Published for SISSA by Springer

Received: *March 18, 2026*
Accepted: *May 31, 2026*
Published: *July 8, 2026*

Measurement of the $|V_{cb}|$ element of the CKM matrix in $t\bar{t}$ decays with the ATLAS detector

The ATLAS collaboration

Full author list at the end of the paper

E-mail: atlas.publications@cern.ch

Abstract: The first measurement of the magnitude of the CKM quark mixing matrix element $|V_{cb}|$ using on-shell W-boson decays is presented. The measurement is made with $t\bar{t}$ events from pp collision data corresponding to an integrated luminosity of 140 fb^{-1} at a centre-of-mass energy of 13 TeV collected by the ATLAS experiment at the Large Hadron Collider. A value of:

$$|V_{cb}| = (50^{+11}_{-14}) \times 10^{-3}$$

is measured, where the uncertainties have roughly equal contributions from the limited size of the data sample and from systematic effects. This is consistent with existing measurements made at much lower energy scales in B hadron decays. While the sensitivity does not yet rival that of previous determinations, this novel approach probes a very different physical situation, namely the rare hadronic $t \to b\bar{b}c$ decay at high momentum-transfer, rather than semileptonic B decays at low momentum-transfer.

Keywords: Hadron-Hadron Scattering

ArXiv ePrint: 2603.16414

Open Access, Copyright CERN,
for the benefit of the ATLAS Collaboration.
Article funded by SCOAP^3.

https://doi.org/10.1007/JHEP07(2026)078

JHEP07(2026)078

Contents

1 Introduction **1**

2 ATLAS detector **3**

3 Data and simulated event samples **4**
3.1 $t\bar{t}$ modelling 5
3.2 Modelling of other backgrounds 6

4 Event reconstruction and selection **7**

5 Overview of the analysis **9**

6 Details of the analysis **10**
6.1 Neural network configuration 10
6.2 *In situ* charm tagging calibration 13

7 Systematic uncertainties **15**
7.1 Experimental uncertainties 15
7.2 Modelling uncertainties 15

8 Statistical analysis and results **17**
8.1 Fit setup 17
8.2 Fit results 19

9 Conclusion **24**

The ATLAS collaboration **32**

JHEP07(2026)078

1 Introduction

The Cabibbo-Kobayashi-Maskawa (CKM) matrix [1, 2] is a 3×3 unitary matrix which parameterises the couplings of the W gauge bosons to the quarks. Its elements are among the fundamental parameters of the Standard Model (SM), which can be determined only by experiment. Its $|V_{cb}|$ element was first determined in 1983, following the initial measurement of the typical B hadron lifetime [3, 4], which was found to be surprisingly long at $\mathcal{O}(1\text{ps})$. This lifetime, in turn, implied that $|V_{cb}| \sim 0.05 \ll |V_{us}|$ [5], heralding for the first time the realisation that the CKM matrix was strongly hierarchical [6]. In the subsequent years, the determination of $|V_{cb}|$ has improved dramatically, both via a sequence of measurements of increasing precision on semileptonic decays of B hadrons, and from improved theoretical understanding [7] of the extraction of $|V_{cb}|$ from the measured quantities. The current PDG average is $|V_{cb}| = (41.1 \pm 1.2) \times 10^{-3}$ [8], but this masks an unresolved discrepancy of around three standard deviations between the determinations made in inclusive and in exclusive semileptonic B decays. It is thus timely to introduce the novel approach to the measurement

of $|V_{cb}|$ reported here, which is based on the method proposed in ref. [9] and uses W bosons produced in the decays of top-quark pairs ($t\bar{t}$).

During LHC Run 2 (2015–2018), $\mathcal{O}(10^8)$ $t\bar{t}$ pairs were produced and decayed in the ATLAS experiment. In such events, assuming the SM, both top quarks decay via an on-shell W boson, and in this sense, the LHC operates effectively as a W boson factory. While single W events are even more numerous, single-lepton $t\bar{t}$ events have a big advantage for studying hadronic W decays in ATLAS. Such events allow relatively easy triggering on the charged lepton, which also helps control hadronic backgrounds in offline analysis. The method used here uses these events, in which one top quark decays into $\bar{b}\ell^-\bar{\nu}$ ($\ell \equiv e$, μ or leptonically decaying τ-lepton), while the other top quark decays hadronically via the $t \to bW^+ \to b\bar{b}c$ decay.[1] The physical context of the measurement is thus very different from those of traditional approaches using B decays, and the experimental uncertainties obtained are of significantly different origins. It is worth noting that on-shell W bosons were first used to measure a CKM matrix element at LEP 2, but only for the much larger $|V_{cs}|$ [10–12].

Traditional measurements of $|V_{cb}|$ [13] exploit the decays of B mesons, and are thus made at an effective momentum-transfer squared (q^2) in the region of $\left(\frac{m_b}{2}\right)^2$, where m_b is the mass of the b-quark. They use a variety of theoretical techniques in low energy hadronic physics to relate the measured quantities to $|V_{cb}|$, including lattice gauge theory for the exclusive semileptonic B decays and the heavy quark expansion for the inclusive B decays. These methods each require the introduction of distinct theoretical uncertainties into the respective measurements. Here, the first measurement of the CKM matrix element $|V_{cb}|$ is presented, made using top quark decays via an on-shell W ($q^2 \simeq M_W^2$). The top quark decays before it hadronises, and the couplings are probed more directly at the parton level. Thus, the measurement described here does not rely on the aforementioned theoretical inputs (lattice, heavy quark expansion) and can provide an independent consistency check. Like other couplings, $|V_{cb}|$ is expected to run above the weak scale, albeit quite slowly [14, 15], although it is expected that such evolution ceases below the weak scale [8]. Therefore, if the value of $|V_{cb}|$ extracted in this measurement were to differ significantly from that determined in B decays, the explanation could be either due to new physics in the $t \to b\bar{b}c$ decay or a poorly understood aspect of the low-q^2 B decay phenomenology.

The measurement determines $|V_{cb}|$ via the ratio of on-shell $W^+ \to c\bar{b}$ decays to $W^+ \to c\bar{q}$, where q is any down-type quark. The leading-order Feynman diagram for the $t \to bW^+ \to b\bar{b}c$ and leptonic $\bar{t}$ decay signal process is shown in figure 1. Taking the ratio of the branching fraction of these decays to that of all similar decays in which the W daughter quark partnering the c-quark has any flavour, determines $|V_{cb}|$ via the following relation, valid in the three-generation SM:[2]

$$|V_{cb}|^2 = \frac{|V_{cb}|^2}{\sum_q |V_{cq}|^2} = \frac{\mathcal{B}(W^+ \to c\bar{b})}{\mathcal{B}(W^+ \to c\bar{q})} = \frac{\mathcal{B}(t \to b\bar{b}c)}{\mathcal{B}(t \to b\bar{q}c)} = \frac{\mathcal{N}(t\bar{t} \to b\bar{b}c\ \bar{b}\ell^-\bar{\nu})}{\mathcal{N}(t\bar{t} \to b\bar{q}c\ \bar{b}\ell^-\bar{\nu})}, \tag{1.1}$$

[1] Charge-conjugate decays are assumed throughout this paper.

[2] The two top-quarks decay independently. Negligible differences in phase space between the three final states in the denominator are ignored. These are calculable from standard formulae (see e.g. ref. [16, section 4.5]) and are found to be at the level of $\lesssim 0.3\%$.

JHEP07(2026)078

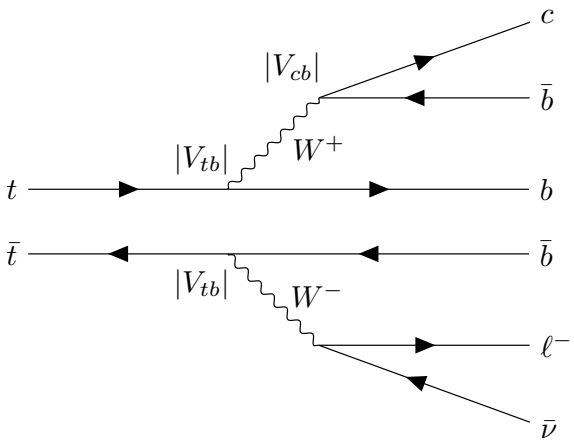

Figure 1. Leading-order Feynman diagram describing the $t\bar{t} \to bW^+\,\bar{b}W^- \to b\bar{b}c\,\bar{b}\ell^-\bar{\nu}$ decay. Vertices are labelled with the appropriate CKM matrix elements.

where $q = d, s, b$, and $\mathcal{N}$ represents the event yield of the decay mode in question. This is a challenging measurement due to the small ratio of event yields, $|V_{cb}|^2 \simeq 1.7 \times 10^{-3}$ [8]. Backgrounds and imperfect detector response complicate the extraction of $|V_{cb}|$ significantly compared with the simple picture implied by eq. (1.1). The phenomenological study of the sensitivity of this measurement reported in ref. [9] did not take account of all experimental backgrounds. The analysis presented here applies this method for the first time, using data collected from the ATLAS detector, with a complete treatment of backgrounds and systematic uncertainties.

2 ATLAS detector

The ATLAS detector [17] at the LHC covers nearly the entire solid angle around the collision point.[3] It consists of an inner tracking detector surrounded by a thin superconducting solenoid, electromagnetic and hadronic calorimeters, and a muon spectrometer incorporating three large superconducting air-core toroidal magnets.

The inner-detector system (ID) is immersed in a 2 T axial magnetic field and provides charged-particle tracking in the range $|\eta| < 2.5$. The high-granularity silicon pixel detector covers the vertex region and typically provides four measurements per track, the first hit generally being in the insertable B-layer (IBL) installed before Run 2 [18, 19]. It is followed by the SemiConductor Tracker (SCT), which usually provides eight measurements per track. These silicon detectors are complemented by the transition radiation tracker (TRT), which enables radially extended track reconstruction up to $|\eta| = 2.0$. The TRT also provides

[3] ATLAS uses a right-handed coordinate system with its origin at the nominal interaction point (IP) in the centre of the detector and the z-axis along the beam pipe. The x-axis points from the IP to the centre of the LHC ring, and the y-axis points upwards. Polar coordinates (r, ϕ) are used in the transverse plane, ϕ being the azimuthal angle around the z-axis. The pseudorapidity is defined in terms of the polar angle θ as $\eta = -\ln\tan(\theta/2)$ and is equal to the rapidity $y = \frac{1}{2}\ln\left(\frac{E+p_z c}{E-p_z c}\right)$ in the relativistic limit. Angular distance is measured in units of $\Delta R \equiv \sqrt{(\Delta y)^2 + (\Delta\phi)^2}$.

JHEP07(2026)078

electron identification information based on the fraction of hits (typically 30 in total) above a higher energy-deposit threshold corresponding to transition radiation.

The calorimeter system covers the pseudorapidity range $|\eta| < 4.9$. Within the region $|\eta| < 3.2$, electromagnetic calorimetry is provided by barrel and endcap high-granularity lead/liquid-argon (LAr) calorimeters, with an additional thin LAr presampler covering $|\eta| < 1.8$ to correct for energy loss in material upstream of the calorimeters. Hadronic calorimetry is provided by the steel/scintillator-tile calorimeter, segmented into three barrel structures within $|\eta| < 1.7$, and two copper/LAr hadronic endcap calorimeters. The solid angle coverage is completed with forward copper/LAr and tungsten/LAr calorimeter modules optimised for electromagnetic and hadronic energy measurements respectively.

The muon spectrometer (MS) comprises separate trigger and high-precision tracking chambers measuring the deflection of muons in a magnetic field generated by the superconducting air-core toroidal magnets. The field integral of the toroids ranges between 2.0 and 6.0 T m across most of the detector. Three layers of precision chambers, each consisting of layers of monitored drift tubes, cover the region $|\eta| < 2.7$, complemented by cathode-strip chambers in the forward region, where the background is highest. The muon trigger system covers the range $|\eta| < 2.4$ with resistive-plate chambers in the barrel, and thin-gap chambers in the endcap regions.

The luminosity is measured mainly by the LUCID-2 [20] detector that records Cherenkov light produced in the quartz windows of photomultipliers located close to the beampipe.

Events are selected by the first-level trigger system implemented in custom hardware, followed by selections made by algorithms implemented in software in the high-level trigger [21]. The first-level trigger accepts events from the 40 MHz bunch crossings at a rate below 100 kHz, which the high-level trigger further reduces in order to record complete events to disk at about 1.25 kHz.

A software suite [22] is used in data simulation, in the reconstruction and analysis of real and simulated data, in detector operations, and in the trigger and data acquisition systems of the experiment.

3 Data and simulated event samples

Proton-proton (pp) collisions at $\sqrt{s} = 13$ TeV collected in 2015–2018 by the ATLAS experiment are analysed [23]. Only the events where all detector components were operational are selected, resulting in a total data sample corresponding to an integrated luminosity of 140 fb^{-1} [24]. Selected events are required to be triggered by one of the single-muon or single-electron triggers which are further described in section 4.

As described in section 1, the analysis focuses on $t\bar{t}$ events with a single electron or muon and four jets in the final state. Monte Carlo (MC) simulated event samples are used to estimate the signal and background contributions in such events, and details are provided below in section 3.1. Heavy-flavour decays are modelled with the EvtGen 1.6.0 program [25] in all parton shower generators, except the Sherpa [26] generator. The modelling of backgrounds with subleading contributions to the phase space is described in section 3.2. The ATLAS simulation infrastructure [27] is used for all the simulated samples, with the detector response simulated using Geant4 [28]. For the signal $t\bar{t}$ sample with $W^+ \to c\bar{b}$ decays, as well as

JHEP07(2026)078

all samples used to evaluate modelling systematic uncertainties, a fast simulation relying on parametrisations of the hadronic showers is used [29]. When evaluating the modelling uncertainties, the fast simulation is used for both the nominal and alternative samples. All simulated samples are processed with the same reconstruction software as the data.

To account for additional pp interactions from the same or close-by bunch crossings (pile-up), a set of minimum-bias interactions generated with Pythia 8.186 [30] using the NNPDF2.3lo parton distribution function (PDF) set [31] with the A3 set of tuned parameters (tune) [32] is superimposed on the hard scattering events. Furthermore, the simulated events are reweighted according to the number of additional pp interactions per bunch-crossing to match the pile-up conditions of each data sample corresponding to the 2015–2018 years of data-taking. Corrections are applied to simulated events to improve agreement between the data and the simulation samples in the object identification efficiencies, energy scales, and energy resolutions, as described in section 4.

3.1 $t\bar{t}$ modelling

All $t\bar{t}$ MC samples used are simulated using Powheg Box-v2 [33–36], which is based on next-to-leading-order (NLO) QCD matrix element (ME) calculations. A suite of $t\bar{t}$ MC samples with various settings are generated to estimate the $t\bar{t}$ contributions and derive systematic uncertainties for the MC modelling of $t\bar{t}$ processes. All $t\bar{t}$ MC samples are normalised to the next-to-next-to-leading-order (NNLO) cross-section including the resummation of soft gluon emissions at next-to-next-to-leading-logarithmic (NNLL) accuracy using Top++ 2.0 [37–43]. The resulting cross-section for the $t\bar{t}$ process is $\sigma_{t\bar{t}} = 834^{+21}_{-30}(\text{scale}) \pm 21(\text{PDF} + \alpha_S)$ pb for $m_t = 172.5$ GeV.

The simulation of $t\bar{t}$ samples is split according to the W boson decay. For single lepton events where the hadronic W boson does not decay via $W^+ \to c\bar{b}$, the simulation uses the simple two-generation quark mixing matrix [44] with Cabibbo angle θ_C [1] given by $\sin\theta_C = 0.225$. Events in the orthogonal single lepton sample, denoted by $t\bar{t}_{|V_{cb}|=1}$, are generated by forcing the hadronic top daughter W boson to decay as $W^+ \to c\bar{b}$. The measurement of $|V_{cb}|$ relies on the ratio constructed from these two samples, which differ only in the quark mixing matrix element settings. All $t\bar{t}$ events that do not feature $W^+ \to c\bar{b}$ decay, including single lepton and dilepton events, are collectively denoted by $t\bar{t}_{|V_{cb}|=0}$. Both $t\bar{t}_{|V_{cb}|=1}$ and $t\bar{t}_{|V_{cb}|=0}$ samples are generated in the five-flavour scheme (5FS) using the Powheg Box-v2 ME generator, the NNPDF3.0nlo PDF [45], the Pythia 8.230 parton shower (PS) generator [46] and the A14 underlying event (UE) tune [47]. They also use $\mu_\text{r} = \mu_\text{f} = \sqrt{m_t^2 + p_{\text{T},t}^2}$ with $m_t = 172.5\,\text{GeV}$, $h_\text{damp} = 1.5 m_t$ and $p_{\text{T,hard}} = 0$, where μ_r and μ_f denote the renormalisation and factorisation scales respectively. The h_damp parameter controls the first high p_T emission after the Born configuration, while $p_{\text{T,hard}}$ is a setting that affects the ME-PS matching. Although the $t\bar{t}_{|V_{cb}|=1}$ sample uses the fast simulation for the detector response, the consistency between fast and full simulation has been validated using the $t\bar{t}_{|V_{cb}|=0}$ sample, where agreement is observed within the MC statistical uncertainty.

The generated $t\bar{t}$ events are categorised based on the presence of additional heavy-flavour (HF) hadrons (b- and c-hadrons), which do not originate from the $t\bar{t}$ system. To identify these, a recursive ancestry check is applied to the generator truth record. The algorithm first

JHEP07(2026)078

counts the total number of HF hadrons in the event. It then subtracts the number of b- and c-quarks that trace their ancestry directly back to the $t\bar{t}$ system. The remaining count defines the number of additional HF hadrons. Events containing at least one additional b-hadron are defined as $t\bar{t}+b$. Events with no additional b-hadrons but at least one additional c-hadron are defined as $t\bar{t}+c$. Both $t\bar{t}+c$ and $t\bar{t}+b$ processes are collectively referred to as $t\bar{t}+\text{HF}$, while events not classified as $t\bar{t}+\text{HF}$ are referred to as $t\bar{t}+\text{light}$.

Alternative samples are used to assess systematic uncertainties associated with the modelling of $t\bar{t}$ in MC samples. Both the $t\bar{t}_{|V_{cb}|=0}$ and $t\bar{t}_{|V_{cb}|=1}$ samples are alternatively interfaced with the Herwig 7.1.3 [48, 49] parton shower generator. Additional $t\bar{t}_{|V_{cb}|=0}$ samples are generated with a variety of m_t, h_{damp}, $p_{\text{T,hard}}$ and UE tuning settings. Furthermore, samples with variations in the final state radiation, b-fragmentation, colour reconnection and the recoil to the top quark transverse momentum $p_{\text{T},t}$ are available to assess systematic uncertainties. An alternative sample is generated with the four-flavour scheme (4FS) at NLO precision using Powheg Box Res [50] and OpenLoops [51–53] using the NNPDF3.1nnlo 4FS PDF set [54]. The mass of the b-quarks in the ME calculation is set to $m_b = 4.95$ GeV. The events are then interfaced to Pythia 8.245 with the A14 tune [47] and the NNPDF2.3lo PDF set [31]. In this sample, the production of additional b-quarks is modelled in the ME, instead of through the PS in the default 5FS sample. This alternative sample is used to define an additional systematic uncertainty for $t\bar{t}+b$.

To serve as pseudo-data for validating the statistical model in section 8.1, an additional $t\bar{t}$ sample is generated. This sample is simulated in the 5FS at NLO precision using Sherpa 2.2.12 [26] and OpenLoops, with the NNPDF3.0nnlo PDF set [45]. The parton showering is performed by Sherpa based on Catani-Seymour dipole factorisation [55, 56] using the MEPS@NLO prescription [57, 58], with parameters tuned by the Sherpa authors.

3.2 Modelling of other backgrounds

Compared to $t\bar{t}$ production, other SM backgrounds make a sub-leading contribution to the event rate. They are predicted with MC simulations, unless stated otherwise, and described in the following.

Single-top processes are split into s-channel, t-channel and tW production. All production modes are modelled with Powheg Box v2 [34–36, 59] at NLO, use the NNPDF3.0nlo PDF set, are interfaced to Pythia 8.230 and use the A14 tune for the UE. To remove overlaps with the $t\bar{t}$ sample in the tW sample, the diagram removal scheme [60] is used. Similar to the $t\bar{t}$ samples described in the previous section, a variety of alternative samples, including a tW alternative sample using the diagram subtraction scheme [60, 61], are generated to assess systematic uncertainties.

The ME, PS and hadronisation for W+jets, Z+jets and diboson (WW, WZ, ZZ) processes is simulated using Sherpa 2.2.11, 2.2.12 or 2.2.14, with the Sherpa version depending on the boson decay modes. The NNPDF3.0nnlo set of PDFs [45] is used in the ME. These samples are matched with the Sherpa parton shower [56] prescription [57, 58, 62, 63] using the set of tuned parameters developed by the Sherpa authors. The production of V+jets is simulated using NLO MEs for up to two partons, and leading-order (LO) matrix elements for up to five partons. They are normalised to an NNLO prediction [64]. Samples of diboson final

JHEP07(2026)078

states (VV) are simulated including off-shell effects and Higgs boson contributions, where appropriate. Fully leptonic final states and single lepton final states, where one boson decays leptonically and the other hadronically, are simulated using matrix elements at NLO accuracy in QCD for up to one additional parton and at LO accuracy for up to three additional parton emissions. Samples for the loop-induced processes $gg \to VV$ are simulated using LO-accurate matrix elements for up to one additional parton emission for both the cases of fully leptonic and single lepton final states. Finally, a small background comes from $t\bar{t}$ + H, $t\bar{t}$ + W and $t\bar{t}$ + Z processes. The production of $t\bar{t}H$ events is modelled using the Powheg Box v2 [33–36, 65] generator at NLO with the NNPDF3.0nlo [45] PDF set. The events are interfaced to Pythia 8.230 [46] using the A14 tune. The production of $t\bar{t}V$ events is modelled using the MadGraph5_aMC@NLO 2.3.3 [66] generator at NLO with the NNPDF3.0nlo [45] PDF. The events are interfaced to Pythia 8.210 [46] using the A14 tune [47] and the NNPDF2.3lo [45] PDF set.

The multijet background is estimated by using the Matrix Method [67] using fake enriched regions orthogonal to the analysis regions. The total fake and non-prompt lepton efficiency is measured using looser lepton identification and isolation requirements and are used to extrapolate the multijet contribution to the analysis regions.

4 Event reconstruction and selection

Events are required to have at least one reconstructed pp interaction vertex with a minimum of two associated tracks with transverse momenta $p_{\mathrm{T}} > 0.5$ GeV. The primary vertex is defined as the vertex with the highest sum of squared transverse momenta of associated tracks [68].

Electron candidates are reconstructed from energy deposits in the EM calorimeter matched to a track in the ID [69]. The track is required to be matched to the primary vertex, where the track longitudinal impact parameter z_0, must satisfy $|z_0 \sin\theta| < 0.5$ mm and the ratio of the transverse impact parameter d_0 to its uncertainty $\sigma(d_0)$ must satisfy $|d_0/\sigma(d_0)| < 5$. Electron candidates are required to be within $|\eta| < 2.47$, excluding the transition region between the barrel and the endcap calorimeters, $1.37 < |\eta| < 1.52$. They must satisfy $p_{\mathrm{T}} > 25$ GeV and the *Tight* likelihood identification criteria and *Tight* isolation criteria [69].

Muon candidates are reconstructed by associating tracks in the ID with tracks or track segments in the MS [70], refined through a global fit that uses hits from both sub-detectors [71]. The track longitudinal and transverse impact parameters must satisfy the requirements $|z_0 \sin\theta| < 0.5$ mm and $|d_0/\sigma(d_0)| < 3$, respectively. Muon candidates must satisfy $p_{\mathrm{T}} > 25$ GeV, $|\eta| < 2.5$ and the *Medium* identification and *Tight* isolation criteria [70].

Jets are reconstructed using the particle flow algorithm, which combines topological clusters of calorimeter cells with tracking information [72, 73]. These objects are then clustered by the anti-k_t algorithm [74, 75] with a jet radius parameter $R = 0.4$. The jet energy scale (JES) is calibrated using both data and simulation, as detailed in ref. [73]. Procedures are adopted to match the jet energy resolution (JER) in simulation to that observed in data [73]. Jets are required to satisfy $p_{\mathrm{T}} > 25$ GeV and $|\eta| < 2.5$. To suppress jets originating from pile-up interactions, the jet vertex tagger (JVT) multivariate likelihood [76] discriminant, using track-based variables, is applied to jets satisfying $p_{\mathrm{T}} < 60$ GeV and $|\eta| < 2.4$, ensuring that the selected jets are matched to the primary vertex.

JHEP07(2026)078

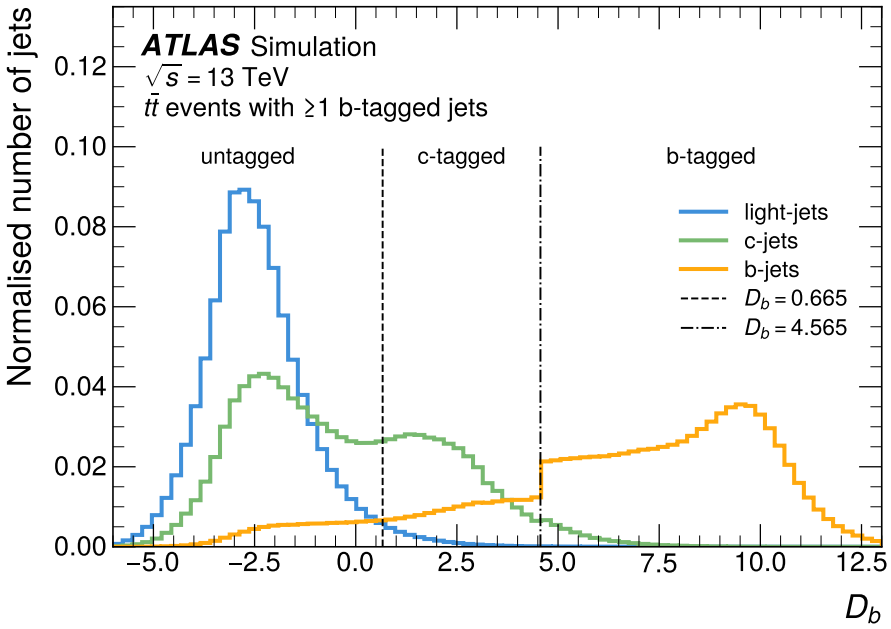

Figure 2. Distribution of the D_b scores for jets from $t\bar{t}$ events after applying the event selection requirements detailed in the text, with the thresholds used to define c- and b-tagged jets shown. For visualisation purposes, the distributions for each flavour are normalised such that the plotted numbers of true light-, c-, and b-jets are equal. Since at least one b-tagged jet is required in the event selection, there is a step in the distribution at the b-tag D_b threshold.

Jets originating from beauty and charm hadrons (b- and c-jets) are identified using the DL1r deep neural network algorithm [77]. This algorithm exploits the distinct features of such jets in terms of track impact parameters and displaced vertices reconstructed in the inner detector. The inputs to the DL1r network include discriminating variables constructed by a recurrent neural network, which exploits the spatial and kinematic correlations between tracks originating from the same b- or c-hadron. The performance of this tagging algorithm is calibrated in data [78–80].

Jets are classified using the single DL1r b-tagging discriminant output score, D_b. A jet is considered b-tagged if its score exceeds the threshold corresponding to a 60% efficiency for correctly identifying b-jets in $t\bar{t}$ events. A jet is considered c-tagged if it is not b-tagged but has a score above the threshold corresponding to an 85% b-jet efficiency. This working point yields a 32% efficiency for correctly identifying c-jets in $t\bar{t}$ events. The chosen b- and c-tagging criteria have a rejection factor of 2500 and of 40 on light-jets, respectively. The distribution of the D_b scores for jets from $t\bar{t}$ events is shown in figure 2.

The missing transverse momentum, $\vec{p}_{\mathrm{T}}^{\,\mathrm{miss}}$, with magnitude $E_{\mathrm{T}}^{\mathrm{miss}}$, is defined as the negative vector-sum of the transverse momenta of all calibrated objects. Tracks that are not associated with any of the physics objects but originate from the primary vertex are taken into account as a $E_{\mathrm{T}}^{\mathrm{miss}}$ soft term [81].

JHEP07(2026)078

To avoid double-counting the same energy deposits in multiple objects due to reconstruction ambiguities, an overlap removal procedure is applied: jets within $\Delta R < 0.2$ of an electron are removed; electrons within $\Delta R < 0.4$ of a remaining jet are removed; jets with less than three ID tracks within $\Delta R < 0.2$ of a muon are removed to avoid rejecting high-energy muons affected by calorimeter energy loss; muons within $\Delta R < 0.4$ of remaining jets are removed.

Events are selected using single-electron or single-muon triggers with offline p_{T} thresholds of 25 GeV for the 2015 data-taking period, and 27 GeV for 2016–2018 [82, 83]. Each selected event is required to contain exactly one reconstructed electron or muon. This lepton must also be matched to the object that fired the trigger. Events containing additional electrons or muons with $p_{\mathrm{T}} > 10$ GeV satisfying the *Loose* identification criteria [69, 70] are vetoed to suppress backgrounds with multiple leptons. Furthermore, events are required to contain exactly four reconstructed jets with $p_{\mathrm{T}} > 25$ GeV and $|\eta| < 2.5$. At least two jets must be identified as either b- or c-tagged, of which at least one must be b-tagged.

5 Overview of the analysis

As noted above, only events with exactly four reconstructed jets satisfying the kinematic selection are used in the analysis. Jets are tagged uniquely as either b-, c- or light-flavoured (for all other jets), and the events are divided into tagging categories (TCs), denoted "$mbnc$", based on the numbers m of b-tagged and n of c-tagged jets they contain. Similarly, production flavours (PFs) are defined using the same $mbnc$ notation, based on the truth-level flavour of jets in each event. The truth-level flavour of a jet is assigned by matching the jet to truth-level hadrons within an angular distance of $\Delta R < 0.3$ and following the priority order $b > c >$ light [77]. TC event yields are different from the corresponding PF event yields, due to jet-flavour mistagging which causes significant numbers of events to migrate between categories.

As suggested by eq. (1.1), sensitivity to $|V_{cb}|$ comes primarily from the ratio of the number of events in the $3b1c$ "signal" TC to that in the $2b1c$ TC: $|V_{cb}|^2 \simeq N(3b1c)/N(2b1c)$. However, a number of effects complicate this simple picture. First, mistagging of jet flavour means that the signal TC contains additional events which need to be accounted for, according to a suitable calculation involving the numbers of events in other PFs and the various jet mistag probabilities which determine the migration between categories. Second, significant numbers of background events enter the signal TC, as a result of physics processes other than pure single lepton weak decays of $t\bar{t}$ pairs. In particular, the most significant backgrounds arise from $t\bar{t}+\mathrm{HF}$ events, in which QCD processes generate an extra pair of heavy quarks ($c\bar{c}$ or $b\bar{b}$) in addition to the usual weak decay products of the $t\bar{t}$ decays, while simultaneously not increasing the number of detected jets. This can happen when, e.g. quark pairs do not form resolved jets, or when one or more jets fall outside the acceptance, leaving just four jets of uncontrolled flavour. The rates of these $t\bar{t}+\mathrm{HF}$ processes are often underestimated in simulation, and the approach taken in this analysis is to determine these rates, simultaneously with the measurement of $|V_{cb}|$.

A final complication of this analysis is that although central ATLAS calibrations of the jet-flavour (mis)tag probabilities (technically, measured weights parameterising data/MC

JHEP07(2026)078

differences) exist for the jet flavours considered, those for true c-jets are calibrated using the same channel as the analysis, namely single lepton $t\bar{t}$ decays [79], with the $|V_{cb}|$ value fixed. Thus, for this analysis the provided c-jet calibration cannot be used directly, and must instead be determined simultaneously with the measurement of $|V_{cb}|$. The sensitivity of this channel to the c-jet tagging efficiency, ϵ_c, comes directly from the fact that the flavour composition of the vast majority of single lepton $t\bar{t}$ decays is very well known from the unitarity of the CKM matrix: hadronic W boson decays to two light-flavoured quarks occur with the same rate as those with one light and one c-quark, up to the small contribution given by $|V_{cb}|^2 \sim 0.2\%$. Thus, the ratio of the yields of events with these flavours after tagging is directly sensitive to the charm tagging efficiency: $N(2b1c)/N(2b0c) \simeq \epsilon_c/(2-\epsilon_c)$, where the dependence on $|V_{cb}|$ makes only a negligible correction. Furthermore, among genuine single lepton $t\bar{t}$ decays, the $3b0c$ PF has negligible rate in the SM as it is suppressed by $|V_{ub}|^2$, and the yield of events seen in the corresponding TC is directly proportional to the c-to-b mistagging probability: $N(3b0c) \propto f_{cb}$, allowing the latter to be determined.

From the above discussion, it is clear that the analysis needs to include the numbers of events in several TCs, in addition to the signal TC, $3b1c$. In practice, eight TCs are used, requiring at least two heavy flavour tags, including at least one b-tag:

$$1b1c,\ 1b2c,\ 1b3c,\ 2b0c,\ 2b1c,\ 2b2c,\ 3b0c,\ 3b1c.$$

The $4b0c$ TC is not used as it does not provide a statistically significant contribution to the analysis.

The $t\bar{t}+\text{HF}$ background events which pass the selection criteria are expected to be incomplete (they have at least six primary partons, with only four jets reconstructed), so that they generally differ kinematically from the primary signal events. Thus, in order to help separate them from the signal, a neural network (NN), trained to distinguish signal events from such incomplete background events, is deployed. The remaining contribution of the $t\bar{t}+\text{HF}$ background to the signal-enriched regions is constrained using background-enriched regions. The NN score, σ, is defined on a scale between 0 and 1, and the events are separated into three distinct regions (NNR) denoted low, med and high. The boundaries of the NNR are obtained by optimising the expected sensitivity to $|V_{cb}|$, resulting in $\sigma_{\text{low}} \leq 0.643$, $0.643 < \sigma_{\text{med}} < 0.736$ and $0.736 \leq \sigma_{\text{high}}$. The same NNR boundaries are used across all eight TCs to give $3 \times 8 = 24$ "fit-regions". Eventually, the event yields in all 24 regions are fitted using a binned profile-likelihood fit [84], while floating $|V_{cb}|^2$, the total $t\bar{t}$ rate, the rates of $t\bar{t}+c$ and $t\bar{t}+b$, and ϵ_c and f_{cb} separately in each of the three NNRs. Figure 3 illustrates the pre-fit NN score distribution in the signal-enriched $3b1c$ TC, as well as the optimal NN score boundaries.

The following sections describe in more detail the architecture of the NN, the *in situ* charm tagging, and details of the fit to extract $|V_{cb}|$.

6 Details of the analysis

6.1 Neural network configuration

A classifier is designed to discriminate between correctly reconstructed $t\bar{t}$ events and background events, defined in the following paragraph. The classification is based on the

JHEP07(2026)078

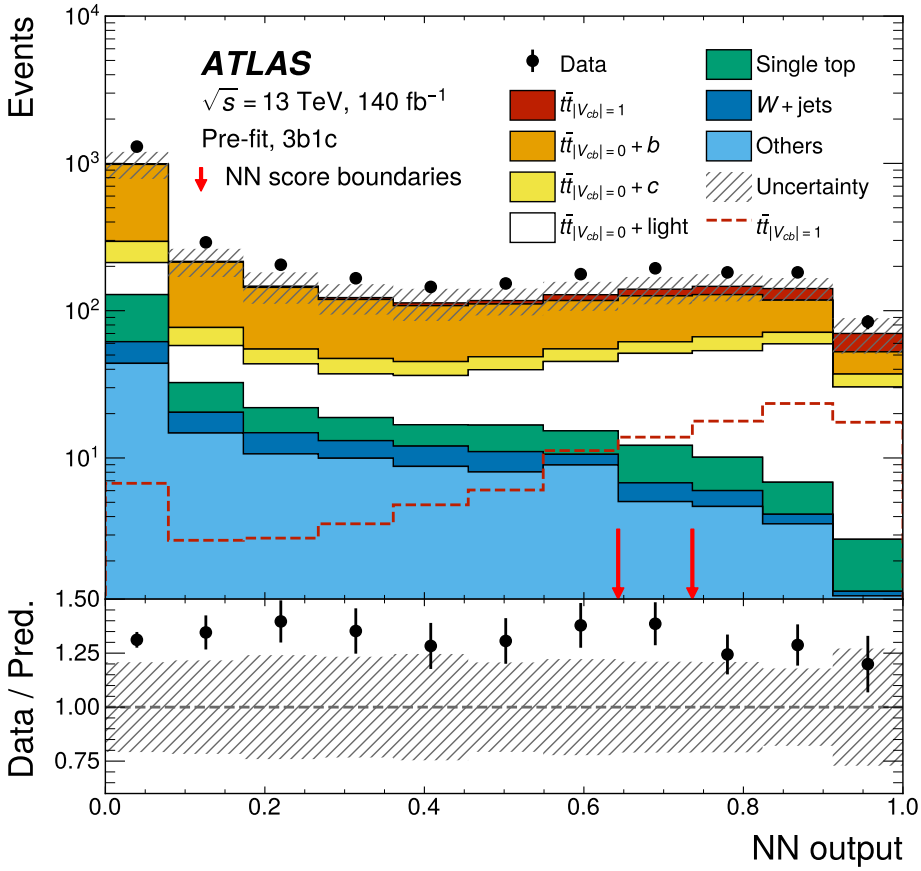

Figure 3. Pre-fit distribution of the Neural Network (NN) output score in the $3b1c$ tagging category. The data are shown as closed circles with statistical uncertainties; the prediction is shown as stacked histograms, broken down into the signal $|V_{cb}| = 1$ and background processes. The signal $|V_{cb}| = 1$ process is also overlaid separately for visualisation. The hatched bands represent the total systematic uncertainties. The lower panels show the ratios of the data to the prediction. The arrows indicate the optimised bin boundaries that are used in the profile-likelihood fit. The "Others" category consists of Z+jets, diboson, $t\bar{t}$ + $H/W/Z$ and multijet events.

output of a NN, which is trained on simulated events and deployed on data and MC. The NN takes a set of reconstructed kinematic inputs from each event, and outputs an activation (score), bound between zero and one, where background events are assigned a low activation, and signal events a high activation. To avoid biasing the extraction of the c-jet tagging probabilities, no flavour-tagging information is used as an input to the NN.

For the NN training, signal events are defined as single lepton $t\bar{t}$ events in simulation, in which the reconstructed lepton and jets can be matched to the corresponding generator-level particle and parton, respectively, within a given angular acceptance. Such events are identified by finding the jet assignment that minimises $\sqrt{\sum_i \Delta R_i^2}$, where ΔR_i is the angular separation between the i'th reconstructed jet and its paired generator-level parton. In accordance with the jet radius used in the jet reconstruction algorithm, a threshold of $\Delta R < 0.4$ is applied to define matched events. In addition, the reconstructed and generator-level leptons are required to be matched within $\Delta R < 0.3$. Single lepton $t\bar{t}$ events that fail the matching criteria, as

JHEP07(2026)078

well as simulated events from other processes (including dilepton $t\bar{t}$ and non-$t\bar{t}$), are labelled as background in the training set and weighted according to their respective cross sections.

A set of reconstructed kinematic features is chosen as input, and is split into two distinct input structures. The first is a vector, containing nine features that are independent of the jet assignment (permutation) to parent W and t-quarks. The other nine features in the second input structure do depend on the selected jet permutation, e.g. the angular distances between the two top candidates, the hadronic W candidate and the lepton. Additionally, the reconstructed masses of the leptonically and hadronically decaying top-quarks ($m(t_{\text{lep}})$ and $m(t_{\text{had}})$), and the hadronic W boson ($m(W_{\text{had}})$) are included. There are 12 unique[4] assignments between four jets and the four partons from a single lepton $t\bar{t}$ decay, each of which yields a unique set of values for the permutation-dependent features. The second NN input structure is therefore a 12×9 matrix, with the rows each representing a fixed jet permutation relative to labels ordered by jet p_{T}. The shapes of the input distributions are standardised to ensure that all inputs have the same absolute scale and width. This is done by applying a Yeo-Johnson power transformation [85], and then normalising each distribution to zero mean and unit standard deviation.

The vector input is processed by a branch of fully connected layers, and the matrix input is processed by a branch of convolutional layers, the latter exploiting the information encoded in the transition between one jet permutation and the next. The outputs of the two branches are processed further by a set of fully connected layers. In addition to background discrimination, the NN is trained to predict the most likely jet permutation as an auxiliary task. This is included as a second output from the NN architecture, and is used for validation plots, but not for the analysis itself.

Two datasets are produced by sorting the full set of simulated events that satisfy the selection criteria into even and odd event numbers. Two NNs with identical architecture are trained, one on each dataset, and are deployed on simulated and observed events in the opposite dataset. For each dataset, 20% is reserved for validation during the training routine. Each NN is trained for a maximum of 50 epochs, the internal weights of each model being saved after each epoch. The final trained model is selected as the one with the minimum loss on the validation set. The trained models select signal events with an efficiency of 81% while the corresponding background efficiency is 18%, and assigns the jet permutation with an efficiency of 63%, when deployed on the validation set.

To verify the importance of the input variables while preserving physical correlations, a local sensitivity analysis [86] is employed based on the partial derivative of the discrimination output σ with respect to each input variable x_i. The importance is quantified by the magnitude of the averaged sensitivity, $|\langle \partial\sigma/\partial x_i \rangle|$, which captures the response to infinitesimal perturbations.[5] As shown in figure 4, the W_{had} mass is the most discriminating variable, followed by the softest jet p_{T} and angular variables; lepton features are retained despite lower sensitivity for their unique information.

[4]The reconstructed quantities used are not sensitive to swapping the assigned W daughter jets.

[5]The perturbation magnitude is set to 1% of the standard deviation for each input variable.

JHEP07(2026)078

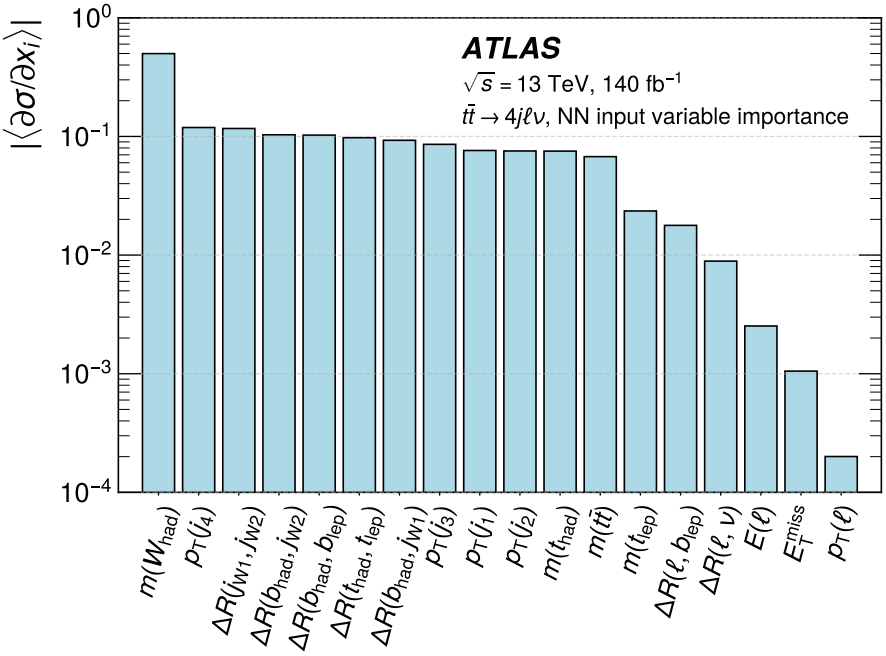

Figure 4. Ranking of the neural network input variables by importance, evaluated with data. The metric is defined as the magnitude of the averaged partial derivative of the discrimination output score with respect to the input. Here, $j_{1,2,3,4}$ refer to the four selected jets in descending order of p_{T}. The reconstructed neutrino is referred to as ν, whose p_x and p_y are defined based on $E_{\mathrm{T}}^{\mathrm{miss}}$, and whose p_z is derived using the W boson invariant mass constraint $m(\ell\nu) = 80.4$ GeV. The hadronic W boson daughter jets are referred to as j_{W1} and j_{W2}, in descending order of p_{T}.

6.2 *In situ* charm tagging calibration

The c-jet tagging efficiencies are calibrated *in situ* using a data-driven method based on the relative event yields in the different TCs. Jet flavour tagging is described by a matrix of tagging rates that encodes both tagging efficiencies and mistag probabilities between light-, charm-, and bottom-flavoured jets,

$$T = \begin{pmatrix} \epsilon_l & f_{lc} & f_{lb} \\ f_{cl} & \epsilon_c & f_{cb} \\ f_{bl} & f_{bc} & \epsilon_b \end{pmatrix}, \tag{6.1}$$

where ϵ_x denotes the tagging efficiency for jets of true flavour x and f_{xy} the probability for a jet of true flavour x to be tagged as flavour y. As each row of T must be normalised to unity, the matrix has six independent parameters, which are chosen to be those in the second and third columns. These tagging rates are defined as kinematically averaged probabilities within the three mutually exclusive NNRs defined in section 5.

Since the standard ATLAS c-jet calibration assumes the SM value of $|V_{cb}|$ and relies on the same data sample used in this analysis, the c-jet tagging efficiency ϵ_c and the c-to-b mistag rate f_{cb} are instead calibrated directly in the fit. On the other hand, for b- and light-flavoured jets, the tagging rates are corrected by applying the simulation-to-data scale

JHEP07(2026)078

factors and associated uncertainties derived in dedicated calibrations [78, 80], to account for the differences between data and simulation.

In a first step, the six independent tagging rates chosen from the T matrix are determined in each NNR from simulation. The simulated events include all events from the fifteen possible PFs without any tagging preselection. They are partitioned into a signal process ($k = S$, including only $|V_{cb}| = 1$) and a background process ($k = B$, including all the other $t\bar{t}$ and single top-quark processes) to reduce correlations with $|V_{cb}|$ and to improve the sensitivity to the tagging rates. The determination of the tagging rates is mainly driven by the $|V_{cb}| = 0$ component of the background. Events are classified into one of the PFs according to their truth-level jet flavour composition, and the probability, $\mathcal{P}_{ij}(T)$, for an event in the i-th PF to be reconstructed in the j-th TC is computed from combinatorial expressions involving only the tagging rates encoded in T. In this calculation, the tagging probabilities for each jet are treated as independent of those for the other jets in the event, an assumption validated by a subsequent closure test. The probability for an event of process k to be tagged into TC j is then given by

$$p_j^k(T) = \sum_i^{\text{PFs}} t_i^k \, \mathcal{P}_{ij}(T), \tag{6.2}$$

where t_i^k is the fraction of events of process k in the i-th PF.

A single, shared set of tagging rates is extracted by minimising a total χ^2 constructed from the separate contributions of the signal and background processes:

$$\chi^2 = \sum_{j,k} \left(\frac{N_j^k - N^k \cdot p_j^k(T)}{\Delta N_j^k} \right)^2, \tag{6.3}$$

where N_j^k is the simulated event yield for process k in TC j, N^k is the total yield, $p_j^k(T)$ is the tagging probability given T. The uncertainty ΔN_j^k is defined as $\sqrt{N_j^k}$, which models the Poisson fluctuation expected in the real data. The subscript j runs over the eight considered TCs, and k runs over the signal and background processes, giving sixteen terms in total. The fit is performed separately in each NNR to reduce the impact of any kinematic differences between the regions. Closure tests are performed by applying the extracted tagging rates to eq. (6.2) to evaluate the predicted event fractions, and then comparing these predictions with the simulated fractions in each TC. Good agreement is observed between the two within the expected statistical fluctuation of the data, as represented by ΔN_j^k.

The second step is performed as part of the final profile-likelihood fit for $|V_{cb}|$, in which the c-jet tagging efficiency ϵ_c and c-to-b mistag rate f_{cb} are incorporated via floated normalisation factors that correct the event yields in each TC to fit the data. In this step, all elements of T except ϵ_c and f_{cb} are fixed to their calibrated values, and distinct tagging rates are used for the low, medium, and high NNRs. The tagging rates, ϵ_c^{NNR} and f_{cb}^{NNR} (NNR = low, med, high), together with their associated uncertainties, are fitted simultaneously with $|V_{cb}|$.

The *in situ* calibration is applied to all $t\bar{t}$ and single top-quark events simulated with Powheg and Pythia. For the other minor processes, a normalisation uncertainty of 30% per true c-jet is assigned.

JHEP07(2026)078

7 Systematic uncertainties

The measurement of $|V_{cb}|$ is affected by systematic uncertainties arising from experimental sources, the modelling of physics processes, and the finite size of MC samples. For two-sided uncertainties, where both upward and downward variations are available, the symmetrised uncertainty is calculated as the signed average of the original variations. In cases of one-sided uncertainties, where only a single alternative scenario is compared against the nominal one, an opposite variation of equal magnitude is assumed.

7.1 Experimental uncertainties

Experimental uncertainties related to the reconstruction of physics objects, pile-up modelling and integrated luminosity are considered. These uncertainties are derived from dedicated measurements using Run 2 data and are applied to all simulated processes. This analysis is primarily sensitive to the experimental uncertainties originating from jet energy and light-jet tagging calibrations.

The uncertainty in the combined 2015–2018 integrated luminosity is 0.83% [24]. Additionally, the distribution of the average number of interactions per bunch crossing in simulation is rescaled to match that in data. Uncertainty in this rescaling process is propagated by varying the corresponding reweighting factors.

Uncertainties associated with electrons and muons arise from the trigger, reconstruction, identification, and isolation efficiencies, as well as their momentum scale and resolution. These are derived from measurements primarily using $Z \to \ell\ell$ ($\ell = e$ or μ) events [69, 70, 82, 83, 87, 88].

Uncertainties in the JES and JER are evaluated using a series of simulation-based techniques and *in situ* measurements [73, 89]. These include uncertainty components related to the jet flavour composition, η-intercalibration, punch-through, single-particle response, calorimeter response to different jet flavours and pile-up effects. They consist of 30 uncorrelated JES components and 13 uncorrelated JER components. An uncertainty associated with the JVT efficiency is also included [76].

Uncertainties related to the calibration of the DL1r flavour tagging algorithm for b-jets and light-flavoured jets are determined from dedicated measurements using events in the dilepton channel of $t\bar{t}$ and $Z+$jets processes, respectively [78, 80]. These uncertainties are decomposed into a set of uncorrelated eigenvectors, including 45 components for b-jets and 20 components for light-jets. Additionally, there are four uncertainty components to account for the extrapolation to high-p_{T} jets, for both flavours. Uncertainties from ref. [79] are not applied to c-jets, since the flavour tagging for c-jets is calibrated within this analysis.

Finally, uncertainties associated with the energy scale and resolution of leptons and jets are propagated to $E_{\mathrm{T}}^{\mathrm{miss}}$. Additional uncertainties in $E_{\mathrm{T}}^{\mathrm{miss}}$ arise from momentum scale and resolution uncertainties of the track-based soft term derived from $Z \to \mu\mu$ events [81].

7.2 Modelling uncertainties

Modelling uncertainties for $t\bar{t}$ and single top-quark processes are estimated by comparing MC samples generated with baseline settings to those generated with alternative settings. The

JHEP07(2026)078

dominant systematic uncertainties in this analysis are related to $t\bar{t}$ modelling, particularly those associated with the modelling of PS and hadronisation.

Uncertainties related to the QCD scale variations in the ME are estimated by varying μ_r and μ_f in the ME calculation independently by factors 2 and 0.5. PDF uncertainties are evaluated using the 30 eigenvectors in the PDF4LHC15 [90] prescription, symmetrising the full difference between the nominal PDF4LHC weight and the variation for each eigenvector. Alternative PDF sets corresponding to different α_s values of 0.117 and 0.119 are also included. Uncertainties in the initial-state radiation (ISR) modelling are estimated according to the VAR 3C set of parameters that are part of the A14 tune [47]. Similarly, the uncertainty related to final-state radiation (FSR) is assessed by varying μ_r for final-state parton-shower emissions up and down by a factor of two. The PS and hadronisation model uncertainty is estimated by comparing the nominal PYTHIA predictions to those obtained from a sample generated with POWHEG BOX v2 using the same settings as the nominal sample for the hard scattering, but interfaced with HERWIG 7.1.3 [48, 49], using the default set of tuned parameters [48] and the MMHT2014LO PDF set [91]. The ME-PS matching uncertainty is estimated by comparing the nominal sample to one with the same settings but using $p_{T,hard} = 1$ instead of 0 in PYTHIA [92].

Since $t\bar{t}$ is the single most important process in this analysis, more detailed modelling uncertainties are considered. The uncertainty arising from the limited precision of the fixed-order NLO QCD ME calculation is evaluated by comparing the baseline differential distributions to the NNLO QCD prediction [93]. The difference is parametrised by reweighting factors derived iteratively using top-quark p_T, $t\bar{t}$ mass and $t\bar{t}$ p_T distributions. The uncertainty related to the modelling of high-p_T radiation is estimated by comparing the nominal sample to one with the h_{damp} parameter increased by a factor of 2 [61]. The uncertainty related to the top-quark mass is propagated by varying its value by ± 0.5 GeV. The uncertainty arising from the ambiguity in the choice of the recoil particle after the first gluon emission [94] in simulating QCD radiation from b-quarks in top-quark decay is evaluated, based on alternative samples in which the top-quark participates in the recoil [95]. The uncertainty in the b-quark fragmentation function is evaluated by comparing samples generated with $r_b = 0.85$, the default value in the A14 tune, with the retuned value $r_b = 1.05$ from ref. [96]. An underlying event and multi-parton interaction (MPI) modelling uncertainty is evaluated with alternative samples generated with varied strong coupling constant for MPI and the colour-reconnection range parameter for the proton beam remnants within the VAR1 parameter set of the A14 tune [47]. The uncertainty related to the modelling of colour reconnection is estimated by comparing samples generated by the "QCD-based" model (CR1) and the "gluon-move" model (CR2) with the baseline sample generated by the "MPI-based" model (CR0). The colour-reconnection uncertainty is then defined by the largest variation for each bin [97, 98].

An additional uncertainty is considered for the choice of flavour scheme in the simulation of $t\bar{t}+b$ events. This is evaluated by comparing the 5FS baseline sample, assuming a massless b-quark, with a 4FS alternative sample, generated with a b-quark mass of 4.95 GeV, which is consistent with the b-quark mass in the top-quark decays.

The $t\bar{t}$ uncertainties are treated as uncorrelated between the single lepton and dilepton processes, as at least two of the selected jets have to come from ISR or FSR in dilepton

JHEP07(2026)078

events. While most modelling uncertainties are correlated between $t\bar{t}_{|V_{cb}|=0}$ and $t\bar{t}_{|V_{cb}|=1}$, the $t\bar{t}$ PS and hadronisation uncertainty is treated as uncorrelated to account for their different heavy-flavour compositions. Furthermore, the PS and hadronisation uncertainty is split into $t\bar{t}+$ light, $t\bar{t}+c$, and $t\bar{t}+b$ components, because c- and b- jets are more likely to be produced via gluon splitting in $t\bar{t}+c$ and $t\bar{t}+b$ processes, respectively. These decorrelation treatments are designed to model the distinct effects independently and prevent unphysical propagation of constraints. Ultimately, the best-fit $|V_{cb}|$ and its uncertainty are not found to depend significantly on these treatments.

For the dominant background process $t\bar{t}_{|V_{cb}|=0}+$ light, the uncertainties related to the PS and hadronisation, FSR, and colour reconnection are decomposed into TC and NN components. The TC component captures event migration between TCs, while the NN component captures event migration between NN score bins within each TC. This treatment prevents the fit from propagating constraints from a sensitive component to an insensitive one, which would otherwise underestimate the total uncertainty. To further reduce the constraint on the NN component of PS and hadronisation uncertainty in $t\bar{t}_{|V_{cb}|=0}+$ light, the original variation is 50% decorrelated across the NN score bins by splitting it into one correlated and three uncorrelated components, each scaled by $1/\sqrt{2}$. This treatment significantly relaxes the constraints associated with this source of the uncertainty while having a minor impact on the $|V_{cb}|$ sensitivity.

An extra uncertainty in the calculation of the interference between tW and $t\bar{t}$ processes is considered for single top-quark modelling. This uncertainty is estimated by comparing the baseline tW sample simulated using diagram-removal, to an alternative sample using diagram-subtraction [60, 61] with otherwise identical settings.

The $t\bar{t}$ normalisation is determined in the fit to data. A cross-section uncertainty of 5.4% is applied to single top-quark processes [99]. For the remaining processes, including $W+$jets, $Z+$jets, diboson and $t\bar{t}+X$, an overall uncertainty of 45–50% is applied [100, 101]. An overall 100% uncertainty is applied to the small multijet background. These uncertainties have a negligible effect on the final results.

8 Statistical analysis and results

8.1 Fit setup

The value of $|V_{cb}|$ is extracted using a binned profile-likelihood fit [84] implemented within the TRExFitter framework [102]. A normalisation factor, $\mu_{|V_{cb}|}$, defined as the ratio of the post-fit value to the pre-fit one, is used throughout this section. The pre-fit value of $|V_{cb}|$ is set to a nominal value of 0.04173, used by the event generators. In addition to $\mu_{|V_{cb}|}$, the overall normalisations of the $t\bar{t}$, $t\bar{t}+c$, and $t\bar{t}+b$ components are treated as free parameters. The c-jet tagging efficiencies and mistag rates are also treated as free parameters and are independent in the three NN score regions. Systematic uncertainties are incorporated as nuisance parameters that affect the predicted event yields through bin-by-bin variations. Most nuisance parameters are constrained by Gaussian probability density functions. The nuisance parameters related to the statistical uncertainty of the simulated samples are constrained

JHEP07(2026)078

Parameter	Affected samples / quantities
$\mu_{\lvert V_{cb}\rvert}$	$t\bar{t}_{\lvert V_{cb}\rvert=1}$ (all), yield scaled with $\mu^2_{\lvert V_{cb}\rvert}$
$\mu_{t\bar{t}}$	$t\bar{t}_{\lvert V_{cb}\rvert=1}$ (all), $t\bar{t}_{\lvert V_{cb}\rvert=0}$ (all)
$\mu_{t\bar{t}+c}$	$t\bar{t}_{\lvert V_{cb}\rvert=1} + c$, $t\bar{t}_{\lvert V_{cb}\rvert=0} + c$
$\mu_{t\bar{t}+b}$	$t\bar{t}_{\lvert V_{cb}\rvert=1} + b$, $t\bar{t}_{\lvert V_{cb}\rvert=0} + b$
$\epsilon_c^{\text{low,med,high}}$	c-jet tagging efficiency in low, med, and high regions
$f_{cb}^{\text{low,med,high}}$	c-to-b mistag rate in low, med, and high regions

Table 1. Overview of the normalisation and tagging parameters used in the fit and their effect on the simulated samples.

by gamma distributions following the Beeston-Barlow technique [103]. The fit is performed simultaneously across 24 bins, comprising eight TCs for each of the three NN score regions.

The likelihood function is the product of Poisson probability terms over all analysis bins, multiplied by constraint terms for the nuisance parameters, and is defined as

$$\mathcal{L}(\text{data} \mid \mu_{|V_{cb}|}, \boldsymbol{\mu}, \boldsymbol{\theta}) = \prod_{k \in \text{bins}} \text{Pois}\left(n_k \mid \nu_k(\mu_{|V_{cb}|}, \boldsymbol{\mu}, \boldsymbol{\theta})\right) \times \prod_i \text{Gauss}\left(\theta_i \mid \theta_{i,0}, 1\right), \tag{8.1}$$

where n_k denotes the observed number of events in bin k, and ν_k is the corresponding expected yield, which depends on the signal strength parameter $\mu_{|V_{cb}|}$, the set of normalisation factors $\boldsymbol{\mu}$, and the nuisance parameters $\boldsymbol{\theta}$. All nuisance parameters, except those accounting for the limited size of the simulated samples, are constrained by Gaussian terms.

Systematic uncertainties with an impact of less than 0.5% on the yield of a given sample in a given bin are omitted for that sample and bin to improve numerical stability and computational performance. It was verified that variations of this threshold have a negligible impact on the fit results.

Table 1 summarises the impact of the fit parameters on the different simulated samples. A common normalisation factor is applied to all $t\bar{t}$ samples, while additional scaling parameters control the relative contributions of the heavy-flavour components. With this parametrisation, the value of $|V_{cb}|$ is directly extracted from the fit through its effect on the $t\bar{t}_{|V_{cb}|=1}$ normalisation.

The model is fit to pseudo-data to validate its robustness. The pseudo-data is constructed from the total prediction, where the contribution of the nominal $t\bar{t}$ sample is replaced by the Sherpa $t\bar{t}$ prediction. The results indicate that the fit to the pseudo-data can recover the inserted values of $\mu_{|V_{cb}|}$ and the other free parameters within the considered modelling uncertainty.

JHEP07(2026)078

8.2 Fit results

The value of $|V_{cb}|$ extracted from the fit is

$$\begin{aligned} |V_{cb}| &= (50^{+7}_{-9}\ (\text{stat.})\ ^{+9}_{-10}\ (\text{syst.})) \times 10^{-3} \\ &= (50^{+11}_{-14}) \times 10^{-3}. \end{aligned}$$

This corresponds to $|V_{cb}|^2 = (2.5 \pm 1.2) \times 10^{-3}$, which scales the decay rate of $W^+ \to c\bar{b}$. The observed (expected) significance relative to the hypothesis in which $|V_{cb}| = 0$ is 2.0σ (1.9σ). The value of $|V_{cb}|$ measured in this analysis is consistent, within one standard deviation, with both inclusive and exclusive measurements from B decays, and with the current world average of $|V_{cb}| = (41.1 \pm 1.2) \times 10^{-3}$ [8]. This consistency supports the Standard Model descriptions of both the low-q^2 phenomenology of B decays, and of the much higher q^2 decays $t \to b\bar{b}c$ which this analysis probes.

The consistency of the high-q^2 measurement of $|V_{cb}|$ with the three generation Standard Model allows the measurement to be re-interpreted in terms of the branching fraction $\mathcal{B}(t \to b\bar{b}c)$. Eq. (1.1) reduces to

$$|V_{cb}|^2 = \frac{\mathcal{B}(t \to b\bar{b}c)}{\mathcal{B}(t \to b\bar{q}c)}, \tag{8.2}$$

while the unitarity of the CKM matrix gives $\mathcal{B}(t \to b\bar{q}c) = \frac{1}{2}\mathcal{B}(t \to b\bar{q}q)$ exactly.[6] Thus

$$\mathcal{B}(t \to b\bar{b}c) = \frac{1}{2}|V_{cb}|^2 \mathcal{B}(t \to b\bar{q}q), \tag{8.3}$$

from which the measured branching fraction, $\mathcal{B}(t \to b\bar{q}q) = (66.5 \pm 1.4)\%$ [106], gives

$$\mathcal{B}(t \to b\bar{b}c) = (8 \pm 4) \times 10^{-4}. \tag{8.4}$$

The post-fit data and predicted yields in all analysis bins are shown in figure 5. The fit has many free parameters and the data are well described by the fitted model in all regions, with an excellent goodness-of-fit, evaluated by a saturated model [84]. Figure 6 shows the post-fit distribution in the 3b1c region. The bottom panel displays the data after subtraction of the predicted background contributions and compares it to the expected signal yields for different values of the $|V_{cb}|$ normalisation factor $\mu_{|V_{cb}|}$, including the best-fit result.

Table 2 summarises the central values and uncertainties of the free-floating parameters of the fit. The overall $t\bar{t}$ normalisation is found to be in good agreement with the SM prediction. The normalisations of the $t\bar{t} + c$ and $t\bar{t} + b$ components are measured to be larger than predicted by simulation, consistent with earlier measurements of the same processes [107, 108]. The uncertainties in these normalisations are larger in this analysis than in the dedicated measurements. This is because the present analysis uses only the four-jet topology, whereas the dedicated measurements use events with higher jet multiplicities, which provide better sensitivity to these processes. An additional validation of these normalisations is performed in regions with 5–6 jets containing at least one additional c- or b-jet, where good agreement

[6] There are corrections of order $\leq 10^{-10}$ to these branching fraction formulae from loop-mediated FCNCs in the SM [104, 105].

JHEP07(2026)078

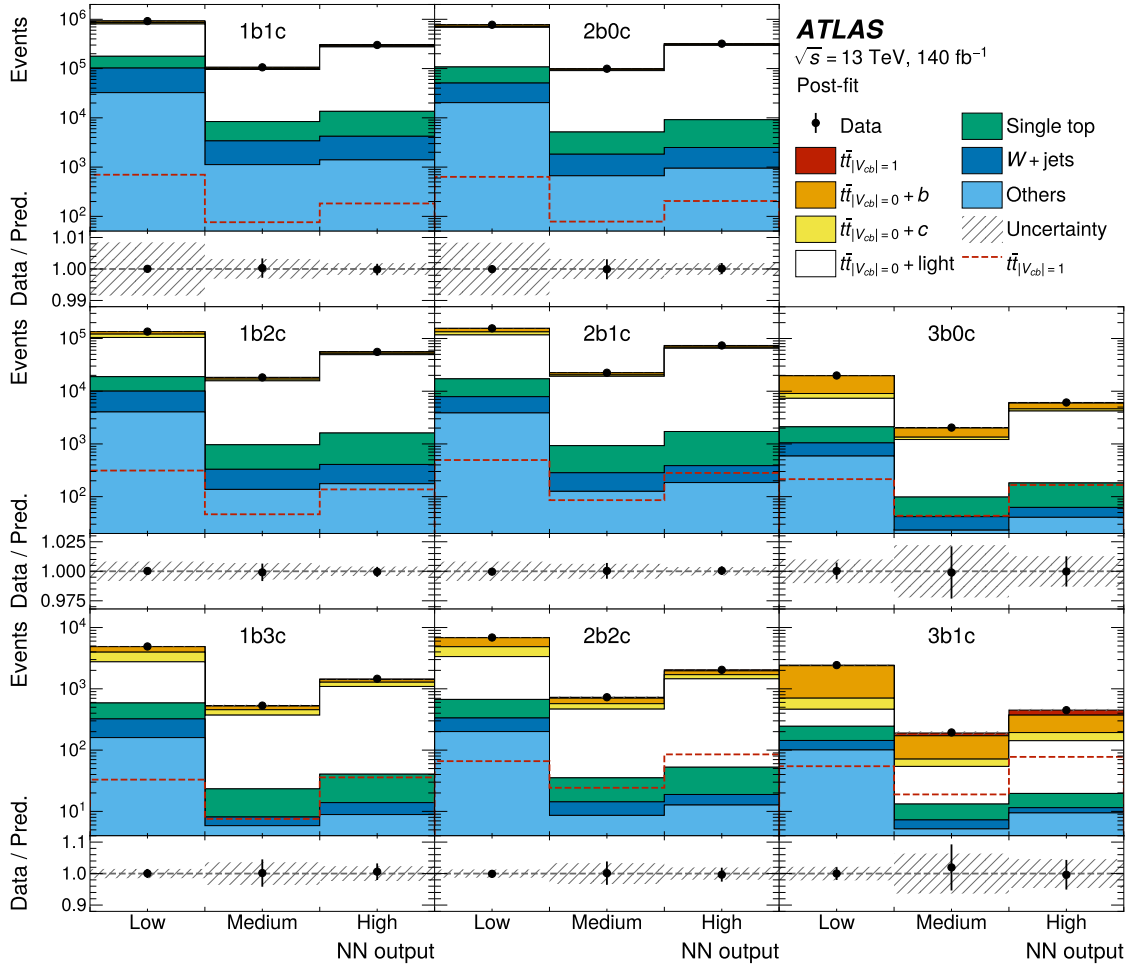

Figure 5. Post-fit distributions of the data and predicted event yields across all bins used in the fit. Each panel in the grid represents a tagging category ($1b1c$-$3b1c$), showing the event yields in the three Neural Network (NN) output score bins (Low, Medium, High). The grid is organised such that regions in the same row contain the same total number of heavy-flavour (b or c) jets and share the same y-axis scales, while regions in the same column contain the same number of b-jets. The data are shown as closed circles with statistical uncertainties; the prediction is shown as stacked histograms, broken down into the signal $|V_{cb}| = 1$ and background processes. The signal $|V_{cb}| = 1$ process is also separately overlaid for visualisation. The hatched bands represent the total systematic uncertainties. The lower panels show the ratios of the data to the predictions.

Parameter	Value	Parameter	Value		
			NN Low	NN Medium	NN High
$\mu_{\lvert V_{cb}\rvert}$	$1.19^{+0.27}_{-0.35}$				
$\mu_{t\bar{t}}$	0.99 ± 0.03	ϵ_c	0.35 ± 0.02	0.34 ± 0.02	$0.33^{+0.02}_{-0.01}$
$\mu_{t\bar{t}+c}$	$1.60^{+0.64}_{-0.60}$	f_{cb} (10^{-3})	25 ± 6	26 ± 3	26 ± 2
$\mu_{t\bar{t}+b}$	$1.45^{+0.54}_{-0.34}$				

Table 2. Best fit values of the freely floating parameters extracted from the fit. The values of ϵ_c and f_{cb} are shown in the three different NN score regions.

JHEP07(2026)078

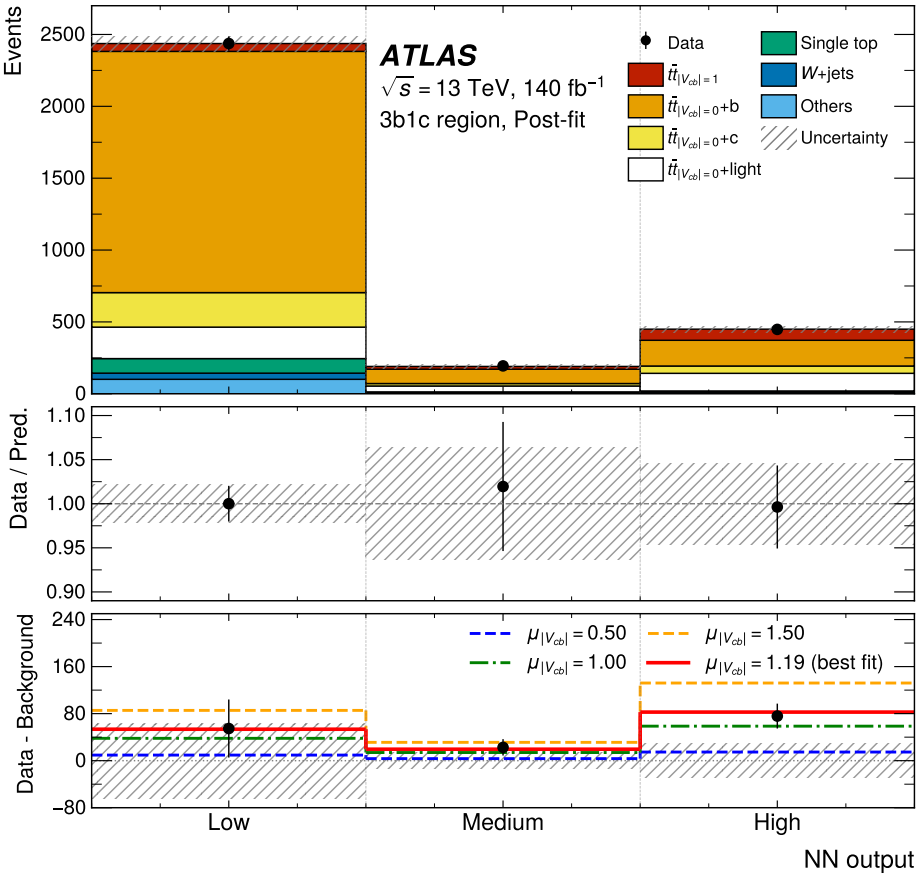

Figure 6. Post-fit distribution of the NN output in the 3b1c region. The upper panel shows the data yield in each bin, and the fitted background and signal MC samples. The middle panel shows the ratio between data and MC. The shaded region marks the total systematic uncertainty, while the error bar on the data symbols represents the statistical uncertainty. The bottom panel shows the data with the background (all samples, excluding $t\bar{t}_{|V_{cb}|=1}$) subtracted, with the lines showing the expected number of $t\bar{t}_{|V_{cb}|=1}$ events at different values of $\mu_{|V_{cb}|}$, together with the best fit value.

is found between the data and the scaled predictions. The fitted c-jet tagging efficiency and mistag rates are both consistent with a constant value across the neural network score regions and with prior ATLAS calibrations [79].

Table 3 shows the contribution of the different sources of systematic uncertainty to the total uncertainty in $|V_{cb}|$. These contributions are estimated by using a toy MC approach, in which 5000 pseudo-experiments are generated for each uncertainty group. The resulting uncertainty breakdown is found to be consistent with the total uncertainty when summed in quadrature. As a cross-check, the impact of each systematic uncertainty is also estimated by using the covariance between $\mu_{|V_{cb}|}$ and the corresponding nuisance parameter [109]. This alternative method yields a similar ranking of the dominant uncertainties. The impact in $\mu_{|V_{cb}|}$ for the 15 highest ranked systematic uncertainties is shown in figure 7. The most important uncertainties are those associated with variations of the parton shower model

JHEP07(2026)078

Uncertainty in $\lvert V_{cb}\rvert$	Up/Down [10^{-3}]
Modelling of $t\bar{t}$	8/9
$\hookrightarrow$ PS and hadronisation	5/6
$\hookrightarrow$ Others	5/6
Jet flavour tagging calibration	2.9/3.1
$\hookrightarrow$ Light-jet	2.5/2.8
$\hookrightarrow$ b-jet	1.2/1.3
Simulation statistical uncertainty	2.6/2.7
Jet calibration	2.4
Modelling of non-$t\bar{t}$ processes	1.6
Others	0.8
Systematic uncertainty	9/10
Statistical uncertainty	7/9
Total uncertainty	11/14

Table 3. Breakdown of the contribution from each source to the total uncertainty in $|V_{cb}|$. The uncertainty components are estimated with a toy MC method, where 5000 toy samples are generated for each uncertainty group. The leading contributions to the 'Others' category in $t\bar{t}$ modelling are from final-state radiation, matrix-element and parton-shower (PS) matching, and colour reconnection. The contribution from *in situ* c-jet calibration cannot be measured using the same approach. Instead, it is incorporated into the statistical uncertainty along with the contributions from other freely floating parameters.

between Pythia and Herwig, which lead to large uncertainties for the $t\bar{t}_{|V_{cb}|=1}$ + light, $t\bar{t}_{|V_{cb}|=0}$ + light, $t\bar{t}_{|V_{cb}|=0} + c$, and $t\bar{t}_{|V_{cb}|=0} + b$ samples.

JHEP07(2026)078

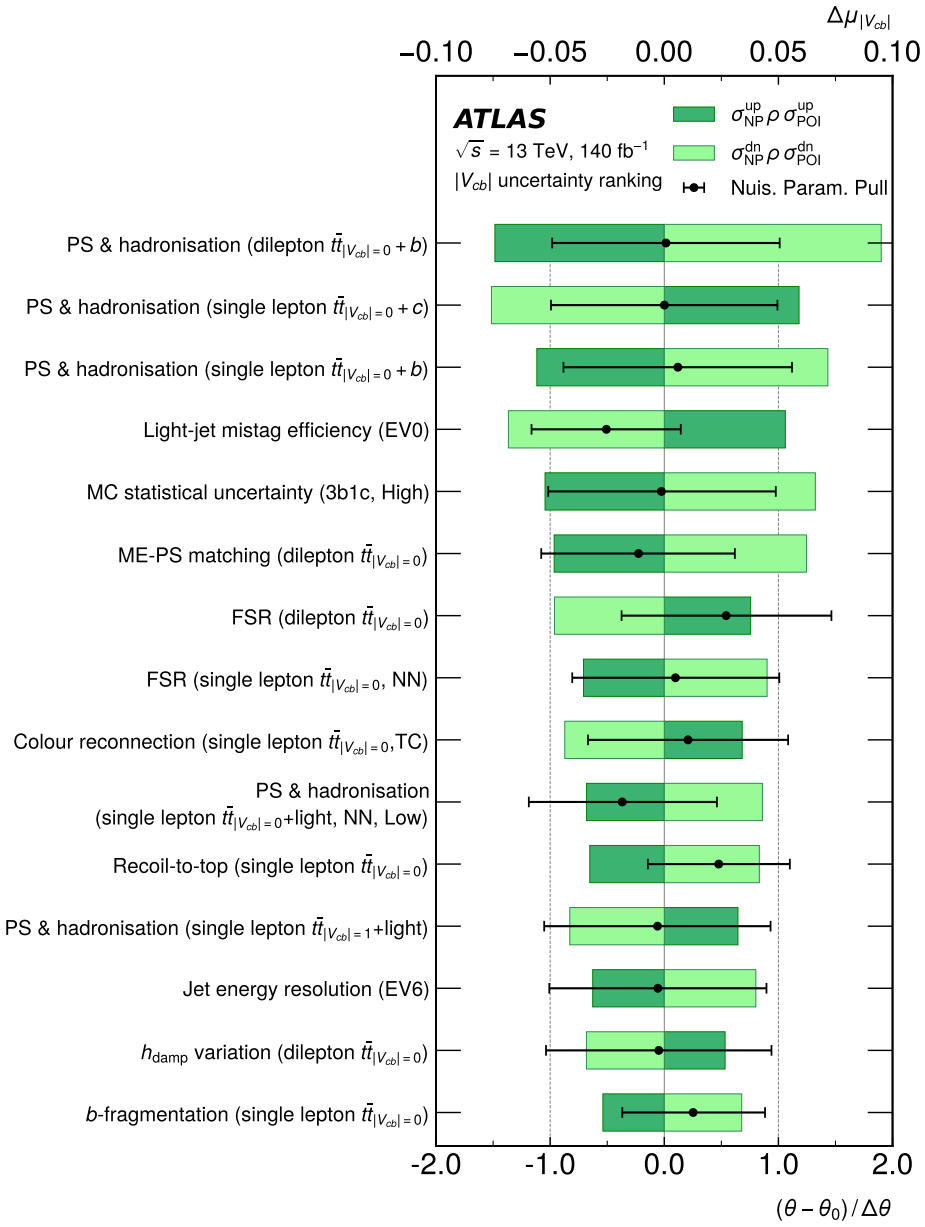

Figure 7. Ranking of the fifteen most significant impacts of individual systematic uncertainties in $\mu_{|V_{cb}|}$ using the covariance method. The dots shows the post-fit value of each nuisance parameter, and the associated band shows the post-fit uncertainty of the parameter. Uncertainties that are decorrelated between samples or regions are labelled with the corresponding sample or region in parentheses. The light-jet mistag efficiency and jet energy resolution uncertainties are split into components; the parentheses indicate the most impactful component.

JHEP07(2026)078

9 Conclusion

The first measurement of the CKM matrix element $|V_{cb}|$ at the weak scale is presented. The measurement uses single lepton $t\bar{t}$ events with exactly four jets, taken from 140 fb^{-1} of pp collision data at $\sqrt{s} = 13$ TeV collected with the ATLAS detector at the LHC. The measurement determines $|V_{cb}|$, via the ratio of on-shell $W^+ \to c\bar{b}$ decays to $W^+ \to c\bar{q}$, where q is any down-type quark. The normalisations of $t\bar{t}$ processes with additional heavy quarks, together with the charm-jet tagging efficiency and mistag rates are determined simultaneously.

The measured value

$$|V_{cb}| = (50^{+11}_{-14}) \times 10^{-3} \tag{9.1}$$

is found to be consistent, within one standard deviation, with earlier measurements made at lower energy scales in B decays. Within the Standard Model, this value can be reinterpreted as the branching fraction

$$\mathcal{B}(t \to b\bar{b}c) = (8 \pm 4) \times 10^{-4}. \tag{9.2}$$

This first measurement of $|V_{cb}|$ using top quark decays demonstrates the potential to measure $|V_{cb}|$ at hadron colliders, and sets the stage for more precise measurements at the LHC in the future. Such measurements will profit from significant progress in flavour tagging algorithms, larger data samples and extended analysis categories.

Acknowledgments

We thank CERN for the very successful operation of the LHC and its injectors, as well as the support staff at CERN and at our institutions worldwide without whom ATLAS could not be operated efficiently.

The crucial computing support from all WLCG partners is acknowledged gratefully, in particular from CERN, the ATLAS Tier-1 facilities at TRIUMF/SFU (Canada), NDGF (Denmark, Norway, Sweden), CC-IN2P3 (France), KIT/GridKA (Germany), INFN-CNAF (Italy), NL-T1 (Netherlands), PIC (Spain), RAL (U.K.) and BNL (U.S.A.), the Tier-2 facilities worldwide and large non-WLCG resource providers. Major contributors of computing resources are listed in ref. [110].

We gratefully acknowledge the support of ANPCyT, Argentina; YerPhI, Armenia; ARC, Australia; BMWFW and FWF, Austria; ANAS, Azerbaijan; CNPq and FAPESP, Brazil; NSERC, NRC and CFI, Canada; CERN; ANID, Chile; CAS, MOST and NSFC, China; Minciencias, Colombia; MEYS CR, Czech Republic; DNRF and DNSRC, Denmark; IN2P3-CNRS and CEA-DRF/IRFU, France; SRNSFG, Georgia; BMFTR, HGF and MPG, Germany; GSRI, Greece; RGC and Hong Kong SAR, China; ICHEP and Academy of Sciences and Humanities, Israel; INFN, Italy; MEXT and JSPS, Japan; CNRST, Morocco; NWO, Netherlands; RCN, Norway; MNiSW, Poland; FCT, Portugal; MNE/IFA, Romania; MSTDI, Serbia; MSSR, Slovakia; ARIS and MVZI, Slovenia; DSI/NRF, South Africa; MICIU/AEI, Spain; SRC and Wallenberg Foundation, Sweden; SERI, SNSF and Cantons of Bern and Geneva, Switzerland; NSTC, Taipei; TENMAK, Türkiye; STFC/UKRI, United Kingdom; DOE and NSF, United States of America.

JHEP07(2026)078

Individual groups and members have received support from BCKDF, CANARIE, CRC and DRAC, Canada; CERN-CZ, FORTE and PRIMUS, Czech Republic; COST, ERC, ERDF, Horizon 2020 and Marie Skłodowska-Curie Actions, European Union; Investissements d'Avenir Labex, Investissements d'Avenir Idex and ANR, France; DFG and AvH Foundation, Germany; Herakleitos, Thales and Aristeia programmes co-financed by EU-ESF and the Greek NSRF, Greece; BSF-NSF and MINERVA, Israel; NCN and NAWA, Poland; La Caixa Banking Foundation, CERCA and AGAUR programs from Generalitat de Catalunya and PROMETEO and GenT Programmes Generalitat Valenciana, Spain; Göran Gustafssons Stiftelse, Sweden; The Royal Society and Leverhulme Trust, United Kingdom; Eric and Wendy Schmidt Fund for Strategic Innovation, United States of America.

In addition, individual members wish to acknowledge support from Chile: Agencia Nacional de Investigación y Desarrollo (ANID FONDECYT reg. 1230987, FONDECYT 1230812, FONDECYT 1240864, Fondecyt 3240661, Fondecyt Regular 1240721); China: Chinese Ministry of Science and Technology (MOST-2023YFA1605700, MOST-2023YFA1609300), National Natural Science Foundation of China (NSFC 12275265, NSFC-W2543005); Czech Republic: Czech Science Foundation (GACR — 24-11373S), Ministry of Education Youth and Sports (ERC-CZ-LL2327, FORTE CZ.02.01.01/00/22_008/0004632), PRIMUS Research Programme (PRIMUS/21/SCI/017); EU: H2020 European Research Council (ERC — 101002463); European Union: European Research Council (BARD No. 101116429, ERC — 101219398, ERC — 948254, ERC 101089007), European Regional Development Fund (HE COFUND GA No.101081355, ERDF), Marie Sklodowska-Curie Actions (GAP-101168829); France: Agence Nationale de la Recherche (ANR-21-CE31-0013, ANR-22-EDIR-0002, ANR-24-CE31-0504-01); Germany: Deutsche Forschungsgemeinschaft (DFG — 469666862); China: Research Grants Council (GRF); Italy: Istituto Nazionale di Fisica Nucleare (LHC-MIUR — 28003/2025), Ministero dell'Università e della Ricerca (NextGenEU 153D23001490006 M4C2.1.1, NextGenEU I53D23000820006 M4C2.1.1, NextGenEU I53D23001490006 M4C2.1.1, SOE2024_0000023); Japan: Japan Society for the Promotion of Science (JSPS KAKENHI JP25H0063, JSPS KAKENHI JP22H01227, JSPS KAKENHI JP22H04944, JSPS KAKENHI JP22KK0227, JSPS KAKENHI JP24K23939, JSPS KAKENHI JP24KK0251, JSPS KAKENHI JP25H00650, JSPS KAKENHI JP25H01291, JSPS KAKENHI JP25K01011, JSPS KAKENHI JP25K01023); Poland: Polish National Science Centre (NCN 2021/42/E/ST2/00350, NCN OPUS 2023/51/B/ST2/02507, NCN OPUS nr 2022/47/B/ST2/03059, NCN UMO-2019/34/E/ST2/00393, UMO-2022/47/O/ST2/00148, UMO-2023/49/B/ST2/04085, UMO-2023/51/B/ST2/00920, UMO-2024/53/N/ST2/00869); Spain: Agència de Gestió d'Ajuts Universitaris i de Recerca. (AGAUR — 2023 BP 00141), Ministry of Science and Innovation (RYC2019-028510-I, RYC2020-030254-I, RYC2021-031273-I, RYC2022-038164-I), Ministerio de Ciencia, Innovación y Universidades/Agencia Estatal de Investigación (EU NextGenerationEU (PRTR-C17.I1), PID2022-142604OB-C22); Sweden: Carl Trygger Foundation (Carl Trygger Foundation CTS 22:2312), Swedish Research Council (Swedish Research Council 2023-04654, VR 2021-03651, VR 2022-03845, VR 2022-04683, VR 2023-03403, VR 2024-05451, VR 2025-05940), Knut and Alice Wallenberg Foundation (KAW 2023.0366); Switzerland: Swiss National Science Foundation (SNSF — PCEFP2_194658); United Kingdom: The Binks Trust, Royal Society

JHEP07(2026)078

(NIF-R1-231091); United States of America: U.S. Department of Energy (ECA DE-AC02-76SF00515), John Templeton Foundation (John Templeton Foundation 63206), Neubauer Family Foundation.

Data Availability Statement. This article has no associated data or the data will not be deposited.

Code Availability Statement. This article has no associated code or the code will not be deposited.

Open Access. This article is distributed under the terms of the Creative Commons Attribution License (CC-BY4.0), which permits any use, distribution and reproduction in any medium, provided the original author(s) and source are credited.

JHEP07(2026)078

References

[1] N. Cabibbo, *Unitary symmetry and leptonic decays*, *Phys. Rev. Lett.* **10** (1963) 531 [INSPIRE].

[2] M. Kobayashi and T. Maskawa, *CP violation in the renormalizable theory of weak interaction*, *Prog. Theor. Phys.* **49** (1973) 652 [INSPIRE].

[3] E. Fernandez et al., *Lifetime of particles containing B quarks*, *Phys. Rev. Lett.* **51** (1983) 1022 [INSPIRE].

[4] N. Lockyer et al., *Measurement of the lifetime of bottom hadrons*, *Phys. Rev. Lett.* **51** (1983) 1316 [INSPIRE].

[5] F.J. Gilman, *Review of particle properties, appendix III the Kobayashi-Maskawa mixing matrix*, in *Review of particle properties*, *Rev. Mod. Phys.* **56** (1984) S296 [INSPIRE].

[6] L. Wolfenstein, *Parametrization of the Kobayashi-Maskawa matrix*, *Phys. Rev. Lett.* **51** (1983) 1945 [INSPIRE].

[7] Flavour Lattice Averaging Group (FLAG) collaboration, *FLAG review 2024*, *Phys. Rev. D* **113** (2026) 014508 [arXiv:2411.04268] [INSPIRE].

[8] A. Ceccucci, Z. Ligeti and Y. Sakai, *Ckm quark-mixing matrix in particle data group review of particle properties*, in *Review of particle physics*, *Phys. Rev. D* **110** (2024) 030001.

[9] P.F. Harrison and V.E. Vladimirov, *A method to determine $|V_{cb}|$ at the weak scale in top decays at the LHC*, *JHEP* **01** (2019) 191 [arXiv:1810.09424] [INSPIRE].

[10] DELPHI collaboration, *Measurement of $|V_{cs}|$ using W decays at LEP-2*, *Phys. Lett. B* **439** (1998) 209 [INSPIRE].

[11] ALEPH collaboration, *A direct measurement of $|V_{cs}|$ in hadronic W decays using a charm tag*, *Phys. Lett. B* **465** (1999) 349 [INSPIRE].

[12] OPAL collaboration, *A measurement of the rate of charm production in W decays*, *Phys. Lett. B* **490** (2000) 71 [hep-ex/0009020] [INSPIRE].

[13] A.X. El-Khadra and P. Urquijo, *Semileptonic b-hadron decays, determination of v_{cb}, v_{ub} in particle data group review of particle properties*, in *Review of particle physics*, *Phys. Rev. D* **110** (2024) 030001.

[14] K.S. Babu, *Renormalization group analysis of the Kobayashi-Maskawa matrix*, *Z. Phys. C* **35** (1987) 69 [INSPIRE].

[15] C. Balzereit, T. Mannel and B. Plumper, *The renormalization group evolution of the CKM matrix*, *Eur. Phys. J. C* **9** (1999) 197 [hep-ph/9810350] [INSPIRE].

[16] M.E. Peskin and D.V. Schroeder, *An introduction to quantum field theory*, Addison-Wesley, Reading, MA, U.S.A. (1995) [DOI:10.1201/9780429503559] [INSPIRE].

[17] ATLAS collaboration, *The ATLAS experiment at the CERN Large Hadron Collider*, 2008 *JINST* **3** S08003 [INSPIRE].

[18] ATLAS collaboration, *ATLAS Insertable B-Layer technical design report*, CERN-LHCC-2010-013 (2010) [INSPIRE].

[19] ATLAS IBL collaboration, *Production and integration of the ATLAS Insertable B-Layer*, 2018 *JINST* **13** T05008 [arXiv:1803.00844] [INSPIRE].

[20] G. Avoni et al., *The new LUCID-2 detector for luminosity measurement and monitoring in ATLAS*, 2018 *JINST* **13** P07017 [INSPIRE].

[21] ATLAS collaboration, *Operation of the ATLAS trigger system in run 2*, 2020 *JINST* **15** P10004 [arXiv:2007.12539] [INSPIRE].

[22] ATLAS collaboration, *The ATLAS collaboration software and firmware*, ATL-SOFT-PUB-2021-001 (2021) [INSPIRE].

[23] ATLAS collaboration, *ATLAS data quality operations and performance for 2015–2018 data-taking*, 2020 *JINST* **15** P04003 [arXiv:1911.04632] [INSPIRE].

[24] ATLAS collaboration, *Luminosity determination in pp collisions at* $\sqrt{s} = 13$ *TeV using the ATLAS detector at the LHC*, *Eur. Phys. J. C* **83** (2023) 982 [arXiv:2212.09379] [INSPIRE].

[25] D.J. Lange, *The EvtGen particle decay simulation package*, *Nucl. Instrum. Meth. A* **462** (2001) 152 [INSPIRE].

[26] SHERPA collaboration, *Event generation with Sherpa 2.2*, *SciPost Phys.* **7** (2019) 034 [arXiv:1905.09127] [INSPIRE].

[27] ATLAS collaboration, *The ATLAS simulation infrastructure*, *Eur. Phys. J. C* **70** (2010) 823 [arXiv:1005.4568] [INSPIRE].

[28] GEANT4 collaboration, *GEANT4 — a simulation toolkit*, *Nucl. Instrum. Meth. A* **506** (2003) 250 [INSPIRE].

[29] ATLAS collaboration, *The simulation principle and performance of the ATLAS fast calorimeter simulation FastCaloSim*, ATL-PHYS-PUB-2010-013 (2010) [INSPIRE].

[30] T. Sjostrand, S. Mrenna and P.Z. Skands, *A brief introduction to PYTHIA 8.1*, *Comput. Phys. Commun.* **178** (2008) 852 [arXiv:0710.3820] [INSPIRE].

[31] R.D. Ball et al., *Parton distributions with LHC data*, *Nucl. Phys. B* **867** (2013) 244 [arXiv:1207.1303] [INSPIRE].

[32] ATLAS collaboration, *The Pythia 8 A3 tune description of ATLAS minimum bias and inelastic measurements incorporating the Donnachie-Landshoff diffractive model*, ATL-PHYS-PUB-2016-017 (2016) [INSPIRE].

[33] S. Frixione, P. Nason and G. Ridolfi, *A positive-weight next-to-leading-order Monte Carlo for heavy flavour hadroproduction*, *JHEP* **09** (2007) 126 [arXiv:0707.3088] [INSPIRE].

[34] P. Nason, *A new method for combining NLO QCD with shower Monte Carlo algorithms*, *JHEP* **11** (2004) 040 [hep-ph/0409146] [INSPIRE].

[35] S. Frixione, P. Nason and C. Oleari, *Matching NLO QCD computations with parton shower simulations: the POWHEG method*, *JHEP* **11** (2007) 070 [arXiv:0709.2092] [INSPIRE].

[36] S. Alioli, P. Nason, C. Oleari and E. Re, *A general framework for implementing NLO calculations in shower Monte Carlo programs: the POWHEG BOX*, *JHEP* **06** (2010) 043 [arXiv:1002.2581] [INSPIRE].

JHEP07(2026)078

[37] M. Beneke, P. Falgari, S. Klein and C. Schwinn, *Hadronic top-quark pair production with NNLL threshold resummation*, *Nucl. Phys. B* **855** (2012) 695 [arXiv:1109.1536] [INSPIRE].

[38] M. Cacciari et al., *Top-pair production at hadron colliders with next-to-next-to-leading logarithmic soft-gluon resummation*, *Phys. Lett. B* **710** (2012) 612 [arXiv:1111.5869] [INSPIRE].

[39] P. Bärnreuther, M. Czakon and A. Mitov, *Percent level precision physics at the Tevatron: first genuine NNLO QCD corrections to $q\bar{q} \to t\bar{t} + X$*, *Phys. Rev. Lett.* **109** (2012) 132001 [arXiv:1204.5201] [INSPIRE].

[40] M. Czakon and A. Mitov, *NNLO corrections to top-pair production at hadron colliders: the all-fermionic scattering channels*, *JHEP* **12** (2012) 054 [arXiv:1207.0236] [INSPIRE].

[41] M. Czakon and A. Mitov, *NNLO corrections to top pair production at hadron colliders: the quark-gluon reaction*, *JHEP* **01** (2013) 080 [arXiv:1210.6832] [INSPIRE].

[42] M. Czakon, P. Fiedler and A. Mitov, *Total top-quark pair-production cross section at hadron colliders through $O(\alpha_S^4)$*, *Phys. Rev. Lett.* **110** (2013) 252004 [arXiv:1303.6254] [INSPIRE].

[43] M. Czakon and A. Mitov, *Top++: a program for the calculation of the top-pair cross-section at hadron colliders*, *Comput. Phys. Commun.* **185** (2014) 2930 [arXiv:1112.5675] [INSPIRE].

[44] S.L. Glashow, J. Iliopoulos and L. Maiani, *Weak interactions with lepton-hadron symmetry*, *Phys. Rev. D* **2** (1970) 1285 [INSPIRE].

[45] NNPDF collaboration, *Parton distributions for the LHC run II*, *JHEP* **04** (2015) 040 [arXiv:1410.8849] [INSPIRE].

[46] T. Sjöstrand et al., *An introduction to PYTHIA 8.2*, *Comput. Phys. Commun.* **191** (2015) 159 [arXiv:1410.3012] [INSPIRE].

[47] ATLAS collaboration, *ATLAS Pythia 8 tunes to 7 TeV data*, ATL-PHYS-PUB-2014-021 (2014) [INSPIRE].

[48] J. Bellm et al., *Herwig 7.0/Herwig++ 3.0 release note*, *Eur. Phys. J. C* **76** (2016) 196 [arXiv:1512.01178] [INSPIRE].

[49] M. Bahr et al., *Herwig++ physics and manual*, *Eur. Phys. J. C* **58** (2008) 639 [arXiv:0803.0883] [INSPIRE].

[50] T. Ježo, J.M. Lindert, N. Moretti and S. Pozzorini, *New NLOPS predictions for $t\bar{t} + b$-jet production at the LHC*, *Eur. Phys. J. C* **78** (2018) 502 [arXiv:1802.00426] [INSPIRE].

[51] F. Cascioli, P. Maierhofer and S. Pozzorini, *Scattering amplitudes with OpenLoops*, *Phys. Rev. Lett.* **108** (2012) 111601 [arXiv:1111.5206] [INSPIRE].

[52] A. Denner, S. Dittmaier and L. Hofer, *Collier: a fortran-based Complex One-Loop LIbrary in Extended Regularizations*, *Comput. Phys. Commun.* **212** (2017) 220 [arXiv:1604.06792] [INSPIRE].

[53] F. Buccioni et al., *OpenLoops 2*, *Eur. Phys. J. C* **79** (2019) 866 [arXiv:1907.13071] [INSPIRE].

[54] NNPDF collaboration, *Parton distributions from high-precision collider data*, *Eur. Phys. J. C* **77** (2017) 663 [arXiv:1706.00428] [INSPIRE].

[55] T. Gleisberg and S. Hoeche, *Comix, a new matrix element generator*, *JHEP* **12** (2008) 039 [arXiv:0808.3674] [INSPIRE].

[56] S. Schumann and F. Krauss, *A parton shower algorithm based on Catani-Seymour dipole factorisation*, *JHEP* **03** (2008) 038 [arXiv:0709.1027] [INSPIRE].

[57] S. Hoeche, F. Krauss, M. Schonherr and F. Siegert, *A critical appraisal of NLO+PS matching methods*, *JHEP* **09** (2012) 049 [arXiv:1111.1220] [INSPIRE].

JHEP07(2026)078

[58] S. Catani, F. Krauss, R. Kuhn and B.R. Webber, *QCD matrix elements + parton showers*, *JHEP* **11** (2001) 063 [hep-ph/0109231] [INSPIRE].

[59] E. Re, *Single-top Wt-channel production matched with parton showers using the POWHEG method*, *Eur. Phys. J. C* **71** (2011) 1547 [arXiv:1009.2450] [INSPIRE].

[60] S. Frixione et al., *Single-top hadroproduction in association with a W boson*, *JHEP* **07** (2008) 029 [arXiv:0805.3067] [INSPIRE].

[61] ATLAS collaboration, *Studies on top-quark Monte Carlo modelling for Top2016*, ATL-PHYS-PUB-2016-020 (2016) [INSPIRE].

[62] S. Hoeche, F. Krauss, M. Schonherr and F. Siegert, *QCD matrix elements + parton showers: the NLO case*, *JHEP* **04** (2013) 027 [arXiv:1207.5030] [INSPIRE].

[63] S. Hoeche, F. Krauss, S. Schumann and F. Siegert, *QCD matrix elements and truncated showers*, *JHEP* **05** (2009) 053 [arXiv:0903.1219] [INSPIRE].

[64] C. Anastasiou, L.J. Dixon, K. Melnikov and F. Petriello, *High precision QCD at hadron colliders: electroweak gauge boson rapidity distributions at NNLO*, *Phys. Rev. D* **69** (2004) 094008 [hep-ph/0312266] [INSPIRE].

[65] H.B. Hartanto, B. Jager, L. Reina and D. Wackeroth, *Higgs boson production in association with top quarks in the POWHEG BOX*, *Phys. Rev. D* **91** (2015) 094003 [arXiv:1501.04498] [INSPIRE].

[66] J. Alwall et al., *The automated computation of tree-level and next-to-leading order differential cross sections, and their matching to parton shower simulations*, *JHEP* **07** (2014) 079 [arXiv:1405.0301] [INSPIRE].

[67] ATLAS collaboration, *Tools for estimating fake/non-prompt lepton backgrounds with the ATLAS detector at the LHC*, 2023 *JINST* **18** T11004 [arXiv:2211.16178] [INSPIRE].

[68] ATLAS collaboration, *Vertex reconstruction performance of the ATLAS detector at* $\sqrt{s} = 13$ *TeV*, ATL-PHYS-PUB-2015-026 (2015) [INSPIRE].

[69] ATLAS collaboration, *Electron and photon efficiencies in LHC run 2 with the ATLAS experiment*, *JHEP* **05** (2024) 162 [arXiv:2308.13362] [INSPIRE].

[70] ATLAS collaboration, *Muon reconstruction and identification efficiency in ATLAS using the full Run 2 pp collision data set at* $\sqrt{s} = 13$ *TeV*, *Eur. Phys. J. C* **81** (2021) 578 [arXiv:2012.00578] [INSPIRE].

[71] ATLAS collaboration, *Muon reconstruction performance of the ATLAS detector in proton–proton collision data at* $\sqrt{s} = 13$ *TeV*, *Eur. Phys. J. C* **76** (2016) 292 [arXiv:1603.05598] [INSPIRE].

[72] ATLAS collaboration, *Jet reconstruction and performance using particle flow with the ATLAS detector*, *Eur. Phys. J. C* **77** (2017) 466 [arXiv:1703.10485] [INSPIRE].

[73] ATLAS collaboration, *Jet energy scale and resolution measured in proton–proton collisions at* $\sqrt{s} = 13$ *TeV with the ATLAS detector*, *Eur. Phys. J. C* **81** (2021) 689 [arXiv:2007.02645] [INSPIRE].

[74] M. Cacciari, G.P. Salam and G. Soyez, *The anti-k_t jet clustering algorithm*, *JHEP* **04** (2008) 063 [arXiv:0802.1189] [INSPIRE].

[75] M. Cacciari, G.P. Salam and G. Soyez, *FastJet user manual*, *Eur. Phys. J. C* **72** (2012) 1896 [arXiv:1111.6097] [INSPIRE].

[76] ATLAS collaboration, *Performance of pile-up mitigation techniques for jets in pp collisions at* $\sqrt{s} = 8$ *TeV using the ATLAS detector*, *Eur. Phys. J. C* **76** (2016) 581 [arXiv:1510.03823] [INSPIRE].

JHEP07(2026)078

[77] ATLAS collaboration, *ATLAS flavour-tagging algorithms for the LHC run 2 pp collision dataset*, *Eur. Phys. J. C* **83** (2023) 681 [arXiv:2211.16345] [INSPIRE].

[78] ATLAS collaboration, *ATLAS b-jet identification performance and efficiency measurement with $t\bar{t}$ events in pp collisions at $\sqrt{s} = 13$ TeV*, *Eur. Phys. J. C* **79** (2019) 970 [arXiv:1907.05120] [INSPIRE].

[79] ATLAS collaboration, *Measurement of the c-jet mistagging efficiency in $t\bar{t}$ events using pp collision data at $\sqrt{s} = 13$ TeV collected with the ATLAS detector*, *Eur. Phys. J. C* **82** (2022) 95 [arXiv:2109.10627] [INSPIRE].

[80] ATLAS collaboration, *Calibration of the light-flavour jet mistagging efficiency of the b-tagging algorithms with Z+jets events using 139 fb^{-1} of ATLAS proton–proton collision data at $\sqrt{s} = 13$ TeV*, *Eur. Phys. J. C* **83** (2023) 728 [arXiv:2301.06319] [INSPIRE].

[81] ATLAS collaboration, *The performance of missing transverse momentum reconstruction and its significance with the ATLAS detector using 140 fb^{-1} of $\sqrt{s} = 13$ TeV pp collisions*, *Eur. Phys. J. C* **85** (2025) 606 [arXiv:2402.05858] [INSPIRE].

[82] ATLAS collaboration, *Performance of the ATLAS muon triggers in run 2*, 2020 *JINST* **15** P09015 [arXiv:2004.13447] [INSPIRE].

[83] ATLAS collaboration, *Performance of electron and photon triggers in ATLAS during LHC run 2*, *Eur. Phys. J. C* **80** (2020) 47 [arXiv:1909.00761] [INSPIRE].

[84] G. Cowan, K. Cranmer, E. Gross and O. Vitells, *Asymptotic formulae for likelihood-based tests of new physics*, *Eur. Phys. J. C* **71** (2011) 1554 [*Erratum ibid.* **73** (2013) 2501] [arXiv:1007.1727] [INSPIRE].

[85] I.-K. Yeo, *A new family of power transformations to improve normality or symmetry*, *Biometrika* **87** (2000) 954.

[86] K. Simonyan, A. Vedaldi and A. Zisserman, *Deep inside convolutional networks: visualising image classification models and saliency maps*, arXiv:1312.6034.

[87] ATLAS collaboration, *Electron and photon energy calibration with the ATLAS detector using LHC run 2 data*, 2024 *JINST* **19** P02009 [arXiv:2309.05471] [INSPIRE].

[88] ATLAS collaboration, *Studies of the muon momentum calibration and performance of the ATLAS detector with pp collisions at $\sqrt{s} = 13$ TeV*, *Eur. Phys. J. C* **83** (2023) 686 [arXiv:2212.07338] [INSPIRE].

[89] ATLAS collaboration, *Dependence of the jet energy scale on the particle content of hadronic jets in the ATLAS detector simulation*, ATL-PHYS-PUB-2022-021 (2022) [INSPIRE].

[90] J. Butterworth et al., *PDF4LHC recommendations for LHC run II*, *J. Phys. G* **43** (2016) 023001 [arXiv:1510.03865] [INSPIRE].

[91] L.A. Harland-Lang, A.D. Martin, P. Motylinski and R.S. Thorne, *Parton distributions in the LHC era: MMHT 2014 PDFs*, *Eur. Phys. J. C* **75** (2015) 204 [arXiv:1412.3989] [INSPIRE].

[92] ATLAS collaboration, *Studies on the improvement of the matching uncertainty definition in top-quark processes simulated with Powheg+Pythia 8*, ATL-PHYS-PUB-2023-029 (2023) [INSPIRE].

[93] M. Czakon et al., *Top-pair production at the LHC through NNLO QCD and NLO EW*, *JHEP* **10** (2017) 186 [arXiv:1705.04105] [INSPIRE].

[94] H. Brooks and P. Skands, *Coherent showers in decays of colored resonances*, *Phys. Rev. D* **100** (2019) 076006 [arXiv:1907.08980] [INSPIRE].

[95] C. Bierlich et al., *A comprehensive guide to the physics and usage of PYTHIA 8.3*, *SciPost Phys. Codeb.* **2022** (2022) 8 [arXiv:2203.11601] [INSPIRE].

JHEP07(2026)078

[96] ATLAS collaboration, *Measurement of the top-quark mass using a leptonic invariant mass in pp collisions at $\sqrt{s} = 13$ TeV with the ATLAS detector*, *JHEP* **06** (2023) 019 [arXiv:2209.00583] [INSPIRE].

[97] ATLAS collaboration, *Measurements of observables sensitive to colour reconnection in $t\bar{t}$ events with the ATLAS detector at $\sqrt{s} = 13$ TeV*, *Eur. Phys. J. C* **83** (2023) 518 [arXiv:2209.07874] [INSPIRE].

[98] ATLAS collaboration, *A study of different colour reconnection settings for Pythia8 generator using underlying event observables*, ATL-PHYS-PUB-2017-008 (2017) [INSPIRE].

[99] N. Kidonakis and N. Yamanaka, *Higher-order corrections for tW production at high-energy hadron colliders*, *JHEP* **05** (2021) 278 [arXiv:2102.11300] [INSPIRE].

[100] ATLAS collaboration, *ATLAS simulation of boson plus jets processes in run 2*, ATL-PHYS-PUB-2017-006 (2017) [INSPIRE].

[101] ATLAS collaboration, *Multi-boson simulation for 13 TeV ATLAS analyses*, ATL-PHYS-PUB-2017-005 (2017) [INSPIRE].

[102] ATLAS collaboration, *Trexfitter*, Zenodo (2026).

[103] R.J. Barlow and C. Beeston, *Fitting using finite Monte Carlo samples*, *Comput. Phys. Commun.* **77** (1993) 219 [INSPIRE].

[104] G. Eilam, J.L. Hewett and A. Soni, *Rare decays of the top quark in the standard and two Higgs doublet models*, *Phys. Rev. D* **44** (1991) 1473 [*Erratum ibid.* **59** (1999) 039901] [INSPIRE].

[105] A. Strumia and N. Tetradis, *Bubble nucleation rates for radiatively induced first order phase transitions*, *Nucl. Phys. B* **554** (1999) 697 [hep-ph/9811438] [INSPIRE].

[106] ATLAS collaboration, *Measurements of the top quark branching ratios into channels with leptons and quarks with the ATLAS detector*, *Phys. Rev. D* **92** (2015) 072005 [arXiv:1506.05074] [INSPIRE].

[107] ATLAS collaboration, *Measurement of $t\bar{t}$ production in association with additional b-jets in the $e\mu$ final state in proton–proton collisions at $\sqrt{s} = 13$ TeV with the ATLAS detector*, *JHEP* **01** (2025) 068 [arXiv:2407.13473] [INSPIRE].

[108] ATLAS collaboration, *Measurement of top-quark pair production in association with charm quarks in proton–proton collisions at $\sqrt{s} = 13$ TeV with the ATLAS detector*, *Phys. Lett. B* **860** (2025) 139177 [arXiv:2409.11305] [INSPIRE].

[109] A. Pinto et al., *Uncertainty components in profile likelihood fits*, *Eur. Phys. J. C* **84** (2024) 593 [arXiv:2307.04007] [INSPIRE].

[110] ATLAS collaboration, *ATLAS computing acknowledgements*, ATL-SOFT-PUB-2026-001, CERN, Geneva, Switzerland (2026).

JHEP07(2026)078

The ATLAS collaboration

G. Aad[102], E. Aakvaag[17], B. Abbott[121], S. Abdelhameed[83b], K. Abeling[54], N.J. Abicht[48], S.H. Abidi[30], M. Aboelela[44], A. Aboulhorma[36e], H. Abramowicz[154], B.S. Acharya[68a,68b,a], A. Ackermann[62a], C. Adam Bourdarios[4], L. Adamczyk[85a], S.V. Addepalli[146], M. J. Addison[101], J. Adelman[117], A. Adiguzel[22c], T. Adye[135], A.A. Affolder[137], Y. Afik[39], M.N. Agaras[13], A. Aggarwal[100], C. Agheorghiesei[28c], A. Ahmad[83a], F. Ahmadov[38,b], S. Ahuja[95], S. Ahuja[165], X. Ai[113c], G. Aielli[75a,75b], A. Aikot[165], M. Ait Tamlihat[36e], T.P.A. Åkesson[98], D. Akiyama[170], N.N. Akolkar[25], S. Aktas[168], G.L. Alberghi[24b], J. Albert[167], U. Alberti[20], P. Albicocco[52], S. Alderweireldt[51], Z.L. Alegria[122], M. Aleksa[37], I.N. Aleksandrov[38], C. Alexa[28b], T. Alexopoulos[10], F. Alfonsi[24b], M. Algren[55], M. Alhroob[169], B. Ali[133], H. M. J. Ali[91,c], S. Ali[32], S.W. Alibocus[92], M. Aliev[34c], G. Alimonti[70a], C. Allaire[65], B.M.M. Allbrooke[149], D. R. Allen[122], J. S. Allen[101], J.F. Allen[51], C.S. Alley[1], E.R. Almazan[137], A. Aloisio[71a,71b], F. Alonso[90], C. Alpigiani[140], A. Alvarez Fernandez[100], M. Alves Cardoso[55], M.G. Alviggi[71a,71b], M. Aly[101], Y. Amaral Coutinho[81b], C. Amelung[37], M. Amerl[101], T. Amezza[128], B. Amini[53], K. Amirie[158], A. Amirkhanov[38], D. Amperiadou[155], S. An[82], C. Anastopoulos[142], T. Andeen[11], J.K. Anders[92], A. C. Anderson[58], A. Andreazza[70a,70b], S. Angelidakis[9], A. Angerami[41], A.V. Anisenkov[38], A. Annovi[73a], C. Antel[37], E. Antipov[148], M. Antonelli[52], F. Anulli[74a], M. Aoki[82], T. Aoki[156], M.A. Aparo[13], L. Aperio Bella[47], M. Apicella[31], C. Appelt[154], A. Apyan[27], M. Arampatzi[10], S. J. Arbiol Val[86], C. Arcangeletti[52], A.T.H. Arce[50], M. Arcuri[43b,43a], J-F. Arguin[108], S. Argyropoulos[155], J.-H. Arling[47], O. Arnaez[4], H. Arnold[148], G. Artoni[74a,74b], H. Asada[111], S. Asatryan[175], N.A. Asbah[37], R. A. Ashby Pickering[169], A. M. Aslam[95], J. Assahsah[36d], K. Assamagan[30], R. Astalos[29a], K. S. V. Astrand[98], S. Atashi[162], R.J. Atkin[34a], H. Atmani[36f], P.A. Atmasiddha[129], K. Augsten[133], A.D. Auriol[40], V.A. Austrup[101], A.S. Avad[94], G. Avolio[37], A. Azzam[13], D. Babal[29b], H. Bachacou[136], K. Bachas[155,d], A. Bachiu[35], E. Bachmann[49], M. J. Backes[62a], A. Badea[39], T.M. Baer[106], M. Bahmani[19], D. Bahner[53], K. Bai[124], L. Baines[94], O.K. Baker[174], D. Bakshi Gupta[8], L.E. Balabram Filho[81b], V. Balakrishnan[121], R. Balasubramanian[4], P. Balek[85a], E. Ballabene[24b,24a], F. Balli[136], L.M. Baltes[62a], W.K. Balunas[127], I. Bamwidhi[83c], E. Banas[86], M. Bandieramonte[130], A. Bandyopadhyay[25], S. Bansal[25], L. Barak[154], M. Barakat[47], E.L. Barberio[105], D. Barberis[18b], M. Barbero[102], M. Z. Barel[116], T. Barillari[110], M-S. Barisits[37], T. Barklow[146], P. Baron[134], D.A. Baron Moreno[101], A. Baroncelli[61], A.J. Barr[127], J.D. Barr[96], F. Barreiro[99], J. Barreiro Guimarães da Costa[14], M.G. Barros Teixeira[131a], F. Bartels[62a], R. Bartoldus[146], A.E. Barton[91], P. Bartos[29a], M. Baselga[48], S. Bashiri[86], A. Bassalat[65,e], M.J. Basso[159a], S. Bataju[44], R. Bate[166], R.L. Bates[58], S. Batlamous[99], M. Battaglia[137], D. Battulga[19], M. Bauce[74a,74b], L. Bauckhage[47], P. Bauer[25], L. T. Bayer[47], L.T. Bazzano Hurrell[31], T. Beau[128], J.Y. Beaucamp[90], S. Beauceron[128], P.H. Beauchemin[161], P. Bechtle[25], H.P. Beck[20,f], K. Becker[169], A.J. Beddall[80], V.A. Bednyakov[38], C.P. Bee[148], L.J. Beemster[16], M. Begalli[81d], M. Begel[30], J.K. Behr[47], J.F. Beirer[37], F. Beisiegel[25], M. Belfkir[83c], G. Bella[154], L. Bellagamba[24b], A. Bellerive[35], C.D. Bellgraph[67], P. Bellos[21], I. Benaoumeur[21], D. Benchekroun[36a], F. Bendebba[36a], Y. Benhammou[154],

JHEP07(2026)078

K.C. Benkendorfer[167], L. Beresford[47], M. Beretta[52], E. Bergeaas Kuutmann[163], N. Berger[4], B. Bergmann[133], J. Beringer[18a], M. Berkat[136], G. Bernardi[5], C. Bernius[146], F.U. Bernlochner[25], A. Berrocal Guardia[13], T. Berry[95], P. Berta[134], A. Berti[131a], R. Bertrand[102], S. Bethke[110], A. Betti[74a,74b], T.F. Beumker[173], A.J. Bevan[94], L. Bezio[55], N.K. Bhalla[53], S. Bharthuar[110], S. Bhatta[148], P. Bhattarai[146], Z.M. Bhatti[118], K. D. Bhide[53], V.S. Bhopatkar[122], R.M. Bianchi[130], G. Bianco[24b,24a], O. Biebel[109], M. Biglietti[76a], P. Bijl[53], C. S. Billingsley[44], Y. Bimgdi[36f], M. Bindi[54], A. Bingham[173], A. Bingul[22b], C. Bini[74a,74b], G.A. Bird[33], M. Biros[134], S. Biryukov[149], T. Bisanz[48], E. Bisceglie[24b,24a], J.P. Biswal[135], D. Biswas[144], M. Biyabi[14], I. Bloch[47], A. Blue[58], U. Blumenschein[94], V.S. Bobrovnikov[38], L. Boccardo[56b,56a], M. Boehler[53], B. Boehm[168], D. Bogavac[13], L. S. Boggia[128], V. Boisvert[95], P. Bokan[163], T. Bold[85a], M. Bomben[5], M. Bona[94], M. Boonekamp[136], A.G. Borbély[58], G. Borissov[91], A. Borkar[168], D. Bortoletto[127], M. Borysova[171], D. Boscherini[24b], M. Bosman[13], K. Bouaouda[36a], L. Boudet[136], J. Boudreau[130], E.V. Bouhova-Thacker[91], D. Boumediene[40], R. Bouquet[56b,56a], A. Boveia[120], D. Boye[30], I.R. Boyko[38], L. Bozianu[55], J. Bracinik[21], N. Brahimi[4], G. Brandt[173], O. Brandt[33], B. Brau[103], R. Brener[171], L. Brenner[116], R. Brenner[163], S. Bressler[171], M. Brettell[96], G. Brianti[116], D. Britton[58], D. Britzger[110], I. Brock[25], R. Brock[107], H. Bronson[129], G. Brooijmans[41], A.J. Brooks[67], E. M. Brooks[159b], E. Brost[30], L.M. Brown[167,159a], L.E. Bruce[60], T.L. Bruckler[127], P.A. Bruckman de Renstrom[86], B. Brüers[47], A. Bruni[24b], G. Bruni[24b], D. Brunner[46a,46b], M. Bruschi[24b], N. Bruscino[74a,74b], T. Buanes[17], Q. Buat[140], D. Buchin[110], A.G. Buckley[58], J. Bucko[134], M. Buhring[49], O. Bulekov[80], B.A. Bullard[146], T. O. Buratovich[90], S. Burdin[92], C.D. Burgard[48], A.M. Burger[89], B. Burghgrave[8], O. Burlayenko[53], J. Burleson[164], J.C. Burzynski[121], V. Büscher[100], P.J. Bussey[58], O. But[25], J.M. Butler[26], C.M. Buttar[58], J.M. Butterworth[96], P. Butti[37], W. Buttinger[135], C.J. Buxo Vazquez[107], A.R. Buzykaev[38], S. Cabrera Urbán[165], L. Cadamuro[65], H. Cai[37], Y. Cai[24b,112c,24a], Y. Cai[112a], M.A. Cairo[129], V.M.M. Cairo[37], O. Cakir[3a], N. Calace[37], P. Calafiura[18a], G. Calderini[128], P. Calfayan[35], L. Calic[98], G. Callea[58], L.P. Caloba[81b], D. Calvet[40], S. Calvet[40], R. Camacho Toro[128], S. Camarda[37], D. Camarero Munoz[27], P. Camarri[75a,75b], C. Camincher[37], M. Campanelli[96], A. Camplani[42], V. Canale[71a,71b], A.C. Canbay[3a], E. Canonero[95], J. Cantero[165], F. Capocasa[27], P. Cappelli[27], M. Capua[43b,43a], A. Carbone[70a,70b], R. Cardarelli[75a], J.C.J. Cardenas[8], M. P. Cardiff[27], G. Carducci[43b,43a], T. Carli[37], G. Carlino[71a], J.I. Carlotto[13], B.T. Carlson[130,g], E.M. Carlson[167], L. Carminati[70a,70b], A. Carnelli[4], M. Carnesale[37], S. Caron[115], E. Carquin[138g], I.B. Carr[105], S. Carrá[72a,72b], G. Carratta[24b,24a], C. Carrion Martinez[165], A.M. Carroll[124], N. Cartalade[40], M.P. Casado[13,h], P. Casolaro[71a,71b], M. Caspar[47], F. Cassinese[90], W.R. Castiglioni[39], F.L. Castillo[4], V. Castillo Gimenez[165], N.F. Castro[131a,131e], A. Catinaccio[37], J.R. Catmore[126], T. Cavaliere[4], V. Cavaliere[30], E. Celebi[80], S. Cella[30], V. Cepaitis[55], K. Cerny[123], A.S. Cerqueira[81a], A. Cerri[73a,i], L. Cerrito[75a,75b], F. Cerutti[18a], B. Cervato[70a,70b], A. Cervelli[24b], G. Cesarini[52], S.A. Cetin[80], V. C. Chabalala[34j], P.M. Chabrillat[128], R. Chakkappai[65], S. Chakraborty[169], A. Chambers[60], J. Chan[18a], J.D. Chapman[33], E. Chapon[136], D.G. Charlton[21], C. Chauhan[132], Y. Che[112a], S. Chekanov[6], G.A. Chelkov[38,j], H. Chen[30], J. Chen[141a],

JHEP07(2026)078

J. Chen[145], M. Chen[59], S. Chen[87], S.J. Chen[112a], X. Chen[141a], X. Chen[15,k], Z. Chen[61], C.L. Cheng[146], H.C. Cheng[63a], S. Cheong[146], A. Cheplakov[38], E. Cherepanova[116], E. Cheu[7], K. Cheung[64], L. Chevalier[136], G. Chiarelli[73a], G. Chiodini[69a], A.S. Chisholm[21], J. L. Chisholm[166], A. Chitan[28b], M. Chitishvili[165], M.V. Chizhov[38,l], K. Choi[11], Y. Chou[140], E.Y.S. Chow[115], G. Christou[51], K.L. Chu[171], M.C. Chu[63a], Z. Chubinidze[52], J. Chudoba[132], J.J. Chwastowski[86], D. Cieri[110], K.M. Ciesla[85a], V. Cindro[93], A. Ciocio[18a], F. Cirotto[71a,71b], Z.H. Citron[171], M. Citterio[70a], D.A. Ciubotaru[28b], A. Clark[55], P.J. Clark[51], N. Clarke Hall[96], C. Clarry[158], S.E. Clawson[47], C. Clement[46a,46b], L. Clissa[24b,24a], Y. Coadou[102], M. Cobal[68a,68c], A. Coccaro[56b], M. G. Cochran Branson[140], R.F. Coelho Barrue[131a], R. Coelho Lopes De Sa[103], S. Coelli[70a], M.M. Cohen[129], L. S. Colangeli[158], B. Cole[41], P. Collado Soto[99], J. Collot[59], M.R. Coluccia[69a], I. Combes[65], P. Conde Muiño[131a,131g], L.H.J. Condren[162], M.P. Connell[34c], S.H. Connell[34c], E.I. Conroy[127], M. Contreras Cossio[11], F. Conventi[71a,m], A.M. Cooper-Sarkar[127], L. Corazzina[74a,74b], F. A. Corchia[24b,24a], A. Cordeiro Oudot Choi[140], L.D. Corpe[40], M. Corradi[74a,74b], F. Corriveau[104,n], A. Cortes-Gonzalez[156], M.J. Costa[165], F. Costanza[4], D. Costanzo[142], J. Couthures[4], G. Cowan[95], K. Cranmer[172], L. Cremer[48], D. Cremonini[24b,24a], S. Crépé-Renaudin[59], F. Crescioli[128], T. Cresta[72a,72b], M. Cristinziani[144], M. Cristoforetti[77a,77b], T. M. Critchley[55], E. Critelli[96], A. Cueto[99], H. Cui[96], Z. Cui[7], B.M. Cunnett[149], W.R. Cunningham[58], E. Cuppini[110], F. Curcio[165], J. R. Curran[51], G. D'amen[30], V. D'Amico[109], M. D'Andrea[56b,56a], G. D'anniballe[73a,73b], S. D'Auria[70a,70b], A. D'Avanzo[71a,71b], L. D'Eramo[40], A. D'Onofrio[71a,71b], M. D'Onofrio[92], M. D'uffizi[101], M.J. Da Cunha Sargedas De Sousa[56b,56a], J.V. Da Fonseca Pinto[81b], C. Da Via[101], W. Dabrowski[85a], T. Dado[37], S. Dahbi[151], T. Dai[106], D. Dal Santo[20], C. Dallapiccola[103], M. Dam[42], J.R. Dandoy[35], D. Dannheim[37], M. Danninger[145], V. Dao[148], G. Darbo[56b], F. Dattola[47], T. Davidek[134], J. Davidson[169], I. Dawson[94], K. De[8], C. De Almeida Rossi[158], N. De Biase[47], S. De Castro[24b,24a], N. De Groot[115], P. de Jong[116], H. De la Torre[117], A. De Maria[112a], S. De Miranda Rimes[81d], A. De Salvo[74a], U. De Sanctis[75a,75b], F. De Santis[69a,69b], A. De Santo[149], J.B. De Vivie De Regie[59], K.G. De Vries[116], J. Debevc[93], D.V. Dedovich[38], J. Degens[92], A.M. Deiana[44], J. Del Peso[99], L. Delagrange[27], F. Deliot[136], C.M. Delitzsch[48], A. Dell'Acqua[37], L. Dell'Asta[70a,70b], M. Della Pietra[71a,71b], D. Della Volpe[55], M. Delmastro[4], C.C. Delogu[56b,56a], P.A. Delsart[59], S. Demers[174], M. Demichev[38], H. Denizli[22a,o], M.G. Depala[92], D. Derendarz[86], L. Derin[56b,56a], F. Derue[128], P. Dervan[92,†], A. M. Desai[1], K. Desch[25], F.A. Di Bello[73a,73b], A. Di Ciaccio[75a,75b], L. Di Ciaccio[4], D. Di Croce[37], C. Di Donato[71a,71b], A. Di Girolamo[37], G. Di Gregorio[65], A. Di Luca[77a,77b], B. Di Micco[76a,76b], R. Di Nardo[76a,76b], K.F. Di Petrillo[39], M. Diamantopoulou[35], F.A. Dias[116], M.A. Diaz[138a,138b], A. R. Didenko[38], M. Didenko[165], S.D. Diefenbacher[18a], E.B. Diehl[106], S. Díez Cornell[47], C. Diez Pardos[144], C. Dimitriadi[147], A. Dimitrievska[21], A. Dimri[148], Y. Ding[61], J. Dingfelder[25], T. Dingley[127], I-M. Dinu[28b], S.J. Dittmeier[62b], F. Dittus[37], M. Divisek[134], B. Dixit[92], F. Djama[102], T. Djobava[152b], C. Doglioni[101,98], A. Dohnalova[29a], Z. Dolezal[134], K. Domijan[85a], K.M. Dona[39], M. Donadelli[81d], B. Dong[107], J. Donini[40], J. Dopke[135], A. Doria[71a], N. Dos Santos Fernandes[131a],

JHEP07(2026)078

I.A. Dos Santos Luz[81e], P. Dougan[44], M.T. Dova[90], A.T. Doyle[58], M.P. Drescher[54], E. Dreyer[171], I. Drivas-koulouris[10], M. Drnevich[118], D. Du[61], T. Du[39], T.A. du Pree[116], Z. Duan[112a], M. Dubau[4], F. Dubinin[38], M. Dubovsky[29a], E. Duchovni[171], G. Duckeck[109], P. K. Duckett[96], O.A. Ducu[28b], D. Duda[51], A. Dudarev[37], M.M. Dudek[86], E. R. Duden[27], L. Duflot[65], M. Dührssen[37], I. Duminica[28g], A.E. Dumitriu[28b], M. Dunford[62a], T. Duong[4], A. Duperrin[102], A.F. Duque Bran[40], H. Duran Yildiz[3a], A. Durglishvili[152b], G.I. Dyckes[18a], M. Dyndal[85a], B.S. Dziedzic[37], G.H. Eberwein[127], B. Eckerova[29a], J.C. Egan[96], S. Eggebrecht[54], E. Egidio Purcino De Souza[81e], G. Eigen[17], K. Einsweiler[18a], T. Ekelof[163], P.A. Ekman[98], S. El Farkh[36b], Y. El Ghazali[61], H. El Jarrari[104], A. El Moussaouy[36a], I. Elbaz[154], D. Elitez[37], M. Ellert[163], F. Ellinghaus[173], T.A. Elliot[95], J. Elmsheuser[30], M. Elsawy[83b], M. Elsing[37], D. Emeliyanov[135], Y. Enari[82], S. Epari[108], D. Ernani Martins Neto[86], F. Ernst[37], M. Escalier[65], C. Escobar[165], R. Estevam De Paula[81c], E. Etzion[154], G. Evans[131a,131b], H. Evans[67], L.S. Evans[47], S. Ezzarqtouni[36a], F. Fabbri[24b,24a], L. Fabbri[24b,24a], G. Facini[96], V. Fadeyev[137], D. Fakoudis[100], S. Falciano[74a], L.F. Falda Ulhoa Coelho[27], F. Fallavollita[110], G. Falsetti[43b,43a], J. Faltova[134], C. Fan[164], K. Y. Fan[63b], Y. Fan[14], Y. Fang[14,112c], M. Fanti[70a,70b], M. Faraj[68a,68c], Z. Farazpay[97], A. Farbin[8], A. Farilla[76a], K. Farman[151], J. N. Farr[174], M. S. Farrington[60], S.M. Farrington[135,51], F. Fassi[36e], D. Fassouliotis[9], L. Fayard[65], G. Fazzino[62b], P. Federic[134], P. Federicova[132], M. Feickert[172], L. Feligioni[102], D.E. Fellers[18a], C. Feng[113b], Y. Feng[14], Z. Feng[65], B. Fernandez Barbadillo[91], P. Fernandez Martinez[66], C. Fernandez Ruiz[33], J. Ferrando[91], A. Ferrari[163], P. Ferrari[116,115], R. Ferrari[72a], D. Ferrere[55], C. Ferretti[106], M. P. Fewell[1], D. Fiacco[74a,74b], F. Fiedler[100], P. Fiedler[133], S. Filimonov[38], M.S. Filip[28b,p], A. Filipčič[93], E.K. Filmer[159a], F. Filthaut[115], M.C.N. Fiolhais[131a,131c,q], L. Fiorini[165], W.C. Fisher[107], T. Fitschen[101], I. Fleck[144], P. Fleischmann[106], T. Flick[173], M. Flores[34d,r], L.R. Flores Castillo[63a], M. Foll[126], F.M. Follega[77a,77b], N. Fomin[33], J.H. Foo[158], A. Formica[136], M. Fornasiero[149], A.C. Forti[101], N. Forti[24b,24a], E. Fortin[102], A.W. Fortman[18a], L. Foster[18a], L. Fountas[9], H. Fox[91], P. Francavilla[73a,73b], S. Francescato[60], S. Franchellucci[20], M. Franchini[24b,24a], S. Franchino[62a], D. Francis[37], L. Franco[47], L. Franconi[47], M. Franklin[60], G. Frattari[37], Y.Y. Frid[154], N. Fritzsche[37], A. Froch[55], D. Froidevaux[37], J.A. Frost[135], Y. Fu[107], S. Fuenzalida Garrido[138g], Y.C. Fujikake[137], M. Fujimoto[148], K. Y. Fung[63a], E. Furtado De Simas Filho[81e], M. Furukawa[156], M. Fuste Costa[47], P. Fuste Martin[13], J. Fuster[165], A. Gaa[54], A. Gabrielli[24b,24a], A. Gabrielli[158], G. Gagliardi[56b,56a], L.G. Gagnon[18a], S. Galantzan[154], J. Gallagher[1], E.J. Gallas[127], A.L. Gallen[163], B.J. Gallop[135], K.K. Gan[120], Y. Gao[51], Z. Gao[112a], A. Garabaglu[140], F.M. Garay Walls[138a,138b], C. García[165], A. Garcia Alonso[116], A.G. Garcia Caffaro[174], J.E. García Navarro[165], M. A. Garcia Ruiz[23b], M. Garcia-Sciveres[18a], G.L. Gardner[129], R.W. Gardner[39], N. Garelli[161], R.B. Garg[146], J.M. Gargan[33], C.A. Garner[158], C.M. Garvey[34a], V. K. Gassmann[161], G. Gaudio[72a], A.J. Gavin[94], J. Gavranovic[93], I.L. Gavrilenko[131a], C. Gay[166], G. Gaycken[124], A. Gekow[120], C. Gemme[56b], M.H. Genest[59], A. D. Gentry[114], S. George[95], T. Geralis[45], A. A. Gerwin[121], P. Gessinger-Befurt[37], M. Ghani[169], K. Ghorbanian[94], A. Ghosal[144], A. Ghosh[162], A. Ghosh[7], B. Giacobbe[24b], S. Giagu[74a,74b], A. Giannini[61], S.M. Gibson[95],

JHEP07(2026)078

D.T. Gil[85b], B.J. Gilbert[41], D. Gillberg[35], G. Gilles[116], D.M. Gingrich[2,s], M.P. Giordani[68a,68c], P.F. Giraud[136], G. Giugliarelli[68a,68c], D. Giugni[70a], F. Giuli[75a,75b,t], I. Gkialas[9,u], B.C. Gladwyn[127], C. Glasman[99], M. Glazewska[20], R. M. Gleason[162], G. Glemža[47], I. Gnesi[24b,24a,v], Y. Go[30], M. Goblirsch-Kolb[37], B. Gocke[48], D. Godin[108], B. Gokturk[22a], S. Goldfarb[105], T. Golling[55], M.G.D. Gololo[34c], A. Golub[140], J.P. Gombas[107], A. Gomes[131a,131b], G. Gomes Da Silva[144], A.J. Gomez Delegido[37], R. Gonçalo[131a], A. Gongadze[152c], F. Gonnella[21], J.L. Gonski[146], R.Y. González Andana[51], S. González de la Hoz[165], M. V. Gonzalez Rodrigues[47], R. Gonzalez Suarez[163], S. Gonzalez-Sevilla[55], L. Goossens[37], B. Gorini[37], E. Gorini[69a,69b], A. Gorišek[93], T.C. Gosart[129], A.T. Goshaw[50], M.I. Gostkin[38], S. Goswami[122], C.A. Gottardo[37], S. A. Gotz[109], M. Gouighri[36b], A.G. Goussiou[140], N. Govender[34c], R. P. Grabarczyk[127], I. Grabowska-Bold[85a], K. Graham[35], E. Gramstad[126], S. Grancagnolo[69a,69b], C.M. Grant[1], P.M. Gravila[28f], F.G. Gravili[69a,69b], H.M. Gray[18a], M. Greco[110], M. J. Green[1], C. Grefe[25], A. S. Grefsrud[17], I.M. Gregor[47], K.T. Greif[162], P. Grenier[146], S.G. Grewe[110], K. Grimm[32], S. Grinstein[13,w], E. Gross[171], J. Grosse-Knetter[54], L.H. Grossman[18b], L. Guan[106], W. Guérin[89], G. Guerrieri[37], R. Guevara[126], R. Gugel[100], J.A.M. Guhit[106], A. Guida[19], E. Guilloton[169], S. Guindon[37], F. Guo[14,112c], J. Guo[141a], L. Guo[47], L. Guo[112b,x], Y. Guo[106], Y. Guo[41], A. Gupta[48], R. Gupta[130], S. Gupta[27], S. Gurbuz[25], S.S. Gurdasani[47], G. Gustavino[74a,74b], P. Gutierrez[121], L.F. Gutierrez Zagazeta[129], M. Gutsche[49], C. Gutschow[96], C. Gwenlan[127], C.B. Gwilliam[92], E.S. Haaland[126], A. Haas[118], M. Habedank[58], C. Haber[18a], R.J. Haberle[171], H.K. Hadavand[8], A. Haddad[40], A. Hadef[49], A.I. Hagan[91], J. J. Hahn[144], M. Haleem[168], J. Haley[122], G.D. Hallewell[102], J.A. Hallford[47], K. Hamano[167], H. Hamdaoui[163], M. Hamer[25], S. E. D. Hammoud[65], E.J. Hampshire[95], L. Han[112a], L. Han[61], S. Han[14], K. Hanagaki[82], M. Hance[137], D.A. Hangal[41], H. Hanif[145], M.D. Hank[129], J.B. Hansen[42], P.H. Hansen[42], T. Harenberg[173], S. Harkusha[175], M.L. Harris[103], Y.T. Harris[25], J. Harrison[13], P.F. Harrison[169], M. L. E. Hart[96], N.M. Hartman[110], N.M. Hartmann[109], R. Z. Hasan[95,135], Y. Hasegawa[143], D. Hashimoto[111], F. Haslbeck[37], S. Hassan[126], R. Hauser[107], M. Haviernik[134], C.M. Hawkes[21], R.J. Hawkings[37], Y. Hayashi[156], D. Hayden[107], R.L. Hayes[116], C.P. Hays[127], J.M. Hays[94], H.S. Hayward[92], M. He[14,112c], Y. He[47], Y. He[96], N.B. Heatley[94], V. Hedberg[98], J. Heilman[35], S. Heim[47], T. Heim[18a], J.J. Heinrich[124], L. Heinrich[110], J. Hejbal[132], M. Helbig[49], A. Held[172], S. Hellesund[17], C.M. Helling[166], F.N.E. Henry[58], H. Herde[98], Y. Hernández Jiménez[148], G. Herten[53], R. Hertenberger[109], L. Hervas[37], M.E. Hesping[100], N.P. Hessey[159a], J. Hessler[110], R. Hicks[129], M. Hidaoui[36b], N. Hidic[134], E. Hill[158], T. S. Hillersoy[17], S.J. Hillier[21], J.R. Hinds[107], F. Hinterkeuser[25], M. Hirose[125], S. Hirose[160], D. Hirschbuehl[173], B. Hiti[93], J. Hobbs[148], R. Hobincu[28e], N. Hod[171], A.M. Hodges[164], M.C. Hodgkinson[142], B.H. Hodkinson[127], A. Hoecker[37], D. D. Hofer[106], J. Hofer[165], J. Hofner[100], M. Holzbock[37], L.B.A.H. Hommels[33], V. Homsak[127], J. J. Hong[67], T.M. Hong[130], B.H. Hooberman[164], W.H. Hopkins[6], M. C. Hoppesch[164], Y. Horii[111], M. E. Horstmann[110], M.M. Horzela[54], S. Hou[151], M. R. Housenga[164], J. Howarth[58], J. Hoya[6], M. Hrabovsky[123], T. Hryn'ova[4], P.J. Hsu[64], S.-C. Hsu[140], T. Hsu[65], M. Hu[18a], P. Hu[63b], Q. Hu[61], S. Huang[33], X. Huang[14,112c],

JHEP07(2026)078

Y. Huang[134], Y. Huang[112b], Y. Huang[14], Z. Huang[65], Z. Hubacek[133], F. Huegging[25], T.B. Huffman[127], M. Hufnagel Maranha De Faria[81a], C. A. Hugli[47], M. Huhtinen[37], S.K. Huiberts[17], R. Hulsken[104], C. E. Hultquist[18a], D.L. Humphreys[103], N. Huseynov[12], J. Huston[107], B. Huth[37], J. Huth[60], L. Huth[47], R. Hyneman[7], G. Iacobucci[55], G. Iakovidis[30], L. Iconomidou-Fayard[65], J. P. Iddon[37], P. Iengo[71a,71b], Y. Iiyama[156], T. Iizawa[156], Y. Ikegami[82], D. Iliadis[155], N. Ilic[158], H. Imam[36a], G. Inacio Goncalves[81d], S. A. Infante Cabanas[138c], T. Ingebretsen Carlson[46a,46b], J. M. Inglis[94], G. Introzzi[72a,72b], M. Iodice[76a], V. Ippolito[74a,74b], R. K. Irwin[92], M. Ishino[156], W. Islam[172], C. Issever[19], S. Istin[22a,y], K. Itabashi[125], H. Ito[170], R. Iuppa[77a,77b], A. Ivina[171], F. Ivone[37], S. Izumiyama[111], V. Izzo[71a], P. Jacka[133], P. Jackson[1], P. R. Jacobson[50], P. Jain[47], K. Jakobs[53], J. Jamieson[58], W. Jang[156], S. Jankovych[116], B. K. Jashal[135], M. Javurkova[103], P. Jawahar[101], L. Jeanty[124], J. Jejelava[152a,z], P. Jenni[53,aa], L. Jerala[93], C.E. Jessiman[35], H. Jia[166], J. Jia[148], X. Jia[110,112c], C. Jiang[51], Q. Jiang[63b], S. Jiggins[47], M. Jimenez Ortega[165], J. Jimenez Pena[13], S. Jin[112a], A. Jinaru[28b], O. Jinnouchi[139], P. Johansson[142], K.A. Johns[7], J.W. Johnson[137], F. A. Jolly[47], D.M. Jones[149], E. Jones[47], K.S. Jones[8], P. Jones[33], R.W.L. Jones[91], T.J. Jones[92], H.L. Joos[37], R. Joshi[120], J. Jovicevic[16], X. Ju[18a], J.J. Junggeburth[37], T. Junkermann[62a], A. Juste Rozas[13,w], M.K. Juzek[86], S. Kabana[138f], A. Kaczmarska[86], S. A. Kadir[146], M. Kado[110], H. Kagan[120], M. Kagan[146], A. Kahn[129], C. Kahra[100], T. Kaji[156], E. Kajomovitz[153], N. Kakati[171], N. Kakoty[13], S. Kandel[8], E. Kanellaki[45], N. Kanellos[10], D. Kar[34j,†], E. Karentzos[25], K. Karki[8], O. Karkout[116], S.N. Karpov[38], Z.M. Karpova[38], V. Kartvelishvili[91,152b], E. Kasimi[155], J. Katzy[47], S. Kaur[35], R. Kavak[164], K. Kawade[143], M.P. Kawale[121], C. Kawamoto[87], E.F. Kay[37], S. Kazakos[107], K. Kazakova[102], J.M. Keaveney[34a], R. Keeler[167], G.V. Kehris[60], J.S. Keller[35], J. M. Kelly[167], J.J. Kempster[149], O. Kepka[132], J. Kerr[159b], B.P. Kerridge[135], B.P. Kerševan[93], L. Keszeghova[29a], R. A. Khan[130], A. Khanov[122], M. Kholodenko[131a], T.J. Khoo[19], G. Khoriauli[168], Y. Khoulaki[36a], Y.A.R. Khwaira[128], D. Kim[6], D.W. Kim[18b], Y.K. Kim[39], N. Kimura[96], M.K. Kingston[54], F. Kirfel[25], J. Kirk[135], A.E. Kiryunin[110], S. Kita[160], O. Kivernyk[25], M. Klassen[161], C. Klein[35], L. Klein[168], M.H. Klein[44], S.B. Klein[55], U. Klein[92], A. Klimentov[30], P. Kluit[116], S. Kluth[110], E. Kneringer[78], T.M. Knight[158], A. Knue[48], M. Kobel[49], D. Kobylianskii[171], S.F. Koch[37], M. Kocian[146], P. Kodyš[134], D.M. Koeck[124], T. Koffas[35], K. Kojima[82], O. Kolay[49], I. Koletsou[4], T. Komarek[86], S. Kondo[156], K. Köneke[54], A.X.Y. Kong[1], T. Kono[119], N. Konstantinidis[96], P. Kontaxakis[55], B. Konya[98], R. Kopeliansky[41], S. Koperny[85a], R. Koppenhofer[53], K. Korcyl[86], K. Kordas[155,ab], A. Korn[96], S. Korn[54], I. Korolkov[13], B. Kortman[116], O. Kortner[110], S. Kortner[110], W.H. Kostecka[117], M. Kostov[29a], V.V. Kostyukhin[144], A. Kotsokechagia[37], A. Kotwal[50], A. Koulouris[37], A. Kourkoumeli-Charalampidi[72a,72b], O. Kovanda[124], R. Kowalewski[167], W. Kozanecki[124], G. Kramberger[93], P. Kramer[25], A. Krasznahorkay[103], A. C. Kraus[117], J.W. Kraus[173], J.A. Kremer[47], N. B. Krengel[144], T. Kresse[158], L. Kretschmann[173], J. Kretzschmar[92], P. Krieger[158], K. Krizka[21], K. Kroeninger[48], H. Kroha[110], J. Kroll[132], J. Kroll[129], K.S. Krowpman[107], U. Kruchonak[38], H. Krüger[25], N. Krumnack[79], J. Krupa[146], M.C. Kruse[50], O. Kuchinskaia[38], S. Kuday[3a], S. Kuehn[37], R. Kuesters[53], T. Kuhl[47],

JHEP07(2026)078

V. Kukhtin[38], Y. Kulchitsky[38], S. Kuleshov[138d,138b], J. Kull[1], E. V. Kumar[109], M. Kumar[34j], N. Kumari[47], P. Kumari[159b], A. Kupco[132], O. Kuprash[53], H. Kurashige[84], L.L. Kurchaninov[159a], O. Kurdysh[4], M. Kuze[139], A.K. Kvam[103], J. Kvita[123], N.G. Kyriacou[140], M. Laassiri[30], C. Lacasta[165], H. Lacker[19], D. Lacour[128], E. Ladygin[38], A. Lafarge[40], B. Laforge[128], T. Lagouri[174], F.Z. Lahbabi[36a], S. Lai[54], W. S. Lai[96], I.K. Lakomiec[54], J.E. Lambert[167], S. Lammers[67], W. Lampl[7], C. Lampoudis[155], G. Lamprinoudis[168], A.N. Lancaster[117], U. Landgraf[53], M.P.J. Landon[94], V.S. Lang[53], A.J. Lankford[162], F. Lanni[37], C. S. Lantz[164], K. Lantzsch[25], A. Lanza[72a], M. Lanzac Berrocal[165], T. Lari[70a], D. Larsen[17], L. Larson[11], F. Lasagni Manghi[24b], M. Lassnig[37], H.C. Lau[167], S.D. Lawlor[142], R. Lazaridou[162], M. Lazzaroni[70a,70b], E. T. T. Le[162], H. D. M. Le[107], E.M. Le Boulicaut[174], D.O. Le Guennec[136], L.T. Le Pottier[18a], B. Leban[24b,24a], F. Ledroit-Guillon[59], T.F. Lee[159b], L.L. Leeuw[34h], M. Lefebvre[167], C. Leggett[18a], L.M. Lehmann[116], G. Lehmann Miotto[37], M. Leigh[55], W.A. Leight[103], W. Leinonen[115], A. Leisos[155,ac], M.A.L. Leite[81c], C.E. Leitgeb[19], R. Leitner[134], K.J.C. Leney[44], T. Lenz[25], S. Leone[73a], C. Leonidopoulos[51], A. Leopold[147], J. LePage-Bourbonnais[35], R. Les[107], C.G. Lester[33], J. Levêque[4], L.J. Levinson[171], G. Levrini[24b,24a], M.P. Lewicki[86], C. Lewis[140], D.J. Lewis[4], L. Lewitt[142], A. Li[30], B. Li[113b], C-Q. Li[110], C. Li[106], H. Li[113b], H. Li[101], H. Li[15], H. Li[61], H. Li[113b], J. Li[141a], L. Li[141a], R. Li[174], S. Li[141b,141a], T. Li[5], Y. Li[14], Z. Li[14,112c], Z. Li[61], S. Liang[14,112c], Z. Liang[14], M. Liberatore[136], B. Liberti[75a], G. B. Libotte[81d], K. Lie[63c], J. Lieber Marin[81e], H. Lien[67], H. Lin[106], S. F. Lin[148], L. Linden[109], R.E. Lindley[7], J.H. Lindon[37], J. Ling[60], E. Lipeles[129], A. Lipniacka[17], A. Lister[166], J.D. Little[67], B. Liu[113a], B.X. Liu[112b], D. Liu[153], D. Liu[137], E. H. L. Liu[21], H. Liu[112b], J.K.K. Liu[118], K. Liu[141b], K. Liu[141b], M. Liu[61], M.Y. Liu[61], P. Liu[113b], Q. Liu[146], S. Liu[148], X. Liu[113b], Y. Liu[112b,112c], Y. Liu[164], Y.L. Liu[113b], Y.W. Liu[61], Z. Liu[65,ad], S.L. Lloyd[94], E.M. Lobodzinska[47], P. Loch[7], E. Lodhi[158], K. Lohwasser[142], E. Loiacono[122], J. D. Lomas[21], I. Longarini[162], R. Longo[24b,24a,v], A. Lopez Solis[13], N.A. Lopez-canelas[7], N. Lorenzo Martinez[4], A.M. Lory[109], M. Losada[83b], G. Löschcke Centeno[4], X. Lou[14,112c], P.A. Love[91], M. Lu[65], S. Lu[129], Y.J. Lu[151], H.J. Lubatti[140], C. Luci[74a,74b], F.L. Lucio Alves[112a], F. Luehring[67], B. S. Lunday[129], O. Lundberg[147], J. Lunde[37], N.A. Luongo[6], M.S. Lutz[158], A.B. Lux[26], D. Lynn[30], R. Lysak[132], V. Lysenko[133], E. Lytken[98], V. Lyubushkin[38], T. Lyubushkina[38], M.M. Lyukova[148], H. Ma[30], K. Ma[61], L.L. Ma[113b], W. Ma[61], Y. Ma[113b], J.C. MacDonald[100], B. Maček[93], P.C. Machado De Abreu Farias[81e], D. Macina[37], R. Madar[40], T. Madula[96], J. Maeda[84], T. Maeno[30], P.T. Mafa[34f], H. Maguire[142], M. Maheshwari[33], V. Maiboroda[65], G. Maineri[70a,70b], A. Maio[131a,131b,131d], K. Maj[85a], O. Majersky[47], S. Majewski[124], A. Makita[156], N. Makovec[65], V. Maksimovic[16], B. Malaescu[128], J. Malamant[126], Pa. Malecki[86], F. Malek[59,ae], M. Mali[93], D. Malito[95], A. Maloizel[5], A. Malvezzi Lopes[81d], S. Malyukov[38], J. Mamuzic[93], G. Mancini[52], M. N. Mancini[27], G. Manco[72a,72b], S.S. Mandarry[149], I. Mandić[93], L. Manhaes de Andrade Filho[81a], I.M. Maniatis[171], J. Manjarres Ramos[89], D.C. Mankad[171], A. Mann[109], T. Manoussos[37], M.N. Mantinan[39], S. Manzoni[37], L. Mao[141a], X. Mapekula[34c], A. Marantis[155], R.R. Marcelo Gregorio[1], G. Marchiori[5], C. Marcon[70a],

JHEP07(2026)078

E. Maricic[16], M. Marinescu[47], S. Marium[47], M. Marjanovic[121], A. Markhoos[53], M. Markovitch[65], M. K. Maroun[103], M. C. Marr[145], T. L. Marsault[136], G. T. Marsden[101], Z. Marshall[18a], S. Marti-Garcia[165], J. Martin[96], T.A. Martin[135], V.J. Martin[51], B. Martin dit Latour[17], S. Martin-Haugh[135], L. Martinelli[74a,74b], V.I. Martinez Outschoorn[103], P. Martinez Suarez[37], G. Martinovicova[134], V.S. Martoiu[28b], A. Martone[89], A.C. Martyniuk[96], A. Marzin[37], D. Mascione[77a,77b], L. Masetti[100], J. Masik[101], A.L. Maslennikov[38], S.L. Mason[41], P. Massarotti[71a,71b], P. Mastrandrea[73a,73b], A. Mastroberardino[43b,43a], R. Mastrofrancesco[72a,72b], T. Masubuchi[125], T.T. Mathew[124], J. Matousek[134], D.M. Mattern[48], K. Mauer[47], J. Maurer[28b], T. Maurin[58], A.J. Maury[65], C. Mavungu Tsava[102], A. E. May[101], E. Mayer[40], R. Mazini[34j], S.M. Mazza[137], E. Mazzeo[37], J.P. Mc Gowan[167], S.P. Mc Kee[106], C.C. McCracken[166], E.F. McDonald[105], L. F. Mcelhinney[91], J.A. Mcfayden[149], R.P. McGovern[129], R.P. Mckenzie[34j], D.J. Mclaughlin[96], S.J. McMahon[135], C.M. Mcpartland[92], R.A. McPherson[167,n], S. Mehlhase[109], A. Mehta[92], D. Melini[165], B.R. Mellado Garcia[14,af], A.H. Melo[54], F. Meloni[47], A.M. Mendes Jacques Da Costa[101], L. Meng[91], S. Menke[110], M. Mentink[37], E. Meoni[43b,43a], G. Mercado[117], S. Merianos[155], C. Merlassino[68a,68c], C. Meroni[70a,70b], J. Metcalfe[6], A.S. Mete[6], E. Meuser[100], C. Meyer[67], J-P. Meyer[136], Y. Miao[112a], R.P. Middleton[135], M. Mihovilovic[65], L. Mijović[51], G. Mikenberg[171], M. Mikestikova[132], M. Mikuž[93], H. Mildner[100], A. Milic[37], D.W. Miller[39], E. H. Miller[146], A. Milov[171], D.A. Milstead[46a,46b], T. Min[112a], I.A. Minashvili[152b], A.I. Mincer[118], B. Mindur[85a], M. Mineev[38], Y. Mino[87], L.M. Mir[13], M. Miralles Lopez[58], M. Mironova[18a], M. Missio[40], A. Mitra[169], V.A. Mitsou[165], Y. Mitsumori[111], P.S. Miyagawa[94], R. Mizuhiki[84], T. Mkrtchyan[37], M. Mlinarevic[96], T. Mlinarevic[96], M. Mlynarikova[134], L. Mlynarska[85a], C. Mo[141a], H. Mobius[47], S. Mobius[20], M. H. Mohamed Farook[114], S. Mohapatra[41], M.F. Mohd Soberi[51], S. Mohiuddin[122], G. Mokgatitswane[34j], R. Mole[21], L. Moleri[171], U. Molinatti[127], L.G. Mollier[20], L. Monaco[37,58], B. Mondal[132], S. Mondal[134], K. Mönig[47], E. Monnier[102], L. Monsonis Romero[165], A. Montella[46a,46b], M. Montella[120], F. Montereali[76a,76b], F. Monticelli[90], S. Monzani[68a,68c], M.E.E. Moors[25], A. Morancho Tarda[42], N. Morange[65], M. Moreno Llácer[165], C. Moreno Martinez[55], J.M. Moreno Perez[23b], P. Morettini[56b], S. Morgenstern[62a], M. Morii[60], M. Morinaga[156], F. Morodei[74a,74b], P. Moschovakos[37], B. Moser[53], M. Mosidze[152b], T. Moskalets[44], P. Moskvitina[115], C.J. Mosomane[34b], J. Moss[32], T. Motta Quirino[81d], A. Moussa[36d], Y. Moyal[171,ag], H. Moyano Gomez[13], E.J.W. Moyse[103], T.G. Mroz[86], S. Muanza[102], M. Mucha[25], J. Mueller[130], D. Muller[144], G.A. Mullier[163], A.J. Mullin[33], J.J. Mullin[50], A.C. Mullins[44], A.E. Mulski[60], D.P. Mungo[158], D. Munoz Perez[122], F.J. Munoz Sanchez[101], W.J. Murray[169,135], E. Musajan[61], M. Muškinja[93], C. Mwewa[47], A.J. Myers[8], G. Myers[106], M. Myska[133], B.P. Nachman[146], K. Nagai[127], K. Nagano[82], R. Nagasaka[156], J.L. Nagle[30,ah], E. Nagy[102], A.M. Nairz[37], T. Nakagawa[87], Y. Nakahama[82], K. Nakamura[82], K. Nakkalil[5], A. Nandi[62b], H. Nanjo[125], E.A. Narayanan[44], Y. Narukawa[156], L. Nasella[70a,70b], S. Nasri[83c], C. Nass[25], G. Navarro[23a], A. Nayaz[19], S. Nechaeva[24b,24a], F. Nechansky[132], L. Nedic[127], A. Negri[72a,72b], M. Negrini[24b], C. Nellist[116], C. Nelson[104], K. Nelson[106], S. Nemecek[132], M. Nessi[37,ai], M.S. Neubauer[164], J. Newell[92], P.R. Newman[21], Y.W.Y. Ng[164], B. Ngair[83b],

JHEP07(2026)078

H.D.N. Nguyen[108], J.D. Nichols[121], R. Nicolaidou[136], J. Nielsen[137], M. Niemeyer[54], J. Niermann[37], N. Nikiforou[37], I. Nikolic-Audit[128], P. Nilsson[30], G. Ninio[154], A. Nisati[74a], D. Nishimura[156], R. Nisius[110], N. Nitika[171], E.K. Nkadimeng[34b], T. Nobe[156], D. Noll[146], T. Nommensen[150], M.B. Norfolk[142], B.J. Norman[35], L.C. Nosler[18a], M. Noury[36a], J. Novak[93], T. Novak[93], P. Novotny[171], R. Novotny[133], L. Nozka[123], K. Ntekas[37], D. Ntounis[146], N.M.J. Nunes De Moura Junior[81b], A.P. O'Neill[20], J. Ocariz[128], I. Ochoa[131a], A. Odella Rodriguez[13], S. Oerdek[47], J.T. Offermann[39], A. Ogrodnik[86], A. Oh[101], C.C. Ohm[147], H. Oide[82], M.L. Ojeda[37], Y. Okumura[156], L.F. Oleiro Seabra[131a], I. Oleksiyuk[55], G. Oliveira Correa[13], D. Oliveira Damazio[30], J.L. Oliver[1], R. Omar[67], Y. Onoda[139], A. Onofre[131a,131e,aj], P.U.E. Onyisi[11], M.J. Oreglia[39], D. Orestano[76a,76b], R. Orlandini[76a,76b], R.S. Orr[158], L.M. Osojnak[41], Y. Osumi[111], G. Otero y Garzón[31], H. Otono[88], M. Ouchrif[36d], F. Ould-Saada[126], T. Ovsiannikova[140], M. Owen[58], R.E. Owen[135], S.A. Oyeniran[114], V.E. Ozcan[22a], F. Ozturk[86], N. Ozturk[8], S. Ozturk[80], H.A. Pacey[127], K. Pachal[159a], A. Pacheco Pages[13], C. Padilla Aranda[13], G. Padovano[74a,74b], S. Pagan Griso[18a], L. Pagani[75a,75b], J. Pampel[25], D.K. Panchal[11], C.E. Pandini[59], J.G. Panduro Vazquez[135], H.D. Pandya[1], H. Pang[136], P. Pani[47], G. Panizzo[68a,68c], L. Panwar[128,ak], L. Paolozzi[21], S. Parajuli[164], A. Paramonov[6], C. Paraskevopoulos[52], D. Paredes Hernandez[63b], S.R. Paredes Saenz[51], A. Pareti[72a,72b], K.R. Park[41], T.H. Park[110], F. Parodi[56b,56a], J.A. Parsons[41], U. Parzefall[53], B.A. Paschen[18a], B. Pascual Dias[40], L. Pascual Dominguez[99], E. Pasqualucci[74a], S. Passaggio[56b], F. Pastore[95], P. Patel[86], U.M. Patel[50], J.R. Pater[101], T. Pauly[37], A. Paunovic[16], F. Pauwels[134], C.I. Pazos[161], M. Pedersen[126], R. Pedro[131a], O. Penc[132], C.C. Penelaud[128], S. Peng[15], G. D. Penn[174], B.S. Peralva[81d], A.P. Pereira Peixoto[140], L. Pereira Sanchez[146], D.V. Perepelitsa[30,ah], G. Perera[103], E. Perez Codina[37], M. Perganti[10], H. Pernegger[37], S. Perrella[74a,74b], K. Peters[47], R.F.Y. Peters[101], B.A. Petersen[37], T.C. Petersen[42], E. Petit[102], V. Petousis[133], A. R. Petri[70a,70b], T. Petru[134], M. Pettee[18a], A. Petukhov[80], K. Petukhova[37], R. Pezoa[138g], L. Pezzotti[24b,24a], G. Pezzullo[174], L. Pfaffenbichler[37], A. J. Pfleger[78], T. Pham[105], T.M. Pham[172], P.W. Phillips[135], G. Piacquadio[148], E. Pianori[18a], F. Piazza[124], R. Piegaia[31], D. Pietreanu[28b], A.D. Pilkington[101], T. Pilusa[34j], M. Pinamonti[68a,68c], J.L. Pinfold[2], G. Pinheiro Matos[41], B.C. Pinheiro Pereira[131a], J. Pinol Bel[13], A. E. Pinto Pinoargote[128], L. Pintucci[68a,68c], K. M. Piper[149], A. Pirttikoski[55], D.A. Pizzi[35], L. Pizzimento[63b], A. Plebani[33], M.-A. Pleier[30], V. Pleskot[134], E. Plotnikova[38], G. Poddar[94], R. Poettgen[98], L. Poggioli[128], S. Polacek[134], G. Polesello[72a], A. Poley[145], A. Polini[24b], C.S. Pollard[169], Z.B. Pollock[120], E. Pompa Pacchi[121], N. I. Pond[96], D. Ponomarenko[67], L. Pontecorvo[37], S. Popa[28a], G.A. Popeneciu[28d], A. Poreba[37], D.M. Portillo Quintero[159a], S. Pospisil[133], M. A. Postill[142], P. Postolache[28c], K. Potamianos[169], P.A. Potepa[85a], I.N. Potrap[38], C.J. Potter[33], H. Potti[150], J. Poveda[165], M.E. Pozo Astigarraga[37], R. Pozzi[37], A. Prades Ibanez[75a,75b], S.R. Pradhan[142], J. Pretel[167], D. Price[101], M. Primavera[69a], L. Primomo[68a,68c], M.A. Principe Martin[99], R. Privara[123], T. Procter[85b], M.L. Proffitt[140], N. Proklova[129], K. Prokofiev[63c], G. Proto[110], J. Proudfoot[6], M. Przybycien[85a], W.W. Przygoda[85b], A. Psallidas[45], D. Pudzha[52], P. Puhl[57], H. I. Purnell[1],

JHEP07(2026)078

D. Pyatiizbyantseva[115], J. Qian[106], R. Qian[107], D. Qichen[127], Y. Qin[13], T. Qiu[51], A. Quadt[54], M. Queitsch-Maitland[101], G. Quetant[55], R.P. Quinn[166], D. Rafanoharana[110], J.L. Rainbolt[39], S. Rajagopalan[30], E. Ramakoti[38], L. Rambelli[56b,56a], I.A. Ramirez-Berend[35], K. Ran[106,112c], S. D. Randles[92], D. S. Rankin[129], N.P. Rapheeha[34j], H. Rasheed[28b], A. Rastogi[18a], S. Rave[100], S. Ravera[56b,56a], B. Ravina[37], I. Ravinovich[171], M. Raymond[37], A.L. Read[126], N.P. Readioff[142], D.M. Rebuzzi[72a,72b], A. S. Reed[58], K. Reeves[27], D. Reikher[37], A. Rej[48], C. Rembser[37], H. Ren[61], M. Renda[28b], F. Renner[47], A.G. Rennie[58], M. Repik[55], A.L. Rescia[56b,56a], S. Resconi[70a], M. Ressegotti[56b], S. Rettie[116], W.F. Rettie[35], M. M. Revering[33], O.L. Rezanova[38], P. Reznicek[134], H. Riani[36d], N. Ribaric[50], B. Ricci[68a,68c], E. Ricci[77a,77b], R. Richter[110], E. Richter-Was[85b], M. Ridel[128], S. Ridouani[36d], P. Riedler[37], E.M. Riefel[46a,46b], J. O. Rieger[116], M. Rimoldi[34c], L. Rinaldi[24b,24a], P. Rincke[163,54], G. Ripellino[163], I. Riu[13], J.C. Rivera Vergara[167], F. Rizatdinova[122], E. Rizvi[94], B.R. Roberts[39], S.S. Roberts[137], D. Robinson[33], A. Robson[58], A. Rocchi[75a,75b], C. Roda[73a,73b], F.A. Rodriguez[117], S. Rodriguez Bosca[37], Y. Rodriguez Garcia[23a], A.M. Rodríguez Vera[117], S. Roe[37], J.T. Roemer[37], O. Røhne[126], R.A. Rojas[37], Z. Rokavec[93], C.P.A. Roland[128], A. Romaniouk[78], E. Romano[72a,72b], M. Romano[24b], N. Rompotis[92], L. Roos[128], S. Rosati[74a], L. Roscher[47], B.J. Rosser[39], E. Rossi[127], E. Rossi[71a,71b], L.P. Rossi[60], L. Rossini[53], R. Rosten[120], M. Rotaru[28b], R. Roth[37], D. Rousseau[65], D. Rousso[47], S. Roy-Garand[55], A. Rozanov[102], Z. M. A. Rozario[58], Y. Rozen[153], A. Rubio Jimenez[165], V.H. Ruelas Rivera[19], T.A. Ruggeri[1], A. Ruggiero[127], A. Ruiz-Martinez[165], A. Rummler[37], G.B. Rupnik Boero[37], N.A. Rusakovich[38], S. Ruscelli[48], H.L. Russell[167], G. Russo[137], J.P. Rutherfoord[7], S. Rutherford Colmenares[118], M. Rybar[134], P. Rybczynski[85a], A. Ryzhov[44], F. Safai Tehrani[74a], S. Saha[1], B. Sahoo[171], B. T. Saifuddin[121], M. Saimpert[136], I. Sainz Saenz Diez[62a], G.T. Saito[81c], M. Saito[156], T. Saito[156], A. Sala[70a,70b], O. T. Salin[65], A. Salnikov[146], J. Salt[165], A. Salvador Salas[154], F. Salvatore[149], A. Salzburger[37], D. Sammel[53], E. Sampson[91], D. Sampsonidis[155,ab], D. Sampsonidou[124], M.A.A. Samy[58], J. Sánchez[165], V. Sanchez Sebastian[165], H. Sandaker[126], C.O. Sander[47], J.A. Sandesara[172], M. Sandhoff[173], C. Sandoval[23b], L. Sanfilippo[62a], D.P.C. Sankey[135], T. Sano[87], A. Sansar[22c], A. Sansoni[52], M. Santana Queiroz[18b], L. Santi[37], C. Santoni[40], H. Santos[131a,131b], L. Santos Pereira Trigo[47], E. Sanzani[24b,24a], K.A. Saoucha[83d], J.G. Saraiva[131a,131d], J. Sardain[7], S. Sarkar[50], O. Sasaki[82], K. Sato[160], C. Sauer[37], E. Sauvan[4], P. Savard[158,s], R. Sawada[156], C. Sawyer[135], L. Sawyer[97], A. M. Sayed[27], C. Sbarra[24b], A. Sbrizzi[24b,24a], R. Scaglioni[72a,72b], T. Scanlon[96], J. Schaarschmidt[140], U. Schäfer[100], A.C. Schaffer[65,44], D. Schaile[109], R.D. Schamberger[148], C. Scharf[19], M.M. Schefer[20], D. Scheirich[134], M. Schernau[138f], C. Scheulen[55], C. Schiavi[56b,56a], M. Schioppa[43b,43a], S. Schlenker[37], T. Schlomer[54], J. Schmeing[173], C. R. Schmidt[49], E. Schmidt[110], M. A. Schmidt[173], K. Schmieden[25], C. Schmitt[100], N. Schmitt[100], S. Schmitt[47], N.A. Schneider[109], L. Schoeffel[136], A. Schoening[62b], P.G. Scholer[35], E. Schopf[144], M. Schott[25], S. Schramm[55], T. Schroer[55], H-C. Schultz-Coulon[62a], M. Schumacher[53], B.A. Schumm[137], Ph. Schune[136], H.R. Schwartz[7], A. Schwartzman[146], T.A. Schwarz[106], Ph. Schwemling[136], R. Schwienhorst[107], F.G. Sciacca[20], A. Sciandra[30],

JHEP07(2026)078

G. Sciolla[27], S. A. Scoville[130], F. Scuri[73a], C.D. Sebastiani[37], K. Sedlaczek[117], A. Sehrawat[138b], S.C. Seidel[114], B.D. Seidlitz[41], C. Seitz[47], J.M. Seixas[81b], G. Sekhniaidze[71a], L. Selem[128], N. Semprini-Cesari[24b,24a], A. Semushin[175], V. Senthilkumar[116], L. Serin[65], M. Sessa[71a,71b], H. Severini[121], F. Sforza[56b,56a], A. Sfyrla[55], Q. Sha[14], H. Shaddix[117], A.H. Shah[33], R. Shaheen[147], J.D. Shahinian[129], M. Shamim[37], L.Y. Shan[14], M. Shapiro[18a], A. Sharma[37], A.S. Sharma[166], P. Sharma[30], K. Shaw[149], S.M. Shaw[101], D. Shemyakin[171], Q. Shen[14], D.J. Sheppard[145], P. Sherwood[96], L. Shi[112b], X. Shi[14], S. Shimizu[82], S. Shirabe[88], M. Shiyakova[38,al], M.J. Shochet[39], D.R. Shope[126], B. Shrestha[121], S. Shrestha[120,am], I. Shreyber[38], M.J. Shroff[104], P. Sicho[132], A.M. Sickles[164], E. Sideras Haddad[34j], A. C. Sidley[116], A. Sidoti[24b], F. Siegert[49], Dj. Sijacki[16], F. Sili[61], J.M. Silva[51], I. Silva Ferreira[81b], M.V. Silva Oliveira[30], S.B. Silverstein[46a], S. Simion[65], R. Simoniello[37], E.L. Simpson[101], H. Simpson[149], L.R. Simpson[6], S. Simsek[80], S. Sindhu[54], S. Singh[30], S. N. Singh[27], S. Sinha[47], S. Sinha[101], M. Sioli[24b,24a], K. Sioulas[9], I. Siral[37], E. Sitnikova[47], J. Sjölin[46a,46b], A. Skaf[54], E. Skorda[21], P. Skubic[121], M. Slawinska[86], I. Slazyk[17], I. Sliusar[126], V. Smakhtin[171], B.H. Smart[135], S.Yu. Smirnov[138b], Y. Smirnov[34c], O. Smirnova[98], J.L. Smith[101], M. B. Smith[35], R. Smith[146], H. Smitmanns[100], M. Smizanska[91], K. Smolek[133], P. Smolyanskiy[133], A.A. Snesarev[38], H.L. Snoek[116], R. M. Snyder[50], S. Snyder[30], R. Sobie[167,n], A. Soffer[154], C.A. Solans Sanchez[37], E.Yu. Soldatov[38], U. Soldevila[165], A.A. Solodkov[34j], S. Solomon[27], A. Soloshenko[38], O.V. Solovyanov[40], P. Sommer[49], A. Sopczak[133], A.L. Sopio[51], F. Sopkova[29b], J. D. Sorenson[114], I.R. Sotarriva Alvarez[139], V. Sothilingam[62a], O. J. Soto Sandoval[138c,138b], S. Sottocornola[67], R. Soualah[83a], D. South[47], N. Soybelman[171], S. Spagnolo[69a,69b], A.S. Spellman[124], D. Sperlich[53], B. Spisso[71a,71b], L. Splendori[102], M. Spousta[134], E.J. Staats[35], R. Stamen[62a], E. Stanecka[86], W. Stanek-Maslouska[47], M.V. Stange[49], B. Stanislaus[18a], M.M. Stanitzki[47], G.H. Stark[137], J. Stark[89], P. Staroba[132], P. Starovoitov[83d], R. Staszewski[86], C. Stauch[109], G. Stavropoulos[45], A. Stefl[37], A. Stein[100], P. Steinberg[30], B. Stelzer[145,159a], H.J. Stelzer[130], O. Stelzer[159a], H. Stenzel[57], T.J. Stevenson[149], G.A. Stewart[47], G. Stoicea[28b], M. Stolarski[131a], S. Stonjek[110], A. Straessner[49], J. Strandberg[147], S. Strandberg[46a,46b], M. Stratmann[173], M. Strauss[121], T. Strebler[102], P. Strizenec[29b], R. Ströhmer[168], D.M. Strom[124], R. Stroynowski[44], A. Strubig[46a,46b], S.A. Stucci[30], B. Stugu[17], J. Stupak[121], N.A. Styles[47], D. Su[146], S. Su[61], X. Su[61], D. Suchy[29a], A. D. Sudhakar Ponnu[54], L. Sudit[171], Y. Sue[82], K. Sugizaki[129], D.M.S. Sultan[127], L. Sultanaliyeva[25], S. Sultansoy[3b], S. Sun[172], W. Sun[14], S. Sundar Raman[166], N. Sur[98], J.P. Surdutovich[120], N. Suri Jr[174], M.R. Sutton[149], M. Svatos[132], P. N. Swallow[33], S.N. Swatman[37], M. Swiatlowski[159a], A. Swoboda[37], I. Sykora[29a], M. Sykora[134], T. Sykora[134], D. Ta[100], K. Tackmann[47,an], A. Taffard[162], R. Tafirout[159a], Y. Takubo[82], M. Talby[102], N.M. Tamir[154], A. Tanaka[156], J. Tanaka[156], R. Tanaka[65], M. Tanasini[148], Z. Tao[166], S. Tapia Araya[138g], S. Tapprogge[100], A. Tarek Abouelfadl Mohamed[37], S. Tarem[153], K. Tariq[14], G. Tarna[37], G.F. Tartarelli[70a], M. J. Tartarin[141b], P. Tas[134], M. Tasevsky[132], E. Tassi[43b,43a], A.C. Tate[164], Y. Tayalati[36e,ao], G.N. Taylor[105], W. Taylor[159b], R.J. Taylor Vara[165], A.S. Tegetmeier[89], P. Teixeira-Dias[95], J.J. Teoh[158], K. Terashi[156],

JHEP07(2026)078

J. Terron[99], S. Terzo[13], M. Testa[52], R.J. Teuscher[158,n], A. Thaler[78], T. Theveneaux-Pelzer[102], J.P. Thomas[21], E.A. Thompson[18a], P.D. Thompson[21], E. Thomson[129], R. E. Thornberry[30], T.M. Thory-Rao[21], C.N. Thotamuna Wijewardhana[148], C. Tian[61], Y. Tian[55], V. Tikhomirov[80], Yu.A. Tikhonov[38], D. Timoshyn[134], E.X.L. Ting[1], P. Tipton[174], A. Tishelman-Charny[30], K. Todome[139], S. Todorova-Nova[134], L. Toffolin[68a,68c], M. Togawa[82], J. Tojo[88], S. Tokár[29a], O. Toldaiev[67], G. Tolkachev[102], M. Tomoto[82], L. Tompkins[146], E. Torrence[124], H. Torres[89], D. I. Torres Arza[138g], E. Torres Reoyo[165], E. Torró Pastor[165], M. Toscani[31], C. Tosciri[39], M. Tost[11], D.R. Tovey[142], T. Trefzger[168], P.M. Tricarico[13], A. Tricoli[30], I.M. Trigger[159a], S. Trincaz-Duvoid[128], D.A. Trischuk[167], A. Tropina[38], D. Truncali[75a,75b], L. Truong[34c], M. Trzebinski[86], A. Trzupek[86], F. Tsai[148], A. Tsiamis[155], P.V. Tsiareshka[38], S. Tsigaridas[159a], A. Tsirigotis[155,ac], V. Tsiskaridze[152a], E.G. Tskhadadze[152a], H. F. Tsoi[129], Y. Tsujikawa[87], V. Tsulaia[18a], K. Tsuri[119], D. Tsybychev[148], Y. Tu[63b], A. Tudorache[28b], V. Tudorache[28b], S. B. Tuncay[127], S. Turchikhin[56b,56a], I. Turk Cakir[3a], R. Turra[70a], T. Turtuvshin[38,ap], P.M. Tuts[41], Y. Uematsu[82], F. Ukegawa[160], P.A. Ulloa Poblete[138c,138b], G. Unal[37], A. Undrus[30], J. Urban[29b], P. Urrejola[138e], G. Usai[8], R. Ushioda[157], M. Usman[108], F. Ustuner[51], Z. Uysal[80], V. Vacek[133], B. Vachon[104], T. Vafeiadis[37], A. Vaitkus[96], C. Valderanis[109], E. Valdes Santurio[46a,46b], M. Valente[37], S. Valentinetti[24b,24a], A. Valero[165], E. Valiente Moreno[165], A. Vallier[89], J.A. Valls Ferrer[165], D. R. Van Arneman[116], R. Van Den Broucke[128], A. Van Der Graaf[48], H. Z. Van Der Schyf[34j], P. Van Gemmeren[6], M. Van Rijnbach[37], S. Van Stroud[96], I. Van Vulpen[116], P. Vana[134], M. Vanadia[75a,75b], U. M. Vande Voorde[147], W. Vandelli[37], E.R. Vandewall[146], D. Vannicola[154], R. Vari[74a], M. Varma[174], E.W. Varnes[7], C. Varni[85a], D. Varouchas[65], L. Varriale[165], K.E. Varvell[150], M.E. Vasile[28b], A. Vasileiadou[9], L. Vaslin[82], M. D. Vassilev[146], A. Vasyukov[38], L. M. Vaughan[122], R. Vavricka[134], T. Vazquez Schroeder[13], J. Veatch[32], V. Vecchio[101], M.J. Veen[103], I. Veliscek[30], I. Velkovska[93], L.M. Veloce[158], F. Veloso[131a,131c], A.G. Veltman[51], S.H. Venetianer[161], S. Veneziano[74a], A. Ventura[69a,69b], A. Verbytskyi[110], M. Verducci[73a,73b], C. Vergis[94], M. Verissimo De Araujo[81b], W. Verkerke[116], J.C. Vermeulen[116], C. Vernieri[146], M. Vessella[162], M.C. Vetterli[145,s], A. Vgenopoulos[100], N. Viaux Maira[138g,aq], L. Vicenik[133], T. Vickey[142], O.E. Vickey Boeriu[142], G.H.A. Viehhauser[127], L. Vigani[62b], M. Vigl[110], M. Villa[24b,24a], M. Villaplana Perez[165], E.M. Villhauer[39], E. Vilucchi[52], M. Vincent[165], M.G. Vincter[35], A. Visibile[116], A. Visive[116], C. Vittori[161], I. Vivarelli[24b,24a], M.I. Vivas Albornoz[47], E. Voevodina[110], F. Vogel[109], J.C. Voigt[49], P. Vokac[133], Yu. Volkotrub[85b], L. Vomberg[25], E. Von Toerne[25], B. Vormwald[37], K. Vorobev[50], M. Vos[165], K. Voss[144], M. Vozak[37], L. Vozdecky[121], N. Vranjes[16], M. Vranjes Milosavljevic[16], M. Vreeswijk[116], N.K. Vu[112a], R. Vuillermet[37], O. Vujinovic[100], I. Vukotic[39], I. K. Vyas[35], J.F. Wack[33], A. Wada[111], S. Wada[160], C. Wagner[146], J.M. Wagner[18a], W. Wagner[173], S. Wahdan[173], H. Wahlberg[90], C. H. Waits[121], J. Walder[135], R. Walker[109], K. Walkingshaw Pass[58], W. Walkowiak[144], A. Wall[129], E.J. Wallin[98], T. Wamorkar[146], K. Wandall-Christensen[165], A. Wang[61], A.Z. Wang[137], C. Wang[47], C. Wang[11], H. Wang[18a], J. Wang[63c], P. Wang[101], P. Wang[96], R. Wang[60], R. Wang[106], R. Wang[6], S. Wang[14], S.M. Wang[151], T. Wang[115],

JHEP07(2026)078

T. Wang[61], W. Wang[113c], W.T. Wang[127], X. Wang[164], X. Wang[141a], X. Wang[47], Y. Wang[148], Y. Wang[114], Z. Wang[106], Z. Wang[14], Z. Wang[63b], C. Wanotayaroj[82], A. Warburton[104], A.L. Warnerbring[144], S. Waterhouse[96], A.T. Watson[21], H. Watson[51], M.F. Watson[21], E. Watton[37], G. Watts[140], B.M. Waugh[96], J. M. Webb[53], C. Weber[30], M.S. Weber[20], C. Wei[61], Y. Wei[53], A.R. Weidberg[127], E.J. Weik[118], J. Weingarten[48], C. Weiser[53], C.J. Wells[47], P.S. Wells[37], T. Wenaus[30], T. Wengler[37], N.S. Wenke[110], N. Wermes[25], D. Werner[47], M. Wessels[62a], A.M. Wharton[91], A. White[8], A.S. White[37], M.J. White[1], D. Whiteson[162], L. Wickremasinghe[125], W. Wiedenmann[172], M. Wielers[135], R. Wierda[147], C. Wiglesworth[42], H.G. Wilkens[37], J. J. H. Wilkinson[33], S. Williams[33], S. Willocq[103], D.J. Wilson[101], P.J. Windischhofer[39], F.I. Winkel[31], F. Winklmeier[124], B.T. Winter[53], M. Wittgen[146], M. Wobisch[97], T. Wojtkowski[59], Z. Wolffs[116], J. Wollrath[37], M.W. Wolter[86], H. Wolters[131a,131c], M.C. Wong[137], E.L. Woodward[41], S.D. Worm[47], B.K. Wosiek[86], K. A. Wozniak[55], K.W. Woźniak[86], S. Wozniewski[54], K. Wraight[58], C. Wu[158], C. Wu[21], J. Wu[156], M. Wu[112b], M. Wu[115], S. Wu[14,ar], S.L. Wu[172], X. Wu[61], Y. Wu[61], Y.Q. Wu[158], Z. Wu[102], Z. Wu[112a], J. Wuerzinger[110], T.R. Wyatt[101], B.M. Wynne[51], S. Xella[42], L. Xia[112a], M. Xie[61], A. Xiong[124], I. Xiotidis[37], D. Xu[14], H. Xu[61], L. Xu[61], R. Xu[129], T. Xu[106], W. Xu[112a], Y. Xu[140], Z. Xu[51], R. Xue[130], B. Yabsley[150], S. Yacoob[11], Y. Yamaguchi[82], E. Yamashita[156], H. Yamauchi[160], T. Yamazaki[18a], Y. Yamazaki[84], S. Yan[58], Z. Yan[103], C. Yang[18a], H.J. Yang[141a], H.T. Yang[61], S. Yang[61], X. Yang[37], X. Yang[14], Y. Yang[156], Y. Yang[61], W-M. Yao[18a], C. L. Yardley[149], J. Ye[14], S. Ye[30], X. Ye[61], I. Yeletskikh[38], B. Yeo[18b], M.R. Yexley[96], T. P. Yildirim[127], K. Yorita[170], C. Young[146], C.J.S. Young[37], I.N.L. Young[58], N.D. Young[124], Y. Yu[61], J. Yuan[14,112c,ar], M. Yuan[106], R. Yuan[141b], L. Yue[96], M. Zaazoua[61], B. Zabinski[86], I. Zahir[36a], Q.U.A. Zahoor[51], A. Zaio[56b,56a], Z.K. Zak[86], T. Zakareishvili[165], S. Zambito[55], J. Zang[156], R. Zanzottera[70a,70b], O. Zaplatilek[133], E. Zaya[147], C. Zeitnitz[173], H. Zeng[14], D.T. Zenger Jr[27], T. Ženiš[29a], S. Zenz[94], D. Zerwas[65], W. Zhan[61], B. Zhang[169], D.F. Zhang[142], G. Zhang[14,ar], J. Zhang[113b], J. Zhang[6], L. Zhang[61], L. Zhang[112a], P. Zhang[14,112c], R. Zhang[112a], S. Zhang[36e], Y. Zhang[140], Y. Zhang[96], Y. Zhang[61], Y. Zhang[112a], Z. Zhang[18a], Z. Zhang[113b], Z. Zhang[65], H. Zhao[140], T. Zhao[113b], Y. Zhao[35], Z. Zhao[61], Z. Zhao[61], A. Zhemchugov[38], J. Zheng[112a], K. Zheng[164], L. Zheng[113b], X. Zheng[61], Z. Zheng[146], D. Zhong[164], B. Zhou[106], B. Zhou[141b,141a], N. Zhou[141a], Y. Zhou[15], Y. Zhou[112a], Y. Zhou[7], Z. Zhou[61], J. Zhu[106], X. Zhu[141b], Y. Zhu[141a], X. Zhuang[14], K. Zhukov[67], P. Ziakas[4], N.I. Zimine[38], J. Zinsser[62b], M. Ziolkowski[144], L. Živković[16], A. Zoccoli[24b,24a], K. Zoch[37], A. Zografos[37], T.G. Zorbas[142], L. Zwalinski[37]

[1] *Department of Physics, University of Adelaide, Adelaide, Australia*
[2] *Department of Physics, University of Alberta, Edmonton AB, Canada*
[3a] *Department of Physics, Ankara University, Ankara, Türkiye*
[3b] *Division of Physics, TOBB University of Economics and Technology, Ankara, Türkiye*
[4] *LAPP, Université Savoie Mont Blanc, CNRS/IN2P3, Annecy, France*
[5] *APC, Université Paris Cité, CNRS/IN2P3, Paris, France*
[6] *High Energy Physics Division, Argonne National Laboratory, Argonne IL, U.S.A.*
[7] *Department of Physics, University of Arizona, Tucson AZ, U.S.A.*
[8] *Department of Physics, University of Texas at Arlington, Arlington TX, U.S.A.*

JHEP07(2026)078

[9] Physics Department, National and Kapodistrian University of Athens, Athens, Greece
[10] Physics Department, National Technical University of Athens, Zografou, Greece
[11] Department of Physics, University of Texas at Austin, Austin TX, U.S.A.
[12] Institute of Physics, Azerbaijan Academy of Sciences, Baku, Azerbaijan
[13] Institut de Física d'Altes Energies (IFAE), Barcelona Institute of Science and Technology, Barcelona, Spain
[14] Institute of High Energy Physics, Chinese Academy of Sciences, Beijing, China
[15] Physics Department, Tsinghua University, Beijing, China
[16] Institute of Physics, University of Belgrade, Belgrade, Serbia
[17] Department for Physics and Technology, University of Bergen, Bergen, Norway
[18a] Physics Division, Lawrence Berkeley National Laboratory, Berkeley CA, U.S.A.
[18b] University of California, Berkeley CA, U.S.A.
[19] Institut für Physik, Humboldt Universität zu Berlin, Berlin, Germany
[20] Albert Einstein Center for Fundamental Physics and Laboratory for High Energy Physics, University of Bern, Bern, Switzerland
[21] School of Physics and Astronomy, University of Birmingham, Birmingham, U.K.
[22a] Department of Physics, Bogazici University, Istanbul, Türkiye
[22b] Department of Physics Engineering, Gaziantep University, Gaziantep, Türkiye
[22c] Department of Physics, Istanbul University, Istanbul, Türkiye
[23a] Facultad de Ciencias y Centro de Investigaciónes, Universidad Antonio Nariño, Bogotá, Colombia
[23b] Departamento de Física, Universidad Nacional de Colombia, Bogotá, Colombia
[24a] Dipartimento di Fisica e Astronomia A. Righi, Università di Bologna, Bologna, Italy
[24b] INFN Sezione di Bologna, Italy
[25] Physikalisches Institut, Universität Bonn, Bonn, Germany
[26] Department of Physics, Boston University, Boston MA, U.S.A.
[27] Department of Physics, Brandeis University, Waltham MA, U.S.A.
[28a] Transilvania University of Brasov, Brasov, Romania
[28b] Horia Hulubei National Institute of Physics and Nuclear Engineering, Bucharest, Romania
[28c] Department of Physics, Alexandru Ioan Cuza University of Iasi, Iasi, Romania
[28d] National Institute for Research and Development of Isotopic and Molecular Technologies, Physics Department, Cluj-Napoca, Romania
[28e] National University of Science and Technology Politechnica, Bucharest, Romania
[28f] West University in Timisoara, Timisoara, Romania
[28g] Faculty of Physics, University of Bucharest, Bucharest, Romania
[29a] Faculty of Mathematics, Physics and Informatics, Comenius University, Bratislava, Slovak Republic
[29b] Department of Subnuclear Physics, Institute of Experimental Physics of the Slovak Academy of Sciences, Kosice, Slovak Republic
[30] Physics Department, Brookhaven National Laboratory, Upton NY, U.S.A.
[31] Universidad de Buenos Aires, Facultad de Ciencias Exactas y Naturales, Departamento de Física, y CONICET, Instituto de Física de Buenos Aires (IFIBA), Buenos Aires, Argentina
[32] California State University, CA, U.S.A.
[33] Cavendish Laboratory, University of Cambridge, Cambridge, U.K.
[34a] Department of Physics, University of Cape Town, Cape Town, South Africa
[34b] iThemba Labs, Western Cape, South Africa
[34c] Department of Mechanical Engineering Science, University of Johannesburg, Johannesburg, South Africa
[34d] National Institute of Physics, University of the Philippines Diliman (Philippines), Philippines
[34e] Department of Physics, Stellenbosch University, Matieland, South Africa
[34f] University of KwaZulu-Natal, School of Agriculture and Science, Mathematics, Westville, South Africa
[34g] University of South Africa, Department of Physics, Pretoria, South Africa
[34h] University of Pretoria, Department of Mechanical and Aeronautical Engineering, Pretoria, South Africa
[34i] University of Zululand, KwaDlangezwa, South Africa
[34j] School of Physics, University of the Witwatersrand, Johannesburg, South Africa
[35] Department of Physics, Carleton University, Ottawa ON, Canada

JHEP07(2026)078

[36a] Faculté des Sciences Ain Chock, Université Hassan II de Casablanca, Morocco
[36b] Faculté des Sciences, Université Ibn-Tofail, Kénitra, Morocco
[36c] Faculté des Sciences Semlalia, Université Cadi Ayyad, LPHEA-Marrakech, Morocco
[36d] LPMR, Faculté des Sciences, Université Mohamed Premier, Oujda, Morocco
[36e] Faculté des sciences, Université Mohammed V, Rabat, Morocco
[36f] Institute of Applied Physics, Mohammed VI Polytechnic University, Ben Guerir, Morocco
[37] CERN, Geneva, Switzerland
[38] Affiliated with an international laboratory covered by a cooperation agreement with CERN
[39] Enrico Fermi Institute, University of Chicago, Chicago IL, U.S.A.
[40] LPC, Université Clermont Auvergne, CNRS/IN2P3, Clermont-Ferrand, France
[41] Nevis Laboratory, Columbia University, Irvington NY, U.S.A.
[42] Niels Bohr Institute, University of Copenhagen, Copenhagen, Denmark
[43a] Dipartimento di Fisica, Università della Calabria, Rende, Italy
[43b] INFN Gruppo Collegato di Cosenza, Laboratori Nazionali di Frascati, Italy
[44] Physics Department, Southern Methodist University, Dallas TX, U.S.A.
[45] National Centre for Scientific Research "Demokritos", Agia Paraskevi, Greece
[46a] Department of Physics, Stockholm University, Sweden
[46b] Oskar Klein Centre, Stockholm, Sweden
[47] Deutsches Elektronen-Synchrotron DESY, Hamburg and Zeuthen, Germany
[48] Fakultät Physik, Technische Universität Dortmund, Dortmund, Germany
[49] Institut für Kern- und Teilchenphysik, Technische Universität Dresden, Dresden, Germany
[50] Department of Physics, Duke University, Durham NC, U.S.A.
[51] SUPA — School of Physics and Astronomy, University of Edinburgh, Edinburgh, U.K.
[52] INFN e Laboratori Nazionali di Frascati, Frascati, Italy
[53] Physikalisches Institut, Albert-Ludwigs-Universität Freiburg, Freiburg, Germany
[54] II. Physikalisches Institut, Georg-August-Universität Göttingen, Göttingen, Germany
[55] Département de Physique Nucléaire et Corpusculaire, Université de Genève, Genève, Switzerland
[56a] Dipartimento di Fisica, Università di Genova, Genova, Italy
[56b] INFN Sezione di Genova, Italy
[57] II. Physikalisches Institut, Justus-Liebig-Universität Giessen, Giessen, Germany
[58] SUPA — School of Physics and Astronomy, University of Glasgow, Glasgow, U.K.
[59] LPSC, Université Grenoble Alpes, CNRS/IN2P3, Grenoble INP, Grenoble, France
[60] Laboratory for Particle Physics and Cosmology, Harvard University, Cambridge MA, U.S.A.
[61] Department of Modern Physics and State Key Laboratory of Particle Detection and Electronics, University of Science and Technology of China, Hefei, China
[62a] Kirchhoff-Institut für Physik, Ruprecht-Karls-Universität Heidelberg, Heidelberg, Germany
[62b] Physikalisches Institut, Ruprecht-Karls-Universität Heidelberg, Heidelberg, Germany
[63a] Department of Physics, Chinese University of Hong Kong, Shatin, N.T., Hong Kong, China
[63b] Department of Physics, University of Hong Kong, Hong Kong, China
[63c] Department of Physics and Institute for Advanced Study, Hong Kong University of Science and Technology, Clear Water Bay, Kowloon, Hong Kong, China
[64] Department of Physics, National Tsing Hua University, Hsinchu, Taiwan
[65] IJCLab, Université Paris-Saclay, CNRS/IN2P3, 91405, Orsay, France
[66] Centro Nacional de Microelectrónica (IMB-CNM-CSIC), Barcelona, Spain
[67] Department of Physics, Indiana University, Bloomington IN, U.S.A.
[68a] INFN Gruppo Collegato di Udine, Sezione di Trieste, Udine, Italy
[68b] ICTP, Trieste, Italy
[68c] Dipartimento Politecnico di Ingegneria e Architettura, Università di Udine, Udine, Italy
[69a] INFN Sezione di Lecce, Italy
[69b] Dipartimento di Matematica e Fisica, Università del Salento, Lecce, Italy
[70a] INFN Sezione di Milano, Italy
[70b] Dipartimento di Fisica, Università di Milano, Milano, Italy
[71a] INFN Sezione di Napoli, Italy

JHEP07(2026)078

[71b] *Dipartimento di Fisica, Università di Napoli, Napoli, Italy*
[72a] *INFN Sezione di Pavia, Italy*
[72b] *Dipartimento di Fisica, Università di Pavia, Pavia, Italy*
[73a] *INFN Sezione di Pisa, Italy*
[73b] *Dipartimento di Fisica E. Fermi, Università di Pisa, Pisa, Italy*
[74a] *INFN Sezione di Roma, Italy*
[74b] *Dipartimento di Fisica, Sapienza Università di Roma, Roma, Italy*
[75a] *INFN Sezione di Roma Tor Vergata, Italy*
[75b] *Dipartimento di Fisica, Università di Roma Tor Vergata, Roma, Italy*
[76a] *INFN Sezione di Roma Tre, Italy*
[76b] *Dipartimento di Matematica e Fisica, Università Roma Tre, Roma, Italy*
[77a] *INFN-TIFPA, Italy*
[77b] *Università degli Studi di Trento, Trento, Italy*
[78] *Universität Innsbruck, Department of Astro and Particle Physics, Innsbruck, Austria*
[79] *Department of Physics and Astronomy, Iowa State University, Ames IA, U.S.A.*
[80] *Istinye University, Sariyer, Istanbul, Türkiye*
[81a] *Departamento de Engenharia Elétrica, Universidade Federal de Juiz de Fora (UFJF), Juiz de Fora, Brazil*
[81b] *Universidade Federal do Rio De Janeiro COPPE/EE/IF, Rio de Janeiro, Brazil*
[81c] *Instituto de Física, Universidade de São Paulo, São Paulo, Brazil*
[81d] *Rio de Janeiro State University, Rio de Janeiro, Brazil*
[81e] *Federal University of Bahia, Bahia, Brazil*
[82] *KEK, High Energy Accelerator Research Organization, Tsukuba, Japan*
[83a] *Khalifa University of Science and Technology, Abu Dhabi, United Arab Emirates*
[83b] *New York University Abu Dhabi, Abu Dhabi, United Arab Emirates*
[83c] *United Arab Emirates University, Al Ain, United Arab Emirates*
[83d] *University of Sharjah, Sharjah, United Arab Emirates*
[84] *Graduate School of Science, Kobe University, Kobe, Japan*
[85a] *AGH University of Krakow, Faculty of Physics and Applied Computer Science, Krakow, Poland*
[85b] *Marian Smoluchowski Institute of Physics, Jagiellonian University, Krakow, Poland*
[86] *Institute of Nuclear Physics Polish Academy of Sciences, Krakow, Poland*
[87] *Faculty of Science, Kyoto University, Kyoto, Japan*
[88] *Research Center for Advanced Particle Physics and Department of Physics, Kyushu University, Fukuoka, Japan*
[89] *L2IT, Université de Toulouse, CNRS/IN2P3, UPS, Toulouse, France*
[90] *Instituto de Física La Plata, Universidad Nacional de La Plata and CONICET, La Plata, Argentina*
[91] *Physics Department, Lancaster University, Lancaster, U.K.*
[92] *Oliver Lodge Laboratory, University of Liverpool, Liverpool, U.K.*
[93] *Department of Experimental Particle Physics, Jožef Stefan Institute and Department of Physics, University of Ljubljana, Ljubljana, Slovenia*
[94] *Department of Physics and Astronomy, Queen Mary University of London, London, U.K.*
[95] *Department of Physics, Royal Holloway University of London, Egham, U.K.*
[96] *Department of Physics and Astronomy, University College London, London, U.K.*
[97] *Louisiana Tech University, Ruston LA, U.S.A.*
[98] *Fysiska institutionen, Lunds universitet, Lund, Sweden*
[99] *Departamento de Física Teorica C-15 and CIAFF, Universidad Autónoma de Madrid, Madrid, Spain*
[100] *Institut für Physik, Universität Mainz, Mainz, Germany*
[101] *School of Physics and Astronomy, University of Manchester, Manchester, U.K.*
[102] *CPPM, Aix-Marseille Université, CNRS/IN2P3, Marseille, France*
[103] *Department of Physics, University of Massachusetts, Amherst MA, U.S.A.*
[104] *Department of Physics, McGill University, Montreal QC, Canada*
[105] *School of Physics, University of Melbourne, Victoria, Australia*
[106] *Department of Physics, University of Michigan, Ann Arbor MI, U.S.A.*
[107] *Department of Physics and Astronomy, Michigan State University, East Lansing MI, U.S.A.*

JHEP07(2026)078

[108] Group of Particle Physics, University of Montreal, Montreal QC, Canada
[109] Fakultät für Physik, Ludwig-Maximilians-Universität München, München, Germany
[110] Max-Planck-Institut für Physik (Werner-Heisenberg-Institut), München, Germany
[111] Graduate School of Science and Kobayashi-Maskawa Institute, Nagoya University, Nagoya, Japan
[112a] Department of Physics, Nanjing University, Nanjing, China
[112b] School of Science, Shenzhen Campus of Sun Yat-sen University, China
[112c] University of Chinese Academy of Science (UCAS), Beijing, China
[113a] School of Physics, Nankai University, Tianjin, China
[113b] Institute of Frontier and Interdisciplinary Science and Key Laboratory of Particle Physics and Particle Irradiation (MOE), Shandong University, Qingdao, China
[113c] School of Physics, Zhengzhou University, China
[114] Department of Physics and Astronomy, University of New Mexico, Albuquerque NM, U.S.A.
[115] Institute for Mathematics, Astrophysics and Particle Physics, Radboud University/Nikhef, Nijmegen, Netherlands
[116] Nikhef National Institute for Subatomic Physics and University of Amsterdam, Amsterdam, Netherlands
[117] Department of Physics, Northern Illinois University, DeKalb IL, U.S.A.
[118] Department of Physics, New York University, New York NY, U.S.A.
[119] Ochanomizu University, Otsuka, Bunkyo-ku, Tokyo, Japan
[120] Ohio State University, Columbus OH, U.S.A.
[121] Homer L. Dodge Department of Physics and Astronomy, University of Oklahoma, Norman OK, U.S.A.
[122] Department of Physics, Oklahoma State University, Stillwater OK, U.S.A.
[123] Palacký University, Joint Laboratory of Optics, Olomouc, Czech Republic
[124] Institute for Fundamental Science, University of Oregon, Eugene, OR, U.S.A.
[125] Graduate School of Science, University of Osaka, Osaka, Japan
[126] Department of Physics, University of Oslo, Oslo, Norway
[127] Department of Physics, Oxford University, Oxford, U.K.
[128] LPNHE, Sorbonne Université, Université Paris Cité, CNRS/IN2P3, Paris, France
[129] Department of Physics, University of Pennsylvania, Philadelphia PA, U.S.A.
[130] Department of Physics and Astronomy, University of Pittsburgh, Pittsburgh PA, U.S.A.
[131a] Laboratório de Instrumentação e Física Experimental de Partículas — LIP, Lisboa, Portugal
[131b] Departamento de Física, Faculdade de Ciências, Universidade de Lisboa, Lisboa, Portugal
[131c] Departamento de Física, Universidade de Coimbra, Coimbra, Portugal
[131d] Centro de Física Nuclear da Universidade de Lisboa, Lisboa, Portugal
[131e] Departamento de Física, Escola de Ciências, Universidade do Minho, Braga, Portugal
[131f] Departamento de Física Teórica y del Cosmos, Universidad de Granada, Granada (Spain), Spain
[131g] Departamento de Física, Instituto Superior Técnico, Universidade de Lisboa, Lisboa, Portugal
[132] Institute of Physics of the Czech Academy of Sciences, Prague, Czech Republic
[133] Czech Technical University in Prague, Prague, Czech Republic
[134] Charles University, Faculty of Mathematics and Physics, Prague, Czech Republic
[135] Particle Physics Department, Rutherford Appleton Laboratory, Didcot, U.K.
[136] IRFU, CEA, Université Paris-Saclay, Gif-sur-Yvette, France
[137] Santa Cruz Institute for Particle Physics, University of California Santa Cruz, Santa Cruz CA, U.S.A.
[138a] Departamento de Física, Pontificia Universidad Católica de Chile, Santiago, Chile
[138b] Millennium Institute for Subatomic physics at high energy frontier (SAPHIR), Santiago, Chile
[138c] Instituto de Investigación Multidisciplinario en Ciencia y Tecnología, y Departamento de Física, Universidad de La Serena, Chile
[138d] Universidad Andres Bello, Department of Physics, Santiago, Chile
[138e] Universidad San Sebastian, Recoleta, Chile
[138f] Instituto de Alta Investigación, Universidad de Tarapacá, Arica, Chile
[138g] Departamento de Física, Universidad Técnica Federico Santa María, Valparaíso, Chile
[139] Department of Physics, Institute of Science, Tokyo, Japan
[140] Department of Physics, University of Washington, Seattle WA, U.S.A.

JHEP07(2026)078

[141a] State Key Laboratory of Dark Matter Physics, School of Physics and Astronomy, Shanghai Jiao Tong University, Key Laboratory for Particle Astrophysics and Cosmology (MOE), SKLPPC, Shanghai, China
[141b] State Key Laboratory of Dark Matter Physics, Tsung-Dao Lee Institute, Shanghai Jiao Tong University, Shanghai, China
[142] Department of Physics and Astronomy, University of Sheffield, Sheffield, U.K.
[143] Department of Physics, Shinshu University, Nagano, Japan
[144] Department Physik, Universität Siegen, Siegen, Germany
[145] Department of Physics, Simon Fraser University, Burnaby BC, Canada
[146] SLAC National Accelerator Laboratory, Stanford CA, U.S.A.
[147] Department of Physics, Royal Institute of Technology, Stockholm, Sweden
[148] Departments of Physics and Astronomy, Stony Brook University, Stony Brook NY, U.S.A.
[149] Department of Physics and Astronomy, University of Sussex, Brighton, U.K.
[150] School of Physics, University of Sydney, Sydney, Australia
[151] Institute of Physics, Academia Sinica, Taipei, Taiwan
[152a] E. Andronikashvili Institute of Physics, Iv. Javakhishvili Tbilisi State University, Tbilisi, Georgia
[152b] High Energy Physics Institute, Tbilisi State University, Tbilisi, Georgia
[152c] University of Georgia, Tbilisi, Georgia
[153] Department of Physics, Technion, Israel Institute of Technology, Haifa, Israel
[154] Raymond and Beverly Sackler School of Physics and Astronomy, Tel Aviv University, Tel Aviv, Israel
[155] Department of Physics, Aristotle University of Thessaloniki, Thessaloniki, Greece
[156] International Center for Elementary Particle Physics and Department of Physics, University of Tokyo, Tokyo, Japan
[157] Graduate School of Science and Technology, Tokyo Metropolitan University, Tokyo, Japan
[158] Department of Physics, University of Toronto, Toronto ON, Canada
[159a] TRIUMF, Vancouver BC, Canada
[159b] Department of Physics and Astronomy, York University, Toronto ON, Canada
[160] Division of Physics and Tomonaga Center for the History of the Universe, Faculty of Pure and Applied Sciences, University of Tsukuba, Tsukuba, Japan
[161] Department of Physics and Astronomy, Tufts University, Medford MA, U.S.A.
[162] Department of Physics and Astronomy, University of California Irvine, Irvine CA, U.S.A.
[163] Department of Physics and Astronomy, University of Uppsala, Uppsala, Sweden
[164] Department of Physics, University of Illinois, Urbana IL, U.S.A.
[165] Instituto de Física Corpuscular (IFIC), Centro Mixto Universidad de Valencia — CSIC, Valencia, Spain
[166] Department of Physics, University of British Columbia, Vancouver BC, Canada
[167] Department of Physics and Astronomy, University of Victoria, Victoria BC, Canada
[168] Fakultät für Physik und Astronomie, Julius-Maximilians-Universität Würzburg, Würzburg, Germany
[169] Department of Physics, University of Warwick, Coventry, U.K.
[170] Waseda University, Tokyo, Japan
[171] Department of Particle Physics and Astrophysics, Weizmann Institute of Science, Rehovot, Israel
[172] Department of Physics, University of Wisconsin, Madison WI, U.S.A.
[173] Fakultät für Mathematik und Naturwissenschaften, Fachgruppe Physik, Bergische Universität Wuppertal, Wuppertal, Germany
[174] Department of Physics, Yale University, New Haven CT, U.S.A.
[175] Yerevan Physics Institute, Yerevan, Armenia

[a] Also at Department of Physics, King's College London, London, U.K.
[b] Also at Institute of Physics, Azerbaijan Academy of Sciences, Baku, Azerbaijan
[c] Also at Imam Mohammad Ibn Saud Islamic University, Saudi Arabia
[d] Also at Department of Physics, University of Thessaly, Greece
[e] Also at An-Najah National University, Nablus, Palestine
[f] Also at Department of Physics, University of Fribourg, Fribourg, Switzerland
[g] Also at Department of Physics, Westmont College, Santa Barbara, U.S.A.
[h] Also at Departament de Fisica de la Universitat Autonoma de Barcelona, Barcelona, Spain

JHEP07(2026)078

[i] Also at University of Siena, Italy
[j] Also at Affiliated with an institute formerly covered by a cooperation agreement with CERN
[k] Also at The Collaborative Innovation Center of Quantum Matter (CICQM), Beijing, China
[l] Also at Faculty of Physics, Sofia University, 'St. Kliment Ohridski', Sofia, Bulgaria
[m] Also at Università di Napoli Parthenope, Napoli, Italy
[n] Also at Institute of Particle Physics (IPP), Canada
[o] Also at Department of Physics, Bolu Abant Izzet Baysal University, Bolu, Türkiye
[p] Also at Faculty of Physics, University of Bucharest, Romania
[q] Also at Borough of Manhattan Community College, City University of New York, New York NY, U.S.A.
[r] Also at National Institute of Physics, University of the Philippines Diliman (Philippines), Philippines
[s] Also at TRIUMF, Vancouver BC, Canada
[t] Also at Universita degli Studi Link, Italy
[u] Also at Department of Financial and Management Engineering, University of the Aegean, Chios, Greece
[v] Also at University and INFN Torino, Torino, Italy
[w] Also at Institucio Catalana de Recerca i Estudis Avancats, ICREA, Barcelona, Spain
[x] Also at Henan University, China
[y] Also at Yeditepe University, Physics Department, Istanbul, Türkiye
[z] Also at Institute of Theoretical Physics, Ilia State University, Tbilisi, Georgia
[aa] Also at CERN, Geneva, Switzerland
[ab] Also at Center for Interdisciplinary Research and Innovation (CIRI-AUTH), Thessaloniki, Greece
[ac] Also at Hellenic Open University, Patras, Greece
[ad] Also at Department of Modern Physics and State Key Laboratory of Particle Detection and Electronics, University of Science and Technology of China, Hefei, China
[ae] Also at Department of Physics, Stellenbosch University, South Africa
[af] Also at School of Physics, University of the Witwatersrand, Johannesburg, South Africa
[ag] Also at Department of Physics, Ben Gurion University of the Negev, Beer Sheva, Israel
[ah] Also at University of Colorado Boulder, Department of Physics, Colorado, U.S.A.
[ai] Also at Département de Physique Nucléaire et Corpusculaire, Université de Genève, Genève, Switzerland
[aj] Also at Centre of Physics of the Universities of Minho and Porto (CF-UM-UP), Portugal
[ak] Also at Indian Institute of Technology (IIT), Jodhpur, India
[al] Also at Institute for Nuclear Research and Nuclear Energy (INRNE) of the Bulgarian Academy of Sciences, Sofia, Bulgaria
[am] Also at Washington College, Chestertown, MD, U.S.A.
[an] Also at Institut für Experimentalphysik, Universität Hamburg, Hamburg, Germany
[ao] Also at Institute of Applied Physics, Mohammed VI Polytechnic University, Ben Guerir, Morocco
[ap] Also at Institute of Physics and Technology, Mongolian Academy of Sciences, Ulaanbaatar, Mongolia
[aq] Also at Millennium Institute for Subatomic physics at high energy frontier (SAPHIR), Santiago, Chile
[ar] Also at University of Chinese Academy of Sciences (UCAS), Beijing, China
[†] Deceased

JHEP07(2026)078